TRACE LEAD ISOTOPE STUDIES WITH GAS SOURCE MASS SPECTROMETRY

by

ARTHUR BRICE LEROY WHITTLES

B.Sc. University of British Columbia, 1959.
M.Sc. University of British Columbia, 1960.

A THESIS SUBMITTED IN PARTIAL FULFILMENT OF

THE REQUIREMENTS FOR THE DEGREE OF

DOCTOR OF PHILOSOPHY

in the Department

of

PHYSICS

We accept this thesis as conforming to the required standard

THE UNIVERSITY OF BRITISH COLUMBIA

April, 1964

In presenting this thesis in partial fulfilment of the requirements for an advanced degree at the University of British Columbia, I agree that the Library shall make it freely available for reference and study. I further agree that permission for extensive copying of this thesis for scholarly purposes may be granted by the Head of my Department or by his representatives. It is understood that copying or publication of this thesis for financial gain shall not be allowed without my written permission.

Department of Physics

The University of British Columbia,
Vancouver 8, Canada

Date April 28, 1964

The University of British Columbia

FACULTY OF GRADUATE STUDIES

PROGRAMME OF THE

FINAL ORAL EXAMINATION

FOR THE DEGREE OF

DOCTOR OF PHILOSOPHY

of

ARTHUR BRICE LEROY WHITTLES

B.Sc., The University of British Columbia, 1959
M.Sc., The University of British Columbia, 1960

IN ROOM 302, HENNINGS BUILDING (PHYSICS)
TUESDAY, APRIL 28th, 1964, at 10:00 A.M.

COMMITTEE IN CHARGE

Chairman: F.H. Soward

J.B. Brown	R.D. Russell
G.M. Griffiths	W.F. Slawson
J.A. Jacobs	R.M. Thompson

External Examiner: J.T. Ulrych
University of Western Ontario

TRACE LEAD ISOTOPE STUDIES WITH GAS SOURCE MASS SPECTROMETRY

ABSTRACT

On the basis of data published prior to 1960, two basic lead isotope models - the isochron model and the primary lead model - were postulated to fit those crustal leads that have had the simplest history. The present writer's analyses of samples from Southern Finland, and the results of other research workers, now indicate that the primary lead model more adequately describes these leads, and that primary "isochrons" are either very short, or else non-existent.

Lead in conformable deposits and in ultrabasic sulfides were postulated by R.L. Stanton to be examples of primary lead. Analyses of samples from several massive lead-zinc conformable deposits have indicated that the leads of many of these deposits possess primary lead characteristics.

The present thesis describes a technique devised to prepare tetramethyllead from the conformable chalcopyrite deposits and ultrabasic sulfides and describes some initial results. This is a free radical technique, involving the reaction of methyl radicals with a lead mirror evaporated out of a sulfide. It appears to be capable of preparing tetramethyllead from samples containing one to two orders of magnitude less lead than previously reported for such a technique. Unfortunately, the full extent of the method cannot be utilized with present gas source mass spectrometer facilities, and only fair precision (0.4%) is possible at 10 ppm. lead.

Samples from the conformable chalcopyrite deposits of Mt. Isa were analysed. The lead isotope ratios were found to be significantly different from those of the massive lead-zinc deposits. The results, interpreted with other lead and sulfur isotope data, suggest that these deposits could be the result of metal-bearing solutions entering a partially enclosed bay. Initial results for two ultrabasic deposits suggest that the lead in the sulfides is not necessarily primary;

for example, that in two Stillwater ultrabasic complex samples appears to be the result of three stages of development. Hence, both the present lead isotope analyses, and those reported earlier by Ostic (1963) indicate that Stanton's geological criteria, while good, are not completely adequate for identifying primary leads. It is here suggested that sulfur isotope analyses might indicate which of these samples have been contaminated by crustal leads.

During the investigation of the gas source mass spectrometric analyses of small tetramethyllead samples, lead isotope fractionation was observed. This occured with molecular flow into the mass spectrometer. Lead isotope fractionation has not been reported previously, and has some interesting geophysical implications. A preliminary study suggests that such fractionation in nature is likely to be rare, except possibly in biological processes in the sea.

GRADUATE STUDIES

Field of Study: Physics

Advanced Geophysics	J.A. Jacobs
Geomagnetism	T. Watanabe
Modern Aspects of Geophysics	J.A. Jacobs
Waves	R.W. Stewart

Related Studies:

Mineral Deposits	W.H. Gross
Mineralogy and Lithology	O.H. Gorman
	P.A. Peach

PUBLICATIONS

Whittles, A.B.L., 1960. Voltage Coefficient of Victoreen High-Meg Resistors. Review of Scientific Instruments, 31, 208.

Whittles, A.B.L., 1962. The Elusive Isochron. Transactions of the American Geophysical Union, 43, 449.

ABSTRACT

On the basis of data published prior to 1960, two basic lead isotope models - the isochron model and the primary lead model - were postulated to fit those crustal leads that have had the simplest history. The present writer's analyses of samples from Southern Finland, and the results of other research workers, now indicate that the primary lead model more adequately describes these leads, and that primary "isochrons" are either very short, or else non-existant.

Lead in conformable deposits and in ultrabasic sulfides were postulated by R.L. Stanton to be examples of primary lead. Analyses of samples from several massive lead-zinc conformable deposits have indicated that the leads of many of these deposits possess primary lead characteristics.

The present thesis describes a technique devised to prepare tetramethyllead from the conformable chalcopyrite deposits and ultrabasic sulfides and describes some initial results. This is a free radical technique, involving the reaction of methyl radicals with a lead mirror evaporated out of a sulfide. It appears to be capable of preparing tetramethyllead from samples containing one to two orders of magnitude less lead than previously reported for such a technique. Unfortunately, the full extent of the method cannot be utilized with present gas source mass spectrometer facilities, and only fair precision (0.4%) is possible

at 10 ppm. lead.

Samples from the conformable chalcopyrite deposits of Mt. Isa were analysed. The lead isotope ratios were found to be significantly different from those of the massive lead-zinc deposits. The results, interpreted with other lead and sulfur isotope data, suggest that these deposits could be the result of metal-bearing solutions entering a partially enclosed bay. Initial results for two ultrabasic deposits suggest that the lead in the sulfides is not necessarily primary; for example, that in two Stillwater Ultrabasic Complex samples appears to be the result of three stages of development. Hence, both the present lead isotope analyses, and those reported earlier by Ostic (1963) indicate that Stanton's geological criteria, while good, are not completely adequate for identifying primary leads. It is here suggested that sulfur isotope analyses might indicate which of these samples have been contaminated by crustal leads.

During the investigation of the gas source mass spectrometric analyses of small tetramethyllead samples, lead isotope fractionation was observed. This occurred with molecular flow into the mass spectrometer. Lead isotope fractionation has not been reported previously, and has some interesting geophysical implications. A preliminary study suggests that such fractionation in nature is likely to be rare, except possibly in biological processes in the sea.

TABLE OF CONTENTS

CHAPTER 4 INTERPRETATION

LIST OF DIAGRAMS

LIST OF TABLES

ACKNOWLEDGEMENTS

Many persons have contributed to the completion of this thesis.

The writer is especially indebted to Dr. W.F. Slawson who supervised the research, and to Drs. R.D. Russell, G.P. Erickson and J.T. Ulrych who made many valuable suggestions. Their guidance and enthusiasm have contributed immeasurably to this research.

The stimulating discussions with Drs. J.R. Richards, R.M. Thompson, E.R. Kanasewich, R.G. Ostic and J.S. Stacey are acknowledged with thanks. The writer also appreciates the suggestions of Dr. E. Peters and Mr. W. Adams, and their permission to use the facilities of the Department of Mining and Metallurgy. The chemical advice of Dr. R. O'Brien is most gratefully acknowledged. The writer would also like to thank the Chemistry Department for providing weighing facilities. Thanks are also due to Miss S. Hanmer and Miss J. Kelly for their technical assistance, and to Miss S. Newman who also helped with the spectra computations and typed the final draft of this thesis.

A very strong vote of thanks must go to Mr. J. Lees, Mr. K.D. Schreiber, and Mr. P. Neukirchner whose technical and philosophical suggestions were especially appreciated, and who persisted with the writer through many variations in the experimental apparatus used in this research.

I have greatly appreciated the encouragement of my wife, family, and friends, without whose help this thesis might never have been completed.

The work was financed by the National Research Council of Canada. I would also like to express my gratitude for a National Research Council Studentship.

INTRODUCTION

"Where do you come from," said the Red Queen, "and where are you going?"
-Lewis Carroll in Through the Looking Glass

Extensive studies of lead isotope variations in natural minerals have been carried out in a number of laboratories throughout the world. At the Geophysics Laboratory of the University of British Columbia the main goal has been to determine the basic model which fits those crustal leads that have had the simplest history. A clear understanding of the correct basic model is essential to the interpretation of leads with more complex histories. On the basis of the data published prior to 1960 (Russell and Farquhar, 1960) two different basic models were proposed.

(1) The leads were presumed to have developed in a number of locally closed systems (containing varying portions of lead, uranium, and thorium) from time t_o, the time of formation of the earth, until time t when mineralization separated the lead from the uranium and thorium. Leads so developed should lie along a straight line on the Pb^{206}/Pb^{204} vs. Pb^{207}/Pb^{204} plot. These straight lines are called primary isochrons, and the model is termed the "isochron model".

(2) The leads were assumed to have developed in a single closed system, probably the lower crust or upper

mantle. If mineralization occurred at a given time t, the leads extracted, separated from the uranium and thorium, and emplaced in the crust without contamination would have identical isotope ratios. This model will be called "primary lead model".

The key to deciding between these two possibilities lay in understanding the effects of errors in measuring the relative Pb^{204} abundance. Such errors - due possibly to contaminants, mass spectrometer errors, and pressure scattering - could cause variations very similar to those expected on the basis of the isochron model. Under the supervision of R.D. Russell, Kollar (1960), Stacey (1962), and the present writer (Whittles, 1960, a and b) were directly concerned with the problem of improving the mass spectrometer precision. Ulrych (1960, 1962) improved the purification of the samples, so that pressure scattering could be reduced and intercomparison carried out under identical conditions. Kollar (1960) and Ostic (1963) devised an empirical pressure scattering correction. Part of the present thesis is involved with this aspect. Slawson and Russell (1962) and Kanasewich (1962a) studied the presence of contaminants in the samples. The results of this research were applied by E.R. Kanasewich and the present writer in the investigation of several suites of lead which apparently indicated the existence of primary isochrons. These analyses have shown that the reported primary isochrons were indeed due to errors in

determining the relative Pb^{204} abundances. Thus the primary lead model appears to be more applicable than the isochron model, the primary isochrons being either extremely short or else non-existent (Kanasewich, 1962a; Whittles, 1962). These results are discussed in more detail in the last chapter of this thesis.

The next step involved exploring, in greater depth, the primary lead model. R.L. Stanton predicted the two types of deposits should best fit this model. These were the conformable base metal deposits and the ultrabasic sulfides (Stanton and Russell, 1959). Ostic (1963) analyzed a large number of samples from conformable massive lead-zinc bodies and showed that the lead of many of these deposits fitted the primary lead model. Part of the present writer's Ph.D. research program involved the analyses of ultrabasic sulfides and conformable chalcopyrites.

Since the ultrabasic sulfides were expected to contain only a few ppm. lead, the first phase of this research required the development of a more sensitive chemical preparation of the tetramethyllead on which the lead isotope analyses are carried out. The type of preparation developed by the present writer was an extension of the technique of Ulrych (1962), and appears capable of preparing tetramethyllead from samples containing between one and two orders magnitude less lead than the minimum 500-1000 micrograms reported by this author. The new technique is described in Chapter 1. The second phase of this research

involved the exploration of the mass spectrometric analyses of small tetramethyllead samples, a topic about which little was known. This phase yielded one of the most exciting results of this thesis - the first lead isotope fractionation to be reported. The present writer has explored not only the mass spectrometric applications (Chapter 2), but also, tentatively, the geophysical implications of this discovery (Chapter 4).

The results of the lead isotopic analyses of some ultrabasic sulfides, and conformable chalcopyrites of Mt. Isa, are also discussed (Chapter 4).

Chapter 1: THE PREPARATION OF TETRAMETHYLLEAD FROM SULFIDES: THE MICRO-LEAD TECHNIQUE.

"The rung of a ladder was never meant to rest upon, but only to hold a man's foot long enough to enable him to put the other somewhat higher."

-T.H. Huxley in On Medical Education

1.0 Introduction

The goal of this portion of the present writer's research program was to produce tetramethyllead from minerals containing as low as a few parts per million lead.

The method used is based on the free radical technique of Ulrych (1962) which was an adaption of the original Paneth technique that has been widely used in free radical research. It was expected, however, that when dealing with small amounts of lead the use of free radicals, while probably a necessary condition, would not be a sufficient one. In particular, it was necessary to investigate and understand the primary causes of lead loss in such a process, and to modify the technique to minimize these losses. This approach has proven sucessful and has allowed the present writer to extend the tetramethyllead preparation to samples containing one to two orders less lead than the 500-1000 micrograms reported earlier.

Three steps are involved in this technique: firstly, a mineral is reduced to yield a reactive lead mirror; secondly, an organic material is decomposed to produce free methyl radicals, which react with the lead mirror to yield tetramethyllead:

$$Pb + 4CH_3\cdot = Pb(CH_3)_4 \quad ;$$

and thirdly, the tetramethyllead is separated from the residual organic materials. Each step will be considered in turn.

1.1 The Preparation of Lead Mirrors

1.1.1 Trace Leads in Minerals

Smith (1963), Mason (1958), Wedepohl (1956), and Goldschmidt (1937) have discussed the average concentration of lead in a variety of igneous rocks and minerals. More detailed studies have been reported by Auger (1941), Tauson and Kravchenko (1956), Fleisher (1955), Azzaria (1960), and Hawley and Nicol (1961). It appears that lead occurs primarily as minute inclusions of galena and is more common in the sulfides of copper ores than in those of nickel or gold ores. These reports also contain valuable suggestions that could be used in selecting suitable samples for the present technique.

For the purpose of this discussion lead-bearing minerals may be divided into three general classes.

(1) Minerals containing lead as a major constituent;

examples are galena, cerussite, and the lead sulfo-salts. Most of the lead isotope determinations using tetramethyllead have been made with minerals of this group.

(2) Minerals containing in the order of ten to several hundred ppm. lead. Examples include the various sulfo-salts; the sulfides: pyrite, sphalerite, pyrrhotite, chalcopyrite, marcasite; and the accessory minerals: magnetite, monazite, zircon, sphene, and apatite.

(3) Minerals containing a few ppm. lead or less; examples include the silicate minerals. Most meteorites also fall into this group. At present only solid source techniques have been applied to determine the lead isotope ratios of minerals of this class.

The micro-lead technique developed by the present writer appears to be capable of preparing tetramethyllead from minerals of all these groups provided their reduction temperature is below 950°C. Unfortunately, present mass spectrometer facilities limit isotope analyses to the first and second groups. If the sensitivity of these instruments could be increased, and if higher reduction temperatures were used, gas source mass spectrometry could be extended to include group (3).

The results of several of the above studies are summarized in Table 1.1.

Table 1.1 Trace Leads in Minerals and the Reduction of Minerals

Mineral	Lead Content ppm.	Reduction Temperature °C.	Present experimental results. Reduction in 2 hrs. at 950°C.
Galena (PbS)		580-780°C. Ref. 4.	Total
Boulangerite ($Pb_3Sb_4S_{11}$)			Total
Anglesite ($PbSO_4$)			Total
Cerussite ($PbCO_3$)			Total
Pyrite (FeS_2)	120-170 (nickel ores) 20-1280 (copper ores) 420 (gold ores) Ref. 1,17.	900°C. Ref. 2,3,4,5, 6,7,8.	90%
Pyrrhotite ($Fe_{1-x}S$)	190 (nickel ores) 200-700 (copper ores) 0 (gold ores) Ref. 1,17.		92%
Pentlandite $(Fe,Ni)_9S_8$			Total
Magnetite (Fe_3O_4)	80 Ref. 9,10,11,12.	90% at 900°C. Ref. 18,19,20.	87%
Chromite $(Mg,Fe)Cr_2O_3$		1600°C. Ref. 13,14,15,16.	10%
Ilmenite ($FeTiO_3$)			48%

Table 1.1 (Continued)

References

(1) Fleisher (1955)
(2) Gallo (1927)
(3) Schwab and Philius (1947)
(4) Sudo (1948)
(5) Mataba and Unotoro (1951)
(6) Gallo and Del Guerra (1951)
(7) Ishihara and Sudo (1954)
(8) Niva et al (1956)
(9) Howie (1955)
(10) Tauson and Kravchenkov (1956)
(11) Tilton et al (1955)
(12) Azzaria (1960)
(13) Pascal (1945)
(14) Kornilov and Kimlaeva (1945)
(15) Baikloh and Henke (1937)
(16) de Wet (1952)
(17) Hawley and Nicol (1961)
(18) Edström (1953)
(19) Quets et al (1960)
(20) McKewan (1960)

1.1.2 The Reduction of Minerals

Step I of the micro-lead technique involved the preparation of trace lead mirrors through the reduction of the mineral hosts. Because of the widespread commercial interest the reduction of minerals has been under study for many years; however, the reduction in order to obtain trace lead mirrors is a relatively new development.

The present writer uses a procedure similar to that of Baskova and Novikov (1957) and Ulrych (1962). The mineral samples are finely crushed then introduced into the micro-lead apparatus in quartz boats. Hydrogen at one atmosphere and 800 c.c./min. is passed through the apparatus, while the furnace temperature is brought slowly up to 950°C. in the first hour, and then maintained at this level for an hour. The mirror is then purified by repeated distillations under the same conditions. A final distillation, at reduced pressure, separates the mirror components out more completely for selective removal with free methyl radicals. A number of minerals have been investigated in this manner and the results have been compared to those available in the literature (Table 1.1).

All the major lead minerals are totally reduced. Chalcopyrite and pentlandite also reduce completely, a molten alloy being left in the quartz boat. The chalcopyrite samples seem to contain more of the volatile metals than pentlandite and are probably more suitable for this

type of preparation. Apart from the lead minerals, pyrite appears to contain the most lead of those listed while pyrrhotite is more comparable to chalcopyrite. Although these last two minerals are not completely reduced in two hours most of the lead must evaporate off during this time since no new mirrors were formed when the samples were subjected to reducing conditions a second time. This is to be expected in view of the porous nature of the free iron that results from the reduction. Magnetite is an easily reduced mineral, and its widespread occurence would make its study extremely interesting. Chromite and ilmenite are not too promising because of the difficulty of reducing them. Both of these minerals retain some of their volatile materials even after two hours since second mirrors were easily obtained. It may well be that the isotopic composition of the first mirror will differ from that of the second as in the case of silicate minerals (Zhirov and Zykov, 1956).

1.1.3 The formation of $xPbO \cdot SiO_2$

During the present writer's experiments it was noticed that under certain conditions lead mirrors were converted to dark brown deposits which could not be totally reduced in the hydrogen furnace. It was later found that this effect could be reproduced at will by first oxidizing the mirror while it was hot (to ensure extensive oxidation). Samples of $Pb(NO_3)_2$ and PbO were

placed in quartz crucibles at 950°C. In all cases the samples converted to a black compound and very little free lead was produced. When subsequently heated in an oxygen stream the deposit turned white; this process was reversible with little or no loss of material. The lead mirrors which had converted to the dark deposits exhibited exactly the same properties. Examination of both the quartz boats containing the lead compounds, and the quartz tubes containing the converted lead mirrors, showed that the lead had apparently reacted with the quartz since the mixture could not be totally removed by scraping. Furthermore, when the quartz tubing was cleaned with HF, the surface was extensively etched at the position of the converted mirrors. One possibility seemed to be the formation of a lead silicate. This was tested by heating, in the hydrogen furnace, a sample of pure lead placed in a quartz boat. No reaction between the lead and the quartz boat could be distinguished. Later experiments with lead mirrors of the order of tens of micrograms deposited on quartz tubing have shown that any reaction between lead and silica must be extremely slow if indeed it occurs at all. It is apparently a difficult task to form even lead feldspars (W.F. Slawson, personal communication). E. Peters, of the U.B.C. Metallurgy Department, suggested instead the formation of a lead mono-oxide silicate. Such a compound, of the form $xPbO \cdot SiO_2$, would indeed be expected on the basis of the $PbO-SiO_2$ phase diagram of Geller, Creamer, and

Bunting (1934), (Diagram 1.1). This silicate will form at all temperatures but is less likely at the lower values where the rates of solid diffusion would be greatly decreased. This was checked experimentally, and at 500°C. most of the lead oxide converted to free lead, although some of the silicate still formed.

Al_2O_3, fused or crystallized, might be more suitable than quartz. Samples of PbO were placed in an alundum crucible and reduced at 950°C. in the hydrogen furnace. Most of the oxide converted to free lead, although a faint black deposit was again evident. In this respect Al_2O_3 seems the better choice, although the phase diagram (Hall and Insley, 1947) suggests the formation of a similar compound: $xPbO \cdot Al_2O_3$.

It should be stressed at this point that the main problem is not the conversion of PbO in the samples to free lead, but the reactivation of the lead mirrors once they have been oxidized. Hence it is not necessary to use alundum crucibles with the samples (which are mostly sulfides) since they contain no source of oxygen. Also, transparent quartz tubes are better than opaque alundum tubes provided the lead mirror is never oxidized.

The solution appears to involve the reduction of the minerals and the formation of the lead mirrors right in the micro-lead apparatus. If the mirrors are immediately

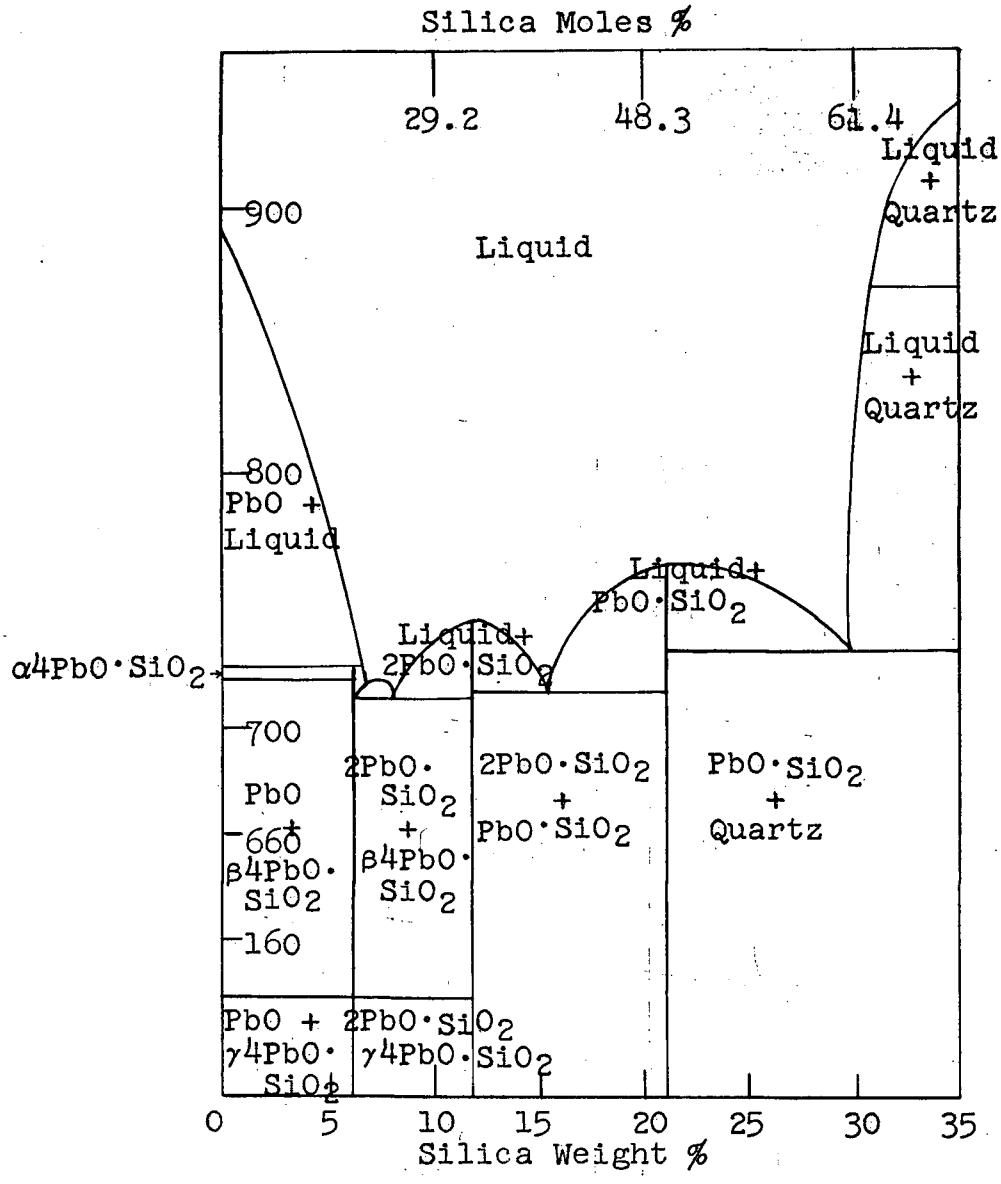

Diagram 1.1. The $PbO-SiO_2$ Phase Diagram
(Geller, Creamer and Bunting, 1934)

removed by the action of methyl radicals the "PbO problem" should not arise. This procedure has been adopted in the present work.

One other point is of interest. The above discussion for PbO applies equally to $Pb(NO_3)_2$ so this would tend to eliminate the use of HNO_3 ($\rightarrow Pb(NO_3)_2 \rightarrow PbO \rightarrow xPbO \cdot SiO_2$) in the cleaning procedure, particularly since HNO_3 is difficult to eliminate even with extensive washing. The use of HF, with subsequent baking in an oxygen stream, provided adequate cleaning.

1.2. Methyl Radical Sources

1.2.1. Free Methyl Radicals and Their Production

Free radicals are defined as neutral atoms or molecules possessing one or more unpaired electrons. In general, they belong to two classes: those which are relatively stable (the Gomberg type, e.g.-the benzl radical, $C_6H_5CH_2\cdot$); and, those which are highly reactive but short lived, such as the methyl radical ($CH_3\cdot$).

One of the first free radicals to be recognized was triphenylmethyl, $(C_6H_5)_3C_2\cdot$, which belonged to the first group (Gomberg, 1900). The existence of the more reactive, short lived radicals was suggested soon after by Bone and Coward (1908) but no conclusive evidence of their existence was obtained until 1929 (Paneth and Hofeditz, 1929). Since this time there has been a great deal of interest in these

entities, and for a more detailed discussion one should refer to the several comprehensive summaries that have been written (Steacie, 1954; Waters, 1948; Rice and Rice, 1935).

This section considers only those points which are of direct interest in the present work.

The nature of covalent bond fission was discussed by Waters (1948). A covalent bond may be broken to give two neutral molecules (homolysis):

$$A{:}B + \text{energy} = A\cdot + B\cdot \qquad (1.1)$$

each of which retains one electron of the bonding pair. Or, it may yield two ions one of which separates with both electrons (heterolysis):

$$A{:}B + \text{energy} = A^{+} + (:B)^{-} \qquad (1.2)$$

More energy is required for heterolysis, particularily in a gas where wide separations are possible, since this process involves both electrostatic and bond-breaking energies. For this reason most gas reactions, unlike reactions in solutions, are of the homolytic type.

Radicals can also result in chain reactions:

$$R\cdot + A{:}B = R{:}A + B\cdot \qquad (1.3)$$

which continue in a series until two active radicals meet and combine, or else are absorbed on the walls of the reaction vessel.

Waters (1948) has also outlined the various methods of producing free radicals. Of these thermal decomposition

seems most satisfactory for the present preparation (Ulrych, 1962). Many stable compounds decompose at higher temperatures into free radicals. Paneth and Hofeditz (1929) used this method with tetramethyllead, and Leermakers (1933a), with azomethane. Rice et al (1932) showed that a wide range of organic compounds decompose at temperatures of 500-1100°C. This method has the virtue of extreme simplicity, requiring only a nichrome-wound quartz tube and a variable auto-transformer. The heated walls also minimize radical-wall recombinations:

$$CH_3\cdot + CH_3\cdot = C_2H_6 \qquad (1.4)$$

1.2.2 The Choice of a Free Methyl Radical Source

1. Possible Methyl Radical Sources

The proper selection of a free radical source is a problem having considerable importance in this work since it can determine to a large extent the details of the tetramethyllead preparation. Since no systematic survey of the possibilities had been made, the present writer undertook the investigation of some 45 organic materials. Several which appeared suitable were investigated experimentally.

The suitability of a source of free radicals was determined by five main criteria:

(1) The experimental ease with which the methyl radicals may be produced. This factor would tend to eliminate compounds which require very high decomposition

temperatures, or which are explosive, very poisonous, or very reactive.

(2) The abundance of free methyl radicals produced per unit weight of the source compound. A more efficient source will result in faster mirror removal, and smaller quantities of by-products to be separated from the tetramethyllead.

(3) The ease with which the breakdown products, and the undecomposed source material, may be separated from the tetramethyllead produced.

(4) Freedom from mass spectral interference. Even after purification, traces of the by-products will remain in the sample. These will be of no importance provided their masses, or the masses of their ionization fragments, do not coincide with those of the trimethyllead spectra.

(5) The freedom from unwanted free radicals. If there are other than methyl radicals present, some of the lead may be converted to compounds other than tetramethyllead. These would decrease the "yield" and might interfere with the isotope measurements. The formation of the solid tetraphenyllead would deactivate the mirror.

The preceding five points have guided the selection of suitable source materials. Compounds of the following types were not considered in detail.

(1) Compounds whose products are extremely complex and unspecified in the literature. The present writer tended to limit the search to the more common compounds

whose products are well known.

(2) Compounds whose decomposition products might deactivate the lead mirror; for example, chlorides, bromides, iodides, and mercury compounds. One of this type, methyl iodide, was tried and found to be eminently unsuitable.

2. The Selection

Many of these sources have been obtained from Steacie's (1954) book; some were discussed by Rice and Rice (1935), Lossing et al (1953a), and Rice and Johnston (1934). The dissociation products are discussed by Steacie, or in the references indicated in the tables. The temperature of abundant free methyl radical production was estimated from one of the above references or from the dissociation energies (Szwarc, 1950; and, Steacie, 1954). These energies give some indication of the ease with which a radical-radical bond may be broken; however, since the mechanism of free radical production is the controlling feature these estimates are not too reliable. The data is summarized in the following tables.

Table 1.2 describes sources that appear unsuitable for the present work, and the reason for this. The (?) inserted behind some of the compounds indicates that it is unclear from the literature to what extent this particular feature applies.

Table 1.2 Undesirable Free Methyl Radical Sources

1. High Temperature Required to Produce Abundant Free Methyl Radicals.

(1)	Acetyldehyde	Ref. 1,2,3,4.
(2)	1 - Butene (?)	Ref. 5,6,7.
(3)	Divinyl Ether	Ref. 8.
(4)	Ethane (?)	Ref. 9,8.
(5)	Ethyl Alcohol (?)	Ref. 11.
(6)	Methane	Ref. 11.
(7)	Methyl Alcohol(?)	Ref. 12.
(8)	Methylamine (?)	Ref. 3.
(9)	Propane	Ref. 13.
(10)	Toluene	Ref. 14.

2. Other Radicals Produced

(1)	Anisole	Ref. 14.
(2)	Azomethane	Ref. 8.
(3)	Azo-iso-Propane	Ref. 8.
(4)	Azo-n-Propene (?)	Ref. 8.
(5)	n-Butane	Ref. 11.
(6)	Dipropyl Peroxide (?)	Ref. 11.
(7)	Ethane	Ref. 9,8.
(8)	Ethyl Alcohol (?)	Ref. 11.
(9)	Methyl Ethyl Ketone	Ref. 11.
(10)	Phenyl Methyl Ether	Ref. 14.
(11)	Propene	Ref. 13.
(12)	Tetrabutyllead	Ref. 11.
(13)	Tetrapropyllead	Ref. 11.
(14)	Toluene	Ref. 14.

Table 1.2 (continued)

3. Inadequate Separation (High Boiling Point Decomposition Products).

(1)	Acetyldehyde	Ref. 1,2,3,4.
(2)	Acetyl Peroxide	Ref. 11.
(3)	Alkyl Nitrates	Ref. 11.
(4)	Alkyl Nitrites	Ref. 11.
(5)	Anisole	Ref. 14.
(6)	Azo-n-Propane	Ref. 8.
(7)	1-Butene (?)	Ref. 5,6,7.
(8)	iso-Butene	Ref. 11.
(9)	Diethyl Peroxide (?)	Ref. 15.
(10)	Dimethyl Ether	Ref. 10,15,16,17,18,19.
(11)	Dipropyl Peroxide	Ref. 11.
(12)	Divinyl Ether	Ref. 8.
(13)	Ethyl Alcohol	Ref. 11.
(14)	Ethyl Benzene	Ref. 20.
(15)	Methyl Alcohol	Ref. 12.
(16)	Methylamine	Ref. 3.
(17)	Methyl Ethyl Ketone	Ref. 11.
(18)	Phenyl Methyl Ether	Ref. 14.
(19)	Propylene Oxide (?)	Ref. 10,21.
(20)	Toluene	Ref. 14.

4. Undesirable for Other Reasons

(1)	Azomethane (Explosive)	Ref. 22,23,24,25,26,27,28,29,30.
(2)	Dimethyl Zinc (very reactive, no data)	
(3)	Tetramethyllead (Contamination)	Ref. 11.
(4)	Trimethyl Aluminum (very reactive)	Ref. 31,32.

Table 1.2 (continued)

References

1. Hinschelwood and Hutchison (1926a)
2. Winkler and Hinschelwood (1935a)
3. Travers (1937a,b)
4. Sweddon and Travers (1936)
5. Szwarc and Sehon (1950)
6. Sehon and Szwarc (1950)
7. Tropsch et al (1936)
8. Lossing et al (1953b)
9. Rice and Dooley (1933)
10. Lossing et al (1953b)
11. Steacie (1954)
12. Terenin et al (1935)
13. Rice, Johnston and Evering (1932)
14. Ingold and Lossing (1953)
15. Rebbert and Laidler (1952)
16. Gay and Travers (1937)
17. Eltenton (1947)
18. Rice and Johnston (1934)
19. Rice and Herzfeld (1934)
20. Szwarc (1949)
21. Thompson and Meissner (1938)
22. Thiele (1909)
23. Ramsperger (1927)
24. Leermakers (1933a,b)
25. Riblett and Rubin (1937)
26. Steel and Trotmann-Dickenson (1959)
27. Forst and Rice (1963)
28. Page et al (1953)
29. John and Taylor (1939)
30. Allen and Rice (1935)
31. Yeddanapalli and Schubert (1946)
32. Laubengayer and Gilliam (1941)

Table 1.3: Possible Free Methyl Radical Sources: I, lists those compounds which appear to be suitable, but which have some reported (but unclarified) bad features.

Table 1.4: Possible Free Methyl Radical Sources II, lists several compounds which seemed particularily suitable, on the basis of the literature survey. Some of these were investigated experimentally by the present writer.

3. Experimental Results

Of the compounds listed in Table 1.4, and studied experimentally, di-t-butyl peroxide was found to be the most satisfactory.

The compounds were studied by passing them through the micro-lead furnace and over a lead mirror. Diagram (1.2) represents a simplified schematic of the apparatus. The decomposition products were trapped in the liquid air trap, transferred to a breakseal, and examined on the mass spectrometer.

(1) Tin Tetramethyl and Other Metal Alkyls

The present writer's experiments have provided the first direct evidence for methyl radicals in the decomposition of tin tetramethyl; however, it was found that as a free radical source for the present work, this compound has several undesirable features.

(a) It is not a very efficient source since con-

Table 1.3 Possible Free Methyl Radical Sources: I

(1) Acetone	Ref. 1,2,3,4,5,6.
(2) 1-Butene	Ref. 5,6,7 (of Table 2.2)
(3) iso-Butane	Ref. 9.
(4) Dimethyl Cadmium	Ref. 8.
(5) Diethyl Peroxide	Ref. 9.
(6) Tetramethyl silicon	Ref. 10,11.

References

(1) Hinschelwood and Hutchison (1926b)
(2) Winkler and Hinschelwood (1935b)
(3) Rice and Vollrath (1929)
(4) McNesley et al (1954)
(5) Rice and Johnston (1934)
(6) Rice and Herzfeld (1934)
(7) Huffman (1936)
(8) Heller and Taylor (1953)
(9) Steacie (1954)
(10) Helm and Mack (1937)
(11) Sathyamurthy et al (1950)

Table 1.4 Possible Free Methyl Radical Sources: II

(1) Dimethylamine	Ref. 1,2,3,4.
(2) Di-tert-butyl Peroxide	Ref. 5,6,7,8,9,10,11, 12,13,23.
(3) Ethylene Oxide	Ref. 2,13,14,15,16, 17,18,19.
(4) Tetramethyl Tin	Ref. 20,21.
(5) Trimethylamine	Ref. 2,3,22.

References:

1. Taylor (1932)
2. Rice and Johnston (1934)
3. Bamford (1939)
4. Rice and Grelecki (1957)
5. Milas and Surgenor (1946)
6. George and Walsh (1946)
7. Raley, Rust and Vaughan (1948)
8. Rust, Seubold and Vaughan (1948)
9. Benson (1960)
10. Murawski et al (1951)
11. Brinton and Volman (1952)
12. Lossing and Tichner (1952)
13. Lossing et al (1953a)
14. Heckert and Mack (1929)
15. Fletcher and Rollefson (1936)
16. Travers (1937b)
17. Simard et al (1948)
18. Mueller and Walters (1951, 1954)
19. Crocco et al (1959)
20. Waring and Horton (1945)
21. Sathyamurthy et al (1950)
22. Gesser et al (1957)
23. Dorfman and Salsburg (1951)

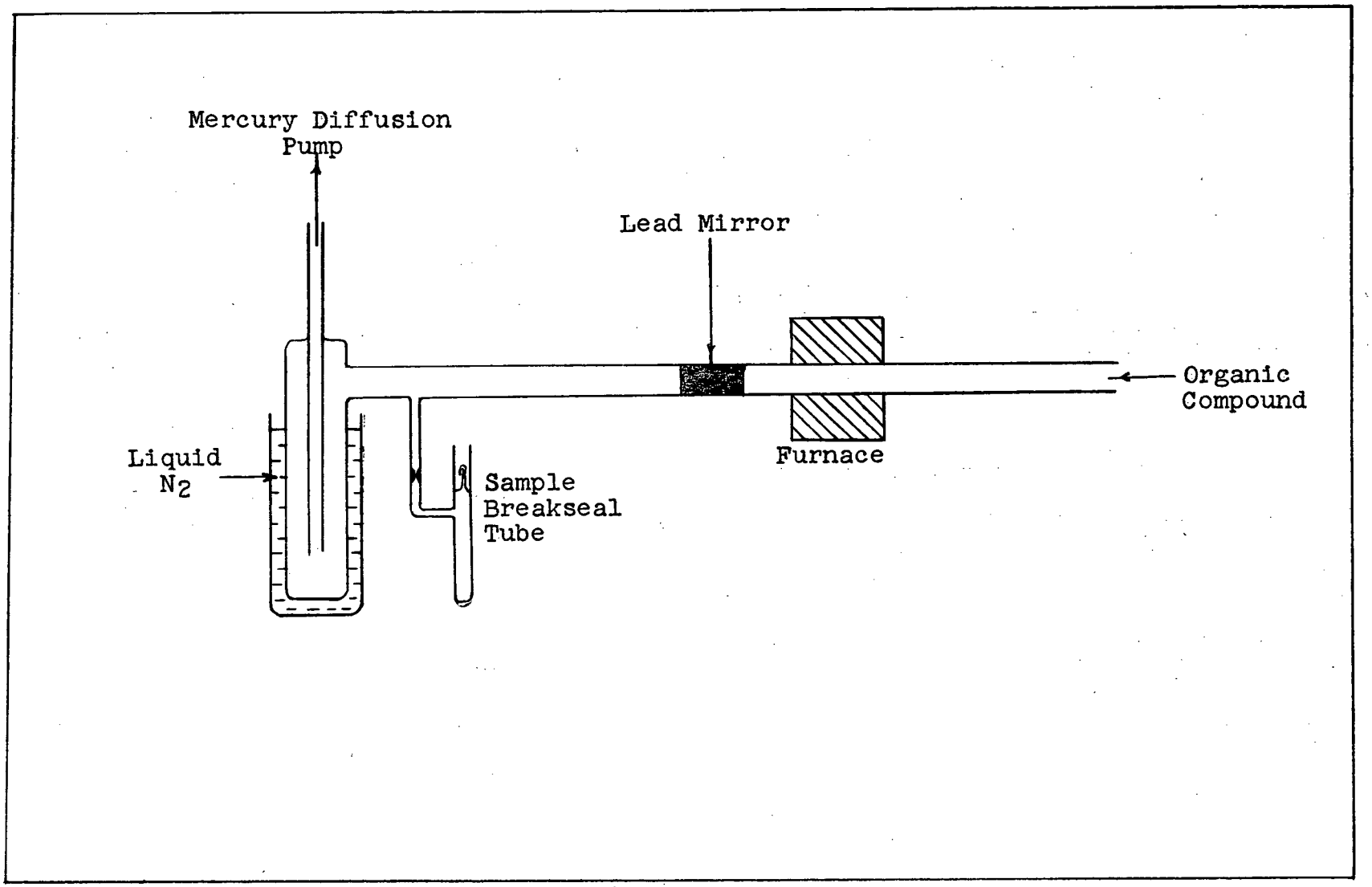

Diagram 1.2. Simplified Schematic of Paneth-Type Micro-Lead Apparatus: The Testing of Methyl Radical Sources.

siderably more $Sn(CH_3)_4$ was decomposed than $Pb(CH_3)_4$ produced. This favors the reaction series described by Sathyamurthy et al (1950) over that of Waring and Horton (1945).

(b) Not all of the $Sn(CH_3)_4$ was decomposed even at the high temperature (950°C.) used.

(c) A carrier gas was necessary for good flow and this complicated the operating procedure.

(d) Many decomposition products were produced which could not be easily separated from the Pb $(CH_3)_4$ by simple vacuum distillation.

(e) Because of the formation of a yellow polymer, and the release of free tin and carbon, cleaning of the apparatus was difficult and necessarily extensive.

Of all the other metal alkyls listed in Table 1.3, tetramethyl silicon would probably be the most similar to tetramethyltin. The literature suggests that trimethyl aluminum might be better than either of these compounds, although it has many similar features. Also, it is highly reactive and difficult to handle. No data appears to be available for dimethyl zinc and it too is very reactive. One other metal alkyl, tetramethyllead, was tested and found to be a very efficient free radical source. Unfortunately, the possible contamination of the sample with source would rule out its use in the present work.

(2) Tri- and dimethylamine and Ethylene Oxide

Trimethylamine was found to give rapid removal for a furnace temperature of 950°C. with no carrier gas. The decomposition products, mainly dimethylamine, methane, and ethane were easily removed from the tetramethyllead by simple vacuum distillation at dry ice temperatures; however, the times required for comparable separation were considerably longer than for di-t-butyl peroxide so the lead loss would be greater. In addition, trimethylamine is much more difficult to handle.

Dimethylamine and ethylene oxide should be as suitable as trimethylamine except that they require a hundred degree higher temperature for comparable methyl radical production.

(3) Di-t-butyl Peroxide

This compound was found to be the most suitable of those tried, provided it was first purified of t-butyl alcohol.

The suitability of this material initially seemed to depend upon the absence of the higher boiling ketone by-products. Decomposition tests showed that acetone and methyl ethyl ketone were the main products. The higher boiling ketones - methyl n-propyl, diethyl, methyl iso-propyl, etc. - would have been present only to about 0.1% of the acetone abundance. t-butyl alcohol, which is not a decomposition product under the present experimental

conditions, was also present. Since di-t-butyl peroxide is often prepared from this alcohol (Milas and Surgenor, 1946) it was perhaps not surprising to find the present supply contained 3%. As it is impossible to separate t-butyl alcohol from tetramethyllead by simple vacuum distillation, the source must first be purified. This involved a distillation at a pressure of 6 cm. Hg and a temperature of 50-60°C. carried out in a grease-free system (Dorfman and Salsburg, 1951).

The tetramethyllead samples prepared from this purified source could be separated to a degree comparable to that obtained using chromatographic techniques. This source was used in preparing all the micro-lead samples.

1.3 Experimental Apparatus and Techniques

1.3.1 Experiment Apparatus and Procedure

1. Design Considerations

The first two of the three steps for obtaining tetramethyllead from sulfides take place in the micro-lead apparatus. A simplified schematic is given in Diagram (1.3). In step I the sample is placed in a quartz boat and heated in a hydrogen flow at 950°C. After two hours the furnace is moved in a series of steps down the tube. This redistills and purifies the lead mirror that has been evaporated from the reduced sulfide. A final distillation is carried out

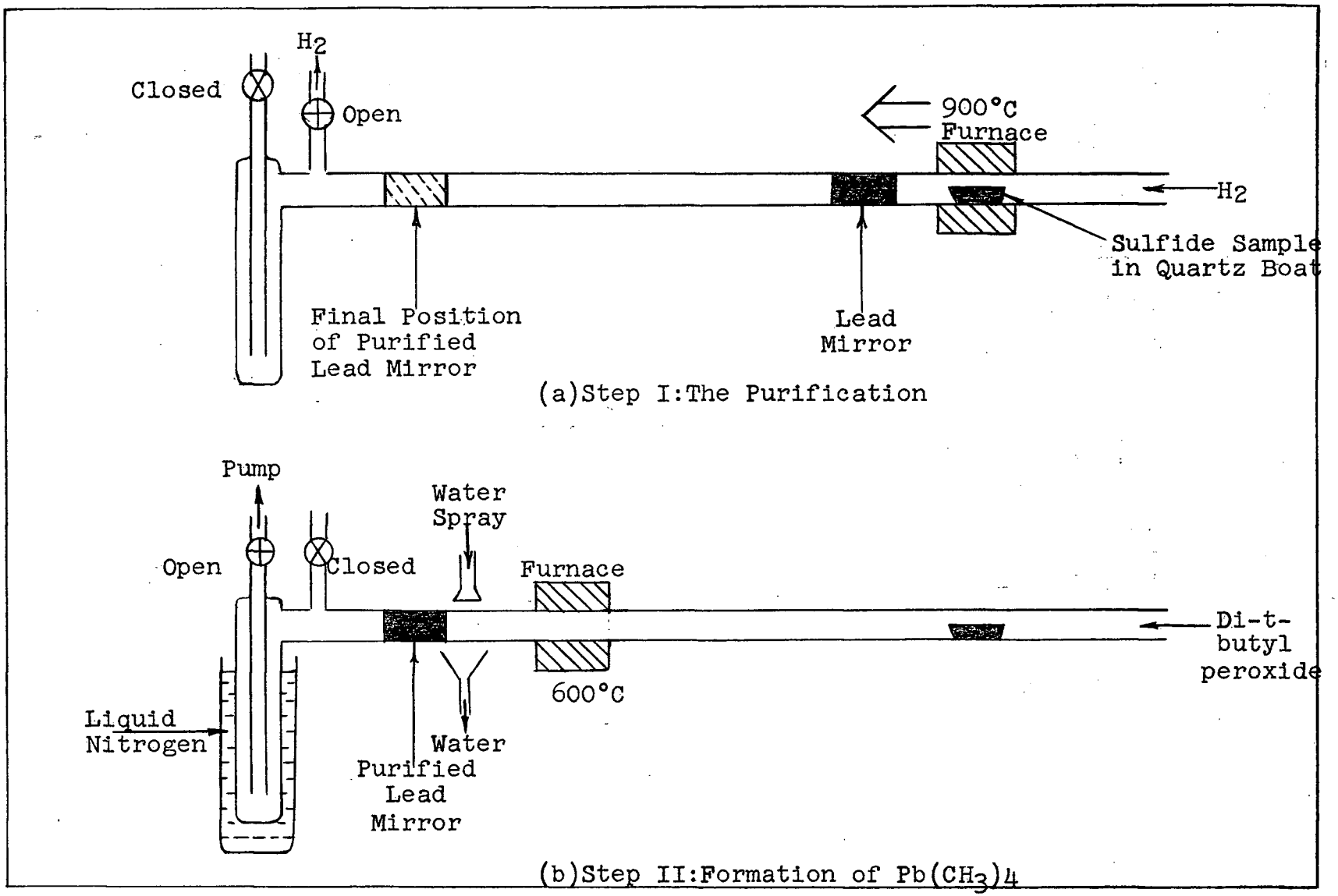

Diagram 1.3.Simplified Schematic of Micro-Lead Tetramethyllead Preparation

at a reduced hydrogen pressure. Step II involves firstly, the cooling of the region between the furnace and the mirror and secondly, the flow, and decomposition of di-t-butyl peroxide. The resulting tetramethyllead is trapped with the decomposition products in the cold trap. The furnace is then cooled, the trapped material transferred to a breakseal tube and sealed off.

Since efficient tetramethyllead production requires that a maximum number of methyl radicals collide with the lead mirror, the very short lifetime of these radicals is a major factor to be considered in the design of the micro-lead apparatus. The methyl radical lifetime is determined partly by the rate of recombination to form ethane:

$$CH_3\cdot + CH_3\cdot = C_2H_6 \qquad (1.5)$$

This occurs in the presence of a third body, usually the wall, that has a sufficiently low thermal energy to absorb the energy released in the recombination. The methyl radicals also react with gas molecules in the region:

$$CH_3\cdot + XR = CH_3X + R\cdot \qquad (1.6)$$

Acetone, the main decomposition product of di-t-butyl peroxide, is converted to ethylmethyl and higher ketones. Hence we can:

(1) minimize the number of radical - wall reactions by:

(a) requiring the ratio of wall area to volume to be small, e.g., the radius of the tube to be large;

(b) placing the mirror as close to the methyl radical source region as possible;

(c) keeping the thermal energy of the walls, between the furnace and the lead mirror, high;

or:

(2) minimize the radical - gas molecule reactions by:

(a) having low pressures in the region the radicals are formed (best removal occurs with total pressures of one or two mm. Hg., or less) either by using high pumping speeds or by slow source material injection, or both;

(b) requiring a large wall area to volume ratio, e.g., a small tube radius.

It is more important to minimize radical - gas molecule reactions since these are more efficient than the radical - wall reactions; only one out of every 1000 wall collisions results in the loss of a radical (Rice and Rice, 1935, p.58).

Conditions (1b) and (1c) can be set independently of the other requirements, and depend mainly upon the experimenter's ability to cool the mirror which must be near room temperature (Rice and Rice, 1935). In order to optimize the competing conditions (1a), (2a), and (2b) the present writer arranged his apparatus so that the mirror, when finally purified, was deposited at the end of a small diameter (15mm.) quartz tube which was placed inside one of larger size (19mm. dia.). The source injection rate gave a mean free path of about 0.1 cm.

Several other factors that affect the activity and removal of metallic lead mirrors by free methyl radicals

must also be considered.

(3) Oxygen - traces may completely deactivate a lead mirror (Harris and Tickner, 1948; Glazebrook and Pearson, 1936) so a good vacuum (10^{-5}mm. Hg.) must be obtained. Additionally, materials which pass over the mirror must not contain free oxygen.

(4) Wall Conditions - fresh quartz surfaces have been found to be about the best (Steacie, 1954).

(5) Back diffusion - of the newly formed tetramethyllead- must also be prevented. In the present system sufficient flow is provided by the decomposition products of the di-t-butyl peroxide source.

2. The Apparatus

The apparatus is given in detail in Diagram (1.4).

Ordinary grade (99.8%) tank hydrogen (hydrocarbon, sulfur content, CO_2, CO, NO, and Hg < 1ppm.; N_2 approximately 23ppm.; O_2 approximately 16 ppm.) was used in Step I, the reduction process. The impurities were effectively removed by passage through a cold trap and activated charcoal held at liquid air temperatures (Lossing and Tickner, 1952; Dushman, 1949). The three glass leaks were made by constricting 2mm.capillary tubing. Leak #1 was used in the initial reduction stage, allowing a H_2 flow of 800 c.c./min. at 1 atmosphere. Leak #2 provided

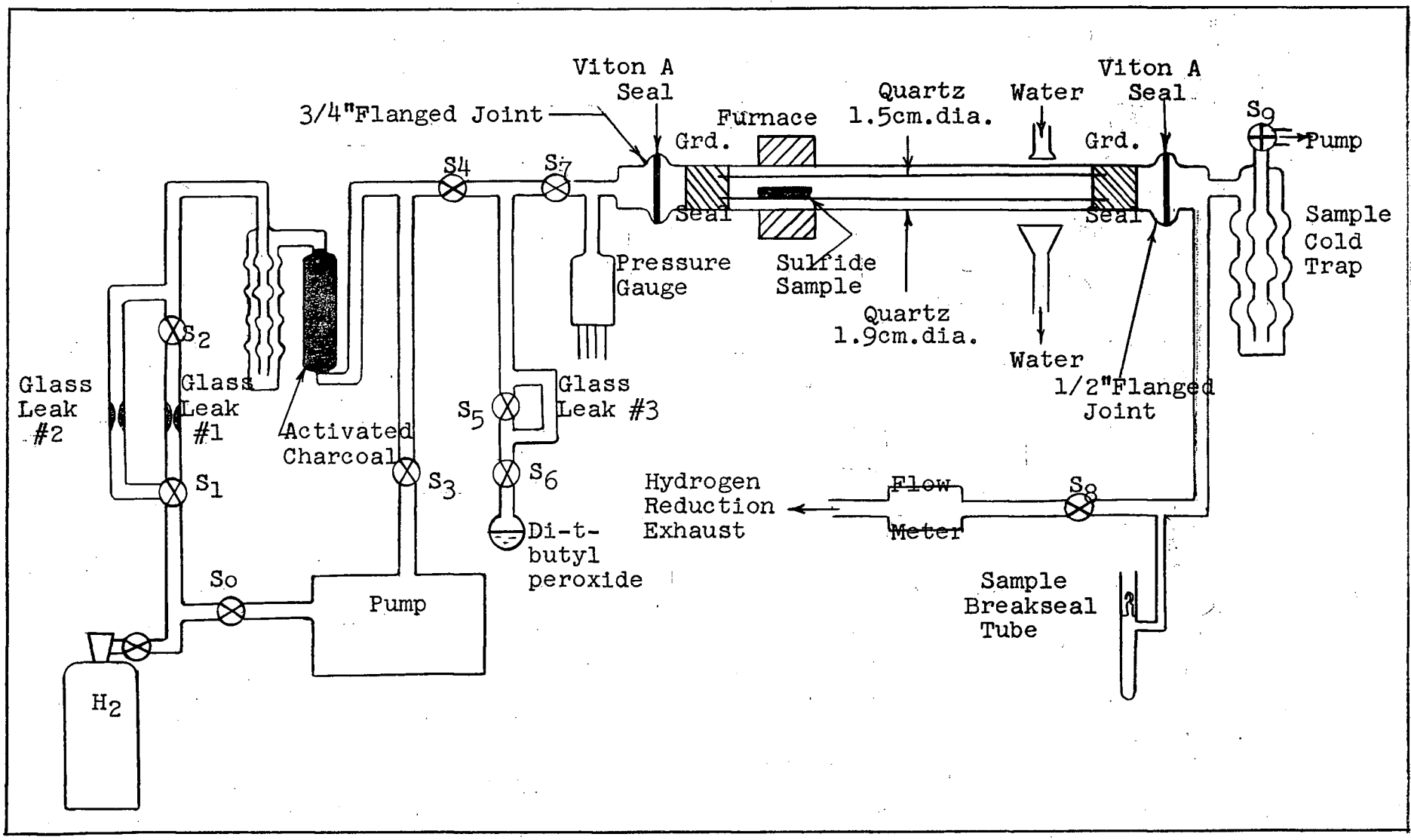

Diagram 1.4:Micro-lead Apparatus for the Preparation of Tetramethyllead

a flow of H_2 at 1 cm. Hg pressure when pumped through the mercury diffusion pump during the final distillation of the lead mirror. Leak #3 allowed a flow of di-t-butyl peroxide at 1 mm. Hg. All the stop-cocks shown, with the exception of S_6, were the usual greased (with Apiezon N, since "silicon" greases must not be used - Kanasewich, 1962a; Slawson and Russell, 1962) vacuum type. S_6 was specially designed to present only a diaphram of Viton-A to the source material. This diaphram of Viton-A was operated by a stainless steel spring and a nylon plunger. An R.C.A. 1946 resistivity gauge was found suitable for monitoring pressures in the apparatus. The flanged joints were Sentinel brand pyrex flanged pipe sets held together by bolted flange sets. Viton-A rings, cut from 1/8" sheeting proved to be excellent vacuum seals. The 19mm. dia. quartz tubing between the graded seals and flanged joints was 70 cm. in length, sufficient to allow six re-distillations of the lead mirror. The furnace consisted of 16 ft. of #22 Nichrome wire wound on a quartz cylinder and several layers of asbestos. A variable auto-transformer provided the necessary control.

3. The Procedure

(1) The sample was finely crushed, 3 gms. were placed in a quartz boat and inserted inside a 50 cm. length of the 15 mm. quartz mirror tubing. This tubing was then placed inside the 19 mm. diameter tubing on which the furnace

moves. Between runs the mirror tubing, boats and furnace quartz were removed and cleaned in HF. They were then baked up to 1/2 hr. at 950°C. in a O_2 stream. The cold trap was removed, cleaned in chromic acid, flushed, and dried at 200°C. All the stopcocks were cleaned and regreased.

(2) A heater (100°C.) was wrapped around the activated charcoal trap and the apparatus pumped on overnight.

(3) The charcoal trap heater was disconnected the following morning and the mercury diffusion pump started.

(4) When the apparatus had pumped down to 1 x 10^{-5}mm. Hg, dry ice and acetone were placed around the di-t-butyl peroxide. With S_4 closed this source was degassed for 1/2 hour.

(5) The hydrogen line was first pumped out through S_o, then flushed with H_2, pumped down again, and finally filled at a pressure of 2 atmospheres with S_1, S_0 closed.

(6) The Hg. diffusion pump was shut off at S_9, and the micro-lead system filled with hydrogen through leak #1. When the pressure was above 1 atmosphere, S_8 was opened. The H_2 line pressure was adjusted to give 800c.c./min. as measured on the flow meter.

(7) Liquid N_2 was added to the activated charcoal and cold traps slowly so as to maintain a positive H_2 pressure.

(8) The furnace was then turned on and the temperature increased in a series of steps;

(a) 250°C. for 1/2 hr.

(b) 350°C. for 1/4 hr.

(c) 500°C. for 1/4 hr.

(d) 950°C. for 1 hr.

Slow heating is recommended (Gallo, 1927) to avoid the formation of free sulfur. The present writer found with this heating procedure and hydrogen flow that little or no free sulfur formed even with 3 grams of initial sulfide.

(9) At the end of the 2 hr. reduction period the furnace temperature was reduced to 750°C. and moved along in a number of steps so as to purify the lead mirror.

(10) When the purified mirror was deposited about 10 cm. from the end of the inner 15 mm. dia. quartz tubing, the furnace was moved away and the mirror cooled. This step was necessary to prevent mirror evaporation when the system was pumped down. The pure lead mirror was grey in color, if not too dense, and exhibited a distinctive "diffraction" pattern.

(11) S_8 was then closed, S_9 opened, and the system pumped down. S_4 was also closed, and S_3 opened.

(12) After several minutes S_2 and S_3 were closed, S_4 opened and hydrogen admitted through leak #2. The H_2 line pressure was adjusted to give 1 cm. Hg pressure in

the system.

(13) The furnace was then moved over the mirror redistilling it for the last time. This step was not always necessary but gave the most consistent results since it tended to separate the mirror components out more completely. The lead mirror converted from the distinctive grey to a dark black deposit.

(14) The furnace was moved back 4 cm. and the mirror cooled before S_4 was closed and the system pumped down. The water spray was adjusted to cool the region between the furnace and mirror but not the mirror directly. The mirror must be maintained at room temperature: if it is too hot its rate of removal will decrease; if too cold it could be deactivated by deposition of the higher boiling point compounds that result in the decomposition of the di-t-butyl peroxide.

(15) Liquid N_2 was placed around the main cold trap.

(16) When the mirror had cooled sufficiently S_5 was closed, and S_6 opened. Di-t-butyl peroxide passed into the system at 1 mm. Hg. This was left on from 1 to 4 minutes, until the mirror was removed.

(17) S_7 and S_6 were then closed. Since tetramethyllead will decompose at 90-110°C., the furnace and tubing must be cooled down.

(18) S_9 was closed, and the sample transferred to the breakseal and sealed off. Step III, the separation by vacuum distillation, was completed on the mass spectrometer where the process could be monitored.

1.3.2 The Purification of Tetramethyllead

The approach to this problem has been guided by three somewhat competing factors:

(1) The tetramethyllead should, for high precision isotope abundance measurements, be separated to a fairly high degree of purity from the other reaction products.

(2) The purification procedure must be such that the lead loss is not significant. This problem is of most importance in the present work, where the sample size is several orders of magnitude smaller than in the normal runs.

(3) If the sample line pressure drops much below the 0.9 cm. Hg range the flow characteristics tend toward the molecular, and considerable fractionation can occur. For this reason the small samples cannot be wholly purified, or if they are, they should be mixed with a carrier.

Gas chromatographic separation has been used for the large Grignard-prepared samples and to some extent for small samples (Ulrych, 1960, 1962). Although these techniques can result in significant lead loss when dealing with the smaller samples, modifications that will overcome

this difficulty may be possible (Abel, Nickless, and Pollard, 1960; Parker, Smith, and Hudson, 1961; and Dawson Jr., 1963).

At any rate, vacuum distillation seems to be sufficient for the present technique provided the methyl radical source is first carefully purified. This type of separation has been shown to result in sample purity comparable to that achieved with the usual chromatographic techniques and the loss rate can be more carefully controlled. All the small samples in this work were purified by vacuum distillation. The distillations were carried out at dry ice temperatures, the length of the distillation depending upon sample size.

The results of several pumping experiments are illustrated in Diagram (1.5). While there is a considerable spread two general features are apparent.

(1) The rate of lead loss is roughly proportional to the amount of lead present. This suggests that the surface area of the frozen-down tetramethyllead is not too dependent upon sample size.

(2) The rate of lead loss is not zero as the sample size goes to zero; e.g. below a certain size the above "masking" effect does not occur. If we assume that the loss rate will be the maximum shown, 400 micrograms per hour, a sample of 30 micrograms can be distilled for only 0.5 to 1.0 minutes. This assumes a 10% lead loss. These

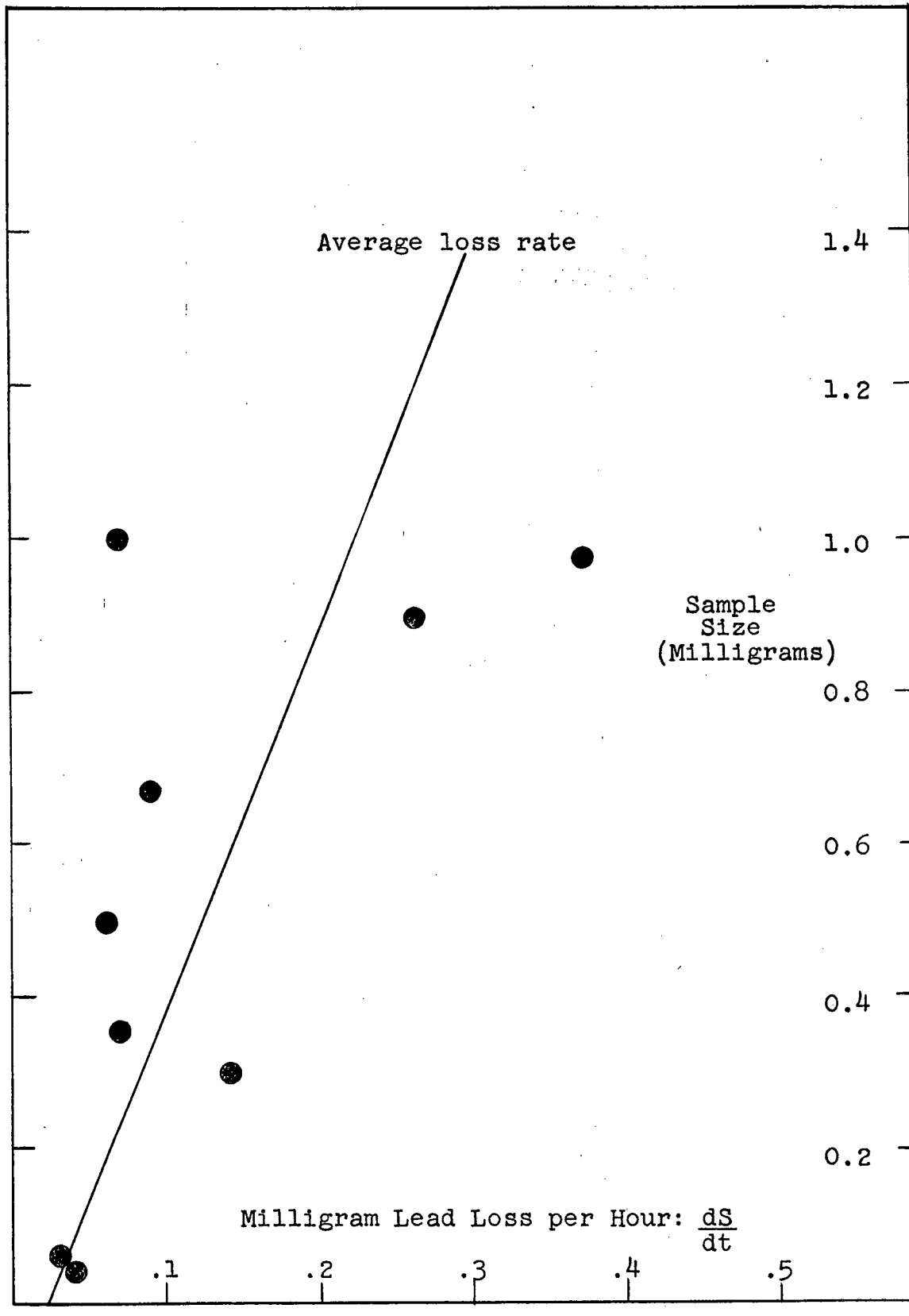

Diagram 1.5. Rate of Tetramethyllead Loss During Vacuum Distillation at Dry Ice Temperatures

times were used in partially purifying the smallest samples although this meant that the operating pressures were 3 to 5 times higher than normally used. The present writer's improved pressure scattering correction compensated for this to a certain extent. As it turned out, such samples could only be run at 1/20 of the normal peak height with a corresponding decrease in mass spectrometer precision, so the pressure scattering correction is not as important as with the large samples.

Actually, the above estimates are quite pessimistic and longer distillation times probably could have been used. A more sophisticated treatment is also possible; for example, Diagram (1.5) suggests that:

$$S = -m \frac{dS}{dt} + b$$

therefore $$\frac{S_o - S}{S_o} = x = \frac{(S_o - b)(1 - e^{-t_x/m})}{S_o}$$

or $$t_x = m \ln \left[\frac{S_o - b}{S_o(1-x) - b} \right]$$

where m = slope of average loss rate

b = intercept

t_x = time of distillation required for a x% sample loss

S_o = initial sample loss

If the rate of loss relations were more exactly known, t_x could be calculated quite closely.

1.3.3 Estimation of Lead Content of Samples

(1) During the development of the micro-lead

technique several carefully weighed samples (22±2 to 1574±2 micrograms of reagent PbS) were studied. It was found that the lengths of the lead mirrors were directly related to size provided that the H_2 flow conditions were maintained identically during reduction (Diagram 1.6). This relationship was used in deciding the maximum time of distillation that could be tolerated; it also gives an estimate of the ppm. lead content in a natural mineral sample.

(2) A more accurate estimate was obtained by comparing the mass spectrometer ion beam intensities of the samples to those of 2 precisely weighed reagent PbS samples (22±2, 76±2 micrograms). By knowing the initial sulfide weight the ppm. lead content can be calculated; these values are listed with the isotopic analyses.

1.3.4 Yields

1. Estimation of yields

The yields were not measured analytically; however, an estimate can be obtained by considering probable losses at each step.

(1) Reduction of sulfide. For such minerals as chalcopyrite or pentlandite, which reduced completely to molten alloys, it is assumed that all but a negligible portion of the lead in the sample is removed during the two hours of reduction. All of the small samples analysed

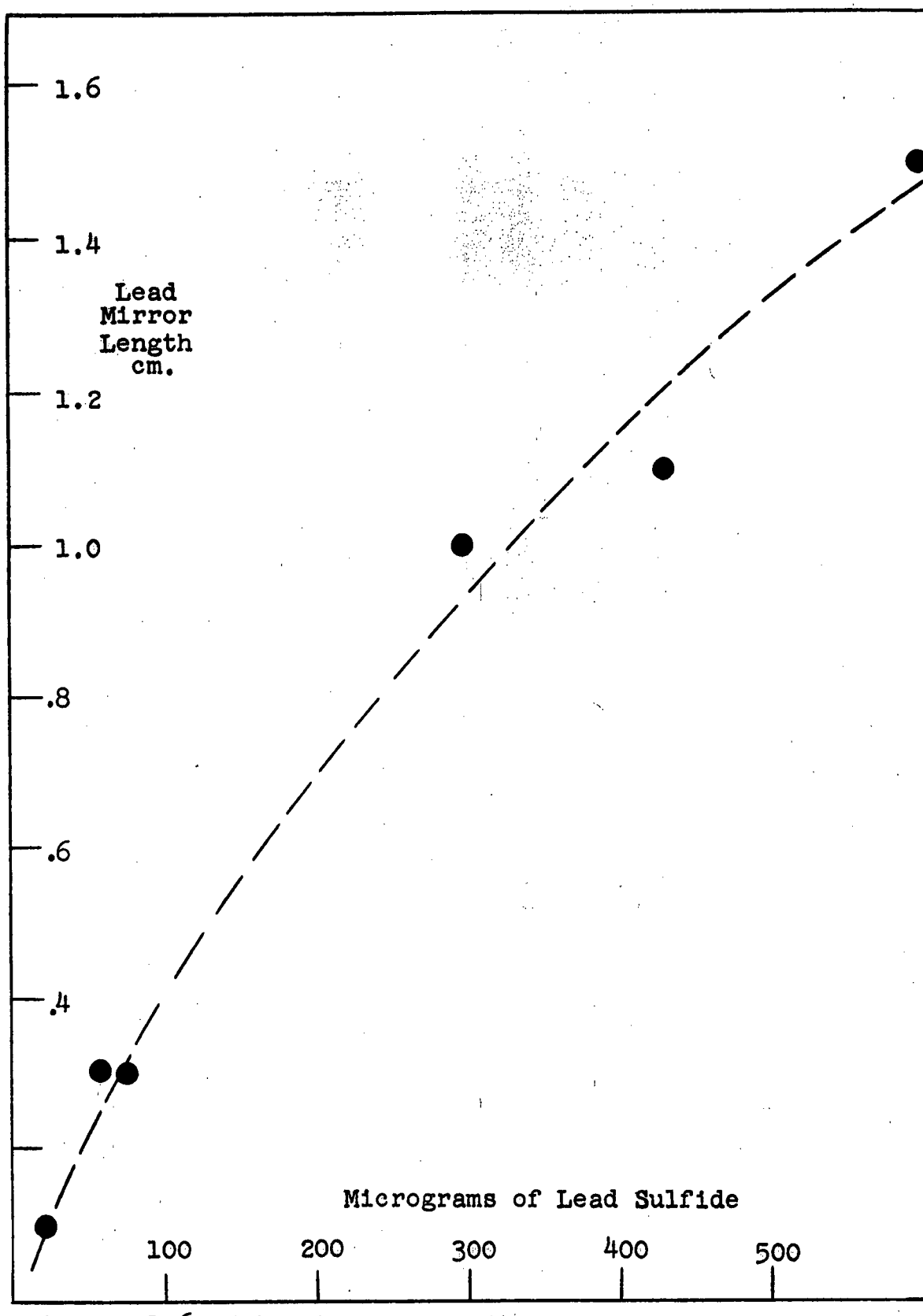

Diagram 1.6. Estimation of Lead Content From Mirror Size

in this work were of this type.

(2) Moving and Purifying the Mirror. One reagent PbS sample of 22±2 micrograms was moved four times. Since 10 micrograms represents the limit of visibility under these conditions the loss at each step could not have been more than about 2 micrograms. As samples are normally re-distilled 6 times, this would represent a maximum 12% loss for a sample of 100 micrograms.

(3) Removal of the Mirror. The removal of the mirrors of several precisely weighed PbS samples ranging from 22±2 to 976±2 micrograms was observed to be visually total. This would represent a maximum 10 microgram loss.

(4) Trapping of the tetramethyllead and by-products. All the condensible material produced in the preparations appeared to be trapped in the first 3 cm. of the specially constructed cold trap, some 21 cm. from the exit to the pump. A maximum loss of 5% does not seem unreasonable.

(5) Transferring to the breakseal tube, and from the breakseal into the mass spectrometer. A number of the small samples were transferred in the mass spectrometer to and from the attached breakseal tube. The loss must have been less than 10% and probably less than 5%.

(6) Distillation losses. The distillation times corresponded to a maximum loss of 10%.

For a sample of about 100 micrograms the yield probably would be better than 60%.

2. The effect of the silicate $xPbO \cdot SiO_2$

A more important question concerned the silicate $xPbO \cdot SiO_2$ which formed if the lead mirror was allowed to oxidize. Its effect was quite variable but appeared to become increasingly serious as the sample size decreased. This is perhaps to be expected since the underlying pure lead would tend to mask the quartz surface from the PbO surface layer. Tests showed that 80% of the small samples (<100 micrograms) could be so lost, compared to 60% for samples of 500-1000 micrograms. Since this represents a significant decrease in the possible yield, the silicate cannot be allowed to form.

1.3.5 Limits of the Micro-lead Technique

Surkan (1956) notes that a good isotope analysis can be carried out with 10 milligrams (10,000 micrograms) of lead using standard techniques, although the equipment and procedure become quite elaborate. It is generally agreed that routine analyses require from 50-150 milligrams for the most precise results.

Surkan, using a free radical technique, was able to obtain sufficiently intense ion beams from about 500 micrograms of lead; he was, however, troubled by the presence of contaminants having mass fragments in the trimethyllead

range. Ulrych (1962) did not extend this lower limit significantly but was able to eliminate the formation of contaminants and carry the process through from mineral to isotope ratios, applying the technique for the first time in a study of a geologically significant suite of samples.

The development of the micro-lead technique has allowed the present writer to extend the preparation of tetramethyllead to samples containing 1 or 2 orders of magnitude less lead than has previously been possible. Unfortunately, the present mass spectrometer facilities limit the most precise analyses (isotope ratios to ± 0.05%) to 500-1000 micrograms of lead. Samples of 20-30 micrograms, prepared with the present writer's technique, have been run with fair precision (0.4%). This represents the practical limit and corresponds to a sample lead content of 10 ppm. with the present apparatus. One isotopic analysis was obtained from a sulfide, of an ultrabasic stock near Hope B.C., which appears to have only 1-2 ppm. lead (3 micrograms). Although the precision is not sufficient for interpretation, because of the low ion signal amplitude, the results are comparable to those expected for the deposit.

The use of larger micro-lead apparatus and multiple runs could reduce the 10 ppm. routine limit to samples containing only 1 ppm. lead. An improvement in the gas source mass spectrometer sensitivity might well extend the analyses to the 0.1-1 ppm. lead range, or lower.

1.3.6 Contamination

1. Lead Contamination

(1) Lead contamination encountered in the micro-lead preparation. One sample (Hope #478) had a very low lead content and was inadvertently in the nature of a "dry" run. If we assume all the lead (above the mass spectrometer background) was picked up in the micro-lead preparation the maximum contamination would be 0.2% for the smallest samples and 0.01% for those of normal sensitivity (500-10000 micrograms).

(2) Contamination between sample lines. Some of the larger samples were compared, using a dual inlet system, to a standard. Tests showed that the cross contamination, in the mass spectrometer, must have been less than 0.01%.

2. Other Contaminants

(1) Samples of the di-t-butyl peroxide source used in this work were examined on the mass spectrometer to determine if this source contained impurities, or had decomposition products, that might have mass fragments in the trimethyllead range. No mass fragments above mass 146 could be detected.

(2) Kanasewich (1962a), Slawson and Russell (1962) reported that a contaminant could form in the Grignard process used to convert galenas to tetramethyllead. This contaminant appeared to be similar to the siloxane

tetrameter $\left[SiO(CH_3)_2\right]$-, with the substitution of two carbon atoms for two silicon atoms. This would give a molecule of mass 264 so the removal of one methyl group would result in a fragment of mass 249. Estimation of the relative lead 204 abundance would thus be in error. This contaminant occured only with galenas of certain deposits and was attributed to the reaction of silicon stopcock grease (triggered by some trace material in the samples) with the Grignard solutions. The formation of this contaminant was avoided by eliminating the use of silicon stopcock greases.

A similar, although unidentified, contaminant formed under certain conditions during the micro-lead preparation. It had a noticeable effect on the 204 lead abundance of the larger samples and a drastic effect on that of the smallest. The contaminent was characterized by three small equally sized peaks in the 280 mass range and as a series of peaks at every mass between 240 and 248. Peaks of masses 249 and 250 were also apparent. The lead isotope ratios of one large (1000 micrograms) sample were found to be 0.6% less than the uncontaminated values when first run, and 0.9% less when the same sample was run a second time. The effect on a small sample of about 10 ppm. lead was much more pronounced; the presence of the contaminant resulted in a 3.6% isotope ratio decrease.

The contaminant was believed to have resulted from

the use of HF in the cleaning procedure. It was possible that the free silicon (from the quartz), or a silicon-fluorine-oxygen compound, may have resulted in the cleaning procedure. The free methyl radicals in contact with the mirror quartz could then have reacted to form the contaminant.

If the apparatus (after cleaning) was baked in a stream of oxygen at 950°C. the contaminent did not form.

1.4 Summary

None of the earlier experimental schemes for obtaining suitably reactive lead mirrors have proven entirely satisfactory since they were developed without the knowledge that PbO can react with SiO_2, and that a significant part of the lead of a sample could be lost through the formation of $xPbO \cdot SiO_2$. The present writer's technique was designed to avoid the formation of this compound.

Once the reactive lead mirror is inside the micro-lead apparatus, tetramethyllead is produced by the decomposition of a suitable methyl radical source. The present writer undertook a systematic survey of 45 methyl radical sources. Several were chosen and investigated experimentally; of these, di-t-butyl peroxide seems to be the most suitable provided it is first carefully purified.

The final step of the micro-lead technique involves the separation of the tetramethyllead from the decomposition products of the organic source material. Gas chromatographic purification has been used in the standard preparation of samples but the present writer's work suggests that it cannot be applied in its present form for samples containing much less than a 1000 micrograms of lead. Vacuum distillation has been found to be a simpler procedure and allows one to control the lead loss more exactly. Larger samples containing 500 or more micrograms of lead can be purified to the degree that chromatographic techniques are capable of, provided that the methyl radical source (di-t-butyl peroxide) is initially pure. With the smaller samples (<100 micrograms of lead) the loss rate is too high even with vacuum distillation to allow a high degree of purity; however, this is not important since at this level the mass spectrometer precision is only 0.4%. In addition, the mass spectrometer sample line pressure must be kept above about 1.0 cm. Hg (corresponding to a minimum of 300-500 micrograms of lead) or isotopic fractionation will occur. On this basis, highly pure small samples are not only unnecessary, but also, undesirable.

The development of the micro-lead technique has allowed the present writer to extend the tetramethyllead preparation to samples containing one to two orders less lead than the 500 to 1000 micrograms reported earlier.

Chapter 2: GAS SOURCE MASS SPECTROMETRY OF MICROGRAM TETRAMETHYLLEAD SAMPLES.

"The test of all knowledge is experiment. Experiment is the sole judge of scientific 'truth'."
-R.P. Feynman in Lectures on Physics

2.0 Introduction

The present writer has explored the mass spectrometric aspects of analysing small tetramethyllead samples, a topic about which little was known. Two main features had to be investigated.

Firstly, the possibility of molecular fractionation (although not previously reported for lead isotopes) had to be considered if the sample size, and hence its pressure in the sample line, was decreased below that necessary for viscous flow.

Secondly, a better understanding of pressure scattering - the scattering of trimethyllead ions during their passage through the mass spectrometer - was required since the low ion signal amplitude of the small samples did not permit the usual tailing corrections to be made directly from measurements of the spectrum.

The experimental studies of these features are discussed in the following sections.

2.1 Lead Isotope Fractionation

Fractionation can occur if a gas sample is introduced into the source region through a constriction - e.g. a "leak". The possibility of fractionation depends mainly upon the size of this leak in relation to the pressure of the gas in the sample line. If the pressure is high so that the mean free path of molecules in the gas is small compared to the dimensions of the leak, the leak is called "viscous". If the pressure is low enough, and the mean free path large, the leak will be "molecular". With a viscous leak, the gas will not be fractionated in passing from the sample line into the source, provided there is sufficient mass flow through the leak so that no back diffusion can occur (Nier, 1947). On the other hand, molecular flow will cause isotopic fractionation.

To evaluate the total fractionation we must consider the combined effects of flow through the leak and flow out of the source region of the mass spectrometer:

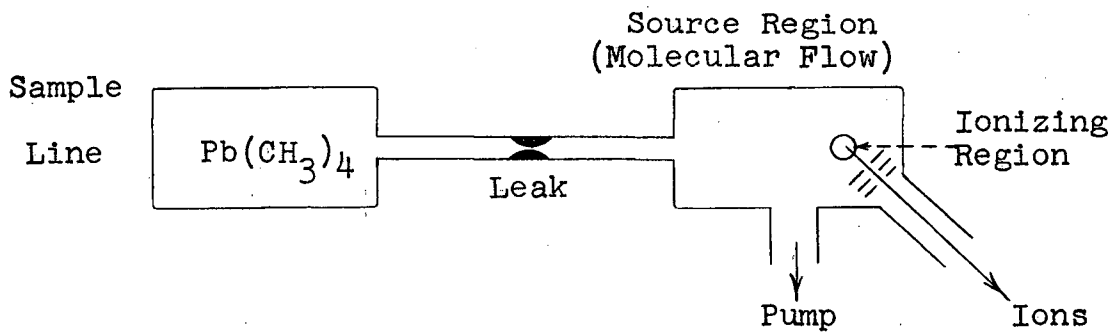

Since the pressure in the mass spectrometer is low (10^{-4} to 10^{-6} mm. Hg) the mean free paths of the gas molecules will be large compared to the dimensions in the source region and connecting tubing; the flow will thus be molecular (Halsted and Nier, 1950; Kistemaker, 1953). We have two possible cases.

1. Viscous Flow in the Leak

If one assumes viscous flow through the leak, and molecular flow from the source it is possible to show that the isotope ratios of source and sample line are different (Halsted and Nier, 1950):

$$\left[\frac{I_1}{I_2}\right]_m \cong \sqrt{\frac{M_1}{M_2}}\left[\frac{P_1}{P_2}\right]_S \qquad (2.1)$$

where I_i = ion beam intensity of isotope i

M_i = mass of isotope i

P_i = partial pressure of isotope i in the sample line (proportional to its abundance in the sample.)

$\left[\frac{I_1}{I_2}\right]_m$ = measured isotope ratios in the source region

$\left[\frac{P_1}{P_2}\right]_s$ = isotope ratio of sample in the sample line.

Halsted and Nier showed that equation (2.1) applied at least for argon - nitrogen, and also HD - H_2 mixtures. Kistemaker (1953) obtained similar results with the oxygen isotopes.

In the case of the lead isotopes, lead-204 will be exhausted preferentially from the source region and the isotope ratios measured in the source will be larger than those in the sample line:

$$\left[\frac{Pb^{206}}{Pb^{204}}\right]_m \cong \sqrt{\frac{266}{264}}\left[\frac{Pb^{206}}{Pb^{204}}\right]_s$$

$$\cong (1.004)\left[\frac{Pb^{206}}{Pb^{204}}\right]_s \qquad (2.2)$$

$$\left[\frac{Pb^{207}}{Pb^{204}}\right]_m \cong (1.006)\left[\frac{Pb^{207}}{Pb^{204}}\right]_s \qquad (2.3)$$

$$\left[\frac{Pb^{208}}{Pb^{204}}\right]_m \cong (1.008)\left[\frac{Pb^{208}}{Pb^{204}}\right]_s \qquad (2.4)$$

These expressions assume that the lead is in tetramethyllead form. If there is sufficient mass flow through the viscous leak the difference between source and sample ratios is constant and does not change with sample depletion. This is not true if the flow through the leak is molecular.

2. Molecular Flow Through the Leak.

The fractionation of a molecular leak will be counteracted by that resulting with flow out of the source, and the isotope ratios of source and sample line will be equal (Halsted and Nier, 1950):

$$\left[\frac{I_1}{I_2}\right]_m \cong \left[\frac{P_1}{P_2}\right]_s \qquad (2.5)$$

In this case, however, the isotope ratios in the sample line will increase as the sample is depleted (Lead-204

will be depleted preferentially).

2.1.1 Viscous Flow: Experimental Results

On the present mass spectrometer the leaks are approximately 0.004 cm. diameter. These leaks were believed to be viscous (Kollar, 1960) over the sample line pressure range at which the analyses were normally carried out (0.9 to 1.6 cm. Hg). This was substantiated by the reproducibility obtained by Ostic (1963). The analyses of J.T. Ulrych (personal communication) showed that this result applied equally well to small samples that were depleted significantly during an analysis (Table 2.1). The variations in isotope ratios between A and B runs were no greater than those obtained with the large samples; hence, it may be concluded that there is sufficient mass flow through the leak, and that the lead isotope ratios in the sample line do not change if the flow is viscous.

2.1.2 Molecular Flow: Theoretical Results

The equation for isotopic fractionation with a molecular leak was derived by the present writer in Appendix A.1:

$$\frac{R}{R_o} \simeq \left[\frac{1}{1-F}\right]^{\sqrt{\frac{M_1}{M_2}}-1} \qquad (2.6)$$

where F = depletion = $(P_o-P)/P_o$

P = total sample pressure at depletion F

P_o = initial total sample pressure

R_o = initial isotope ratio

Table 2.1 Reproducibility of Lead Isotope Ratios under Viscous Flow Conditions (Ulrych, personal communication).

Sample Number	Run	$\frac{Pb(206)}{Pb(204)}$	$\frac{Pb(207)}{Pb(204)}$	$\frac{Pb(208)}{Pb(204)}$	Initial Sample Line Pressure (cm. Hg) ⧫	Maximum Total Depletion ⧫⧫
2	A	15.013	14.905	36.262	1.5	.095
	B	14.990	14.862	35.203	1.5	.277
4	A	14.902	14.866	35.151	1.6	.079
	B	14.911	14.874	35.184	1.9	.321
6	A	14.804	14.909	35.037	1.7	.139
	B	14.785	14.880	34.990	1.9	.430
21	A	15.730	15.179	35.802	1.5	.026
	B	15.728	15.170	35.790	1.4	.075

⧫ The initial sample line pressure can be obtained by direct measurement, or by relating the sample line pressure to the mass spectrometer vacuum gauge pressure.

⧫⧫ Determined from the ion beam intensity decrease during an analysis:

$$= \frac{I_o - I}{I_o}$$

where I_o = ion beam intensity at beginning of analysis.

I = ion beam intensity at end of analysis.

R = isotope ratio of a sample with a total depletion F.

M_i = molecular weight of isotopic species i.

The ratio R/R_o has been computed for Pb^{206}/Pb^{204}, Pb^{207}/Pb^{204} and Pb^{208}/Pb^{204} for a given depletion (Diagrams 2.1, 2.2, 2.3). This calculation assumes that the lead is in tetramethyllead form.

From these diagrams one can construct the relations expected between viscous flow isotope ratios and molecular flow ratios at various stages of depletion. These are given in Diagrams (2.4) and (2.5). If the flow is changed from viscous to molecular, the lead isotope ratios drop from those of equations (2.2), (2.3), and (2.4) to those represented by equation (2.5). Then as the sample is depleted its ratios will increase (Pb-204 being depleted preferentially) along the curve shown. These calculations correspond closely to the observed results.

2.1.3 Molecular Flow: Experimental Results

Several small samples, from the Sullivan base metal deposit, were analysed by the present writer at pressures of less than 1 cm. Hg (Table 2.2, Diagrams 2.6 and 2.7). The lead in this deposit appears to be primary and the samples are assumed to have identical isotope ratios; this has proven to be correct for the four samples (320, 321, 323, 324A) analysed under viscous flow conditions.

Samples 321 and 323 were large samples prepared by

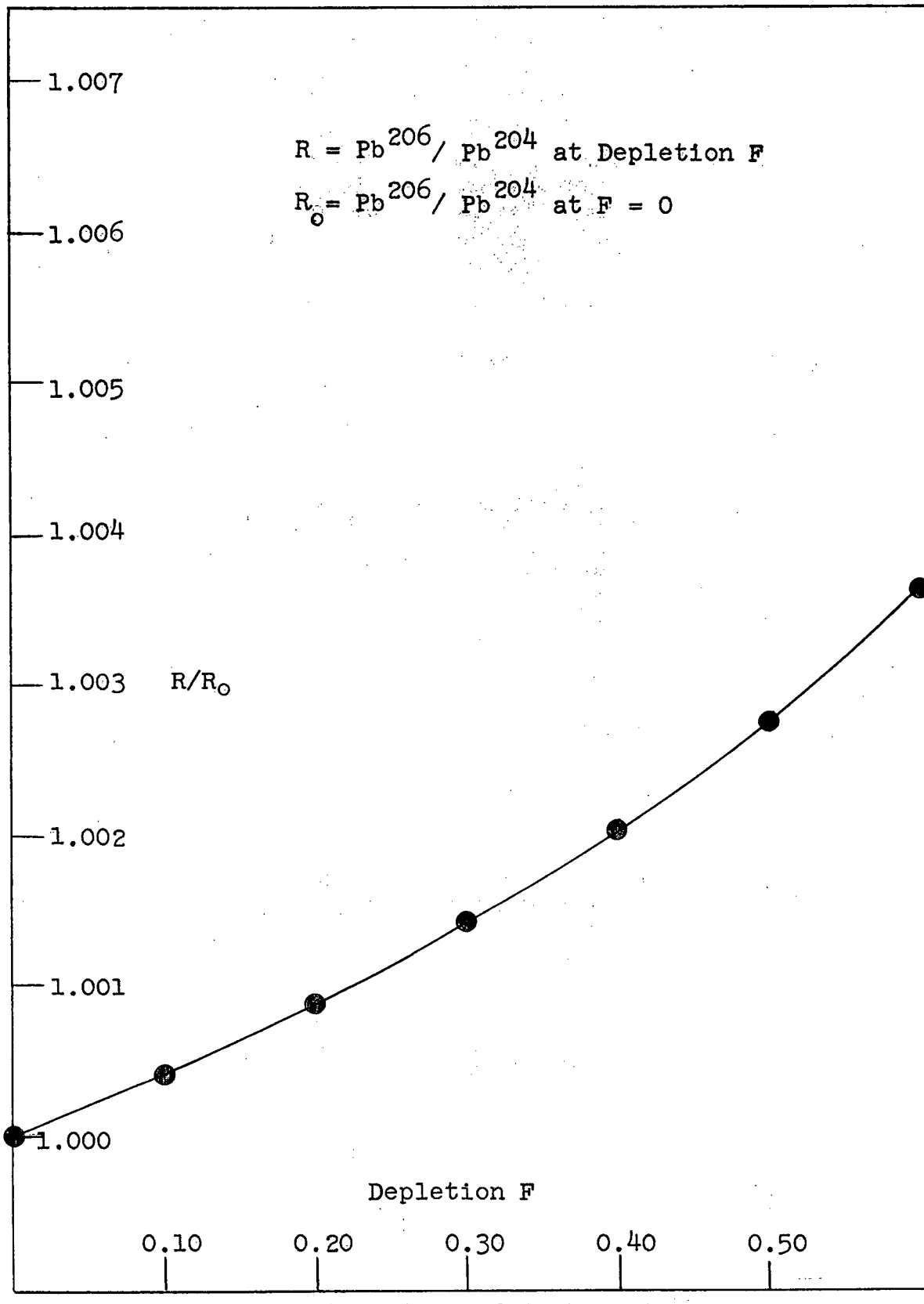

Diagram 2.1.Molecular Flow Model.Theoretical Change of Lead Isotope Ratios with Sample Depletion:I.

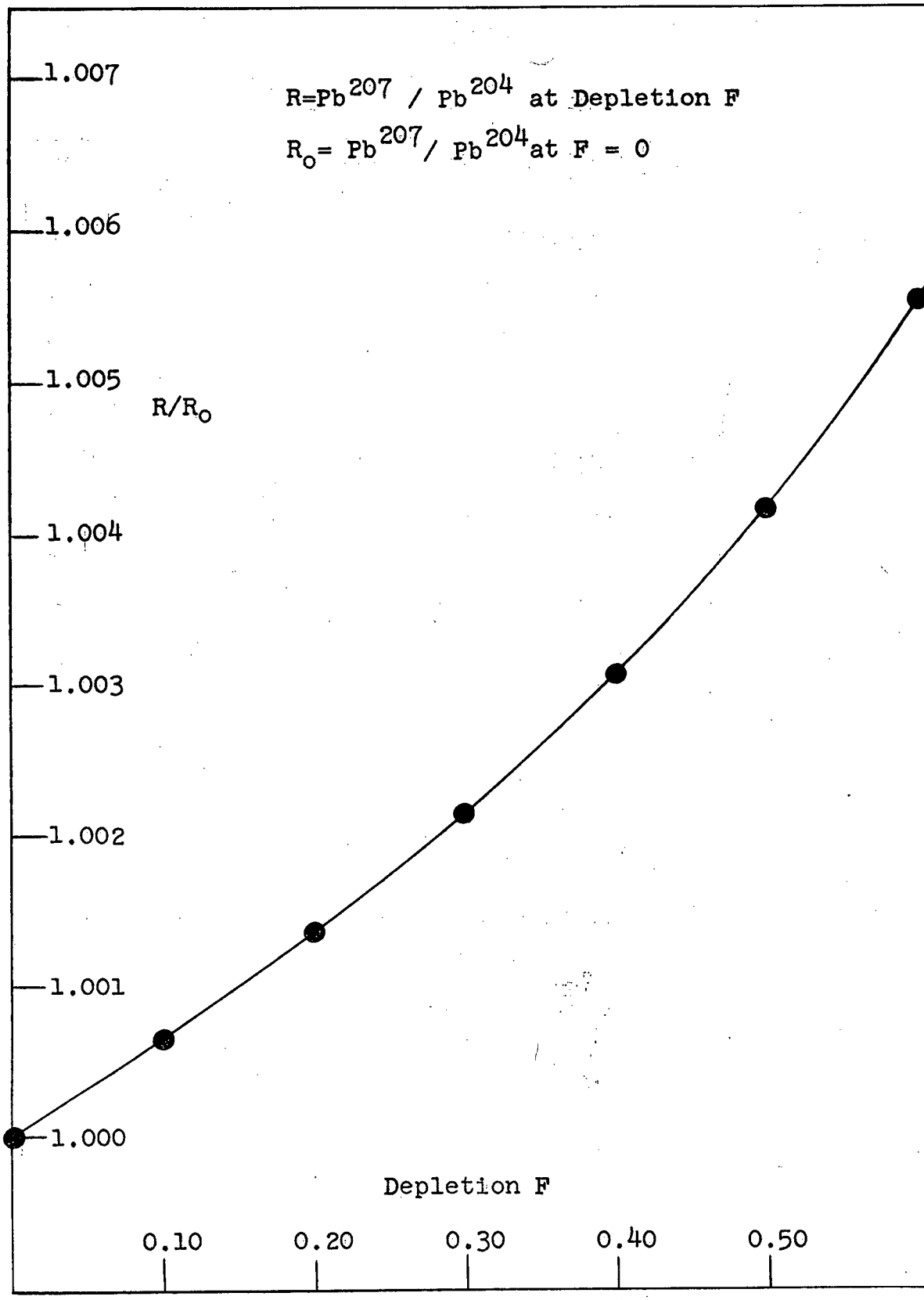

Diagram 2.2. Molecular Flow Model. Theoretical Change of Lead Isotope Ratios with Sample Depletion:II.

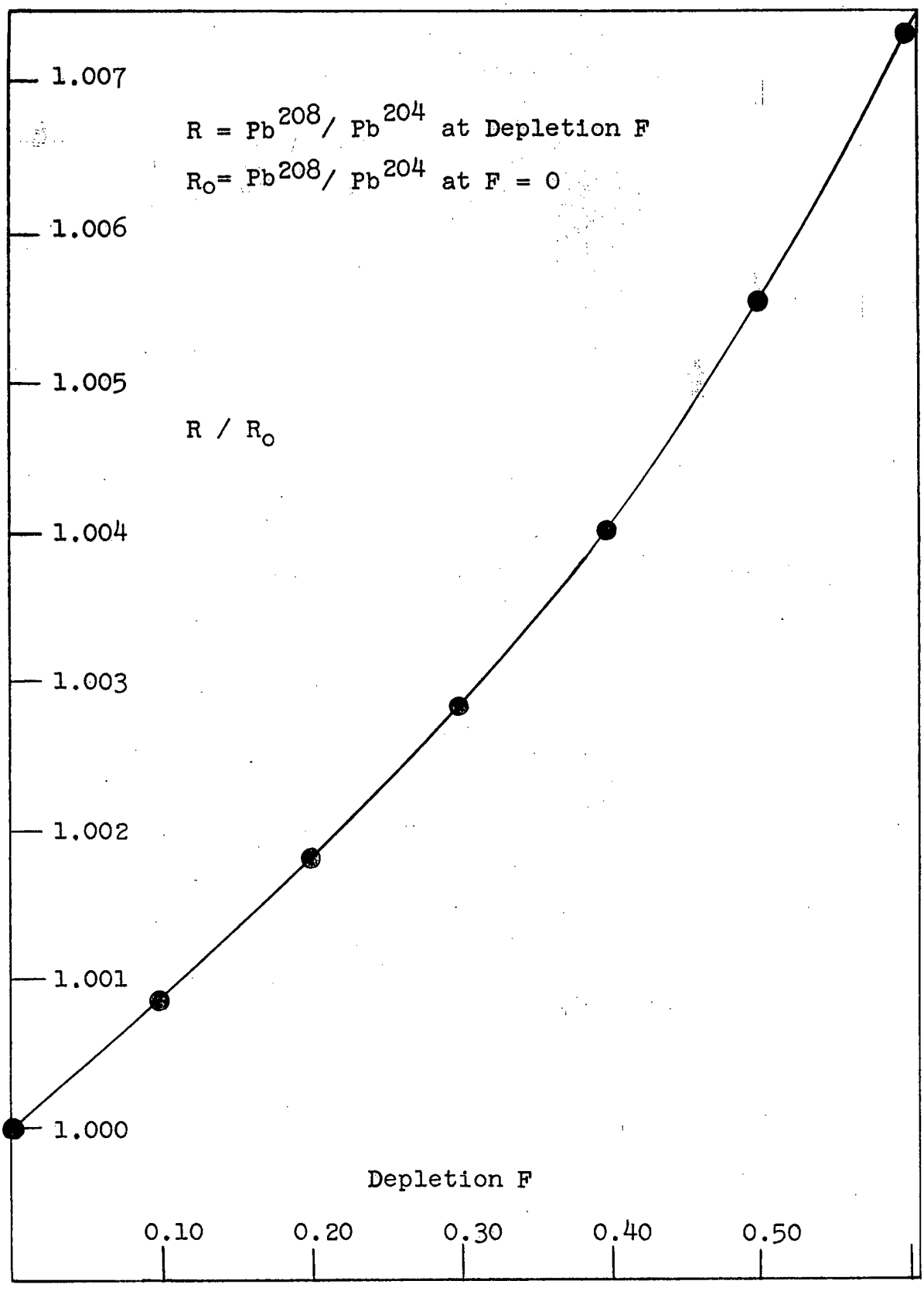

Diagram 2.3.Molecular Flow Model. Theoretical Change of Lead Isotope Ratios with Sample Depletion:III.

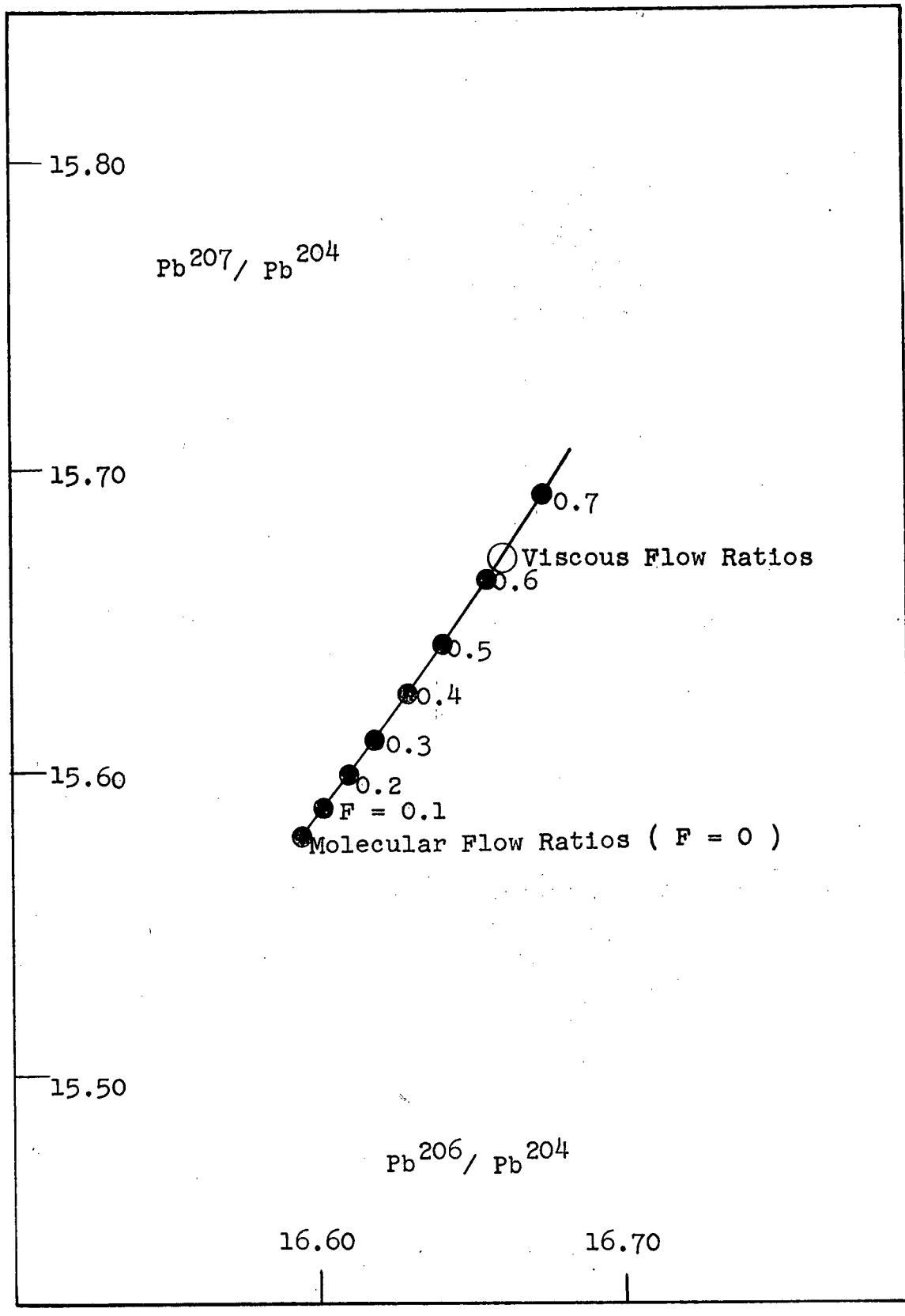

Diagram 2.4. Theoretical Flow Model. Viscous Flow and Molecular Flow at Various Depletions:I.

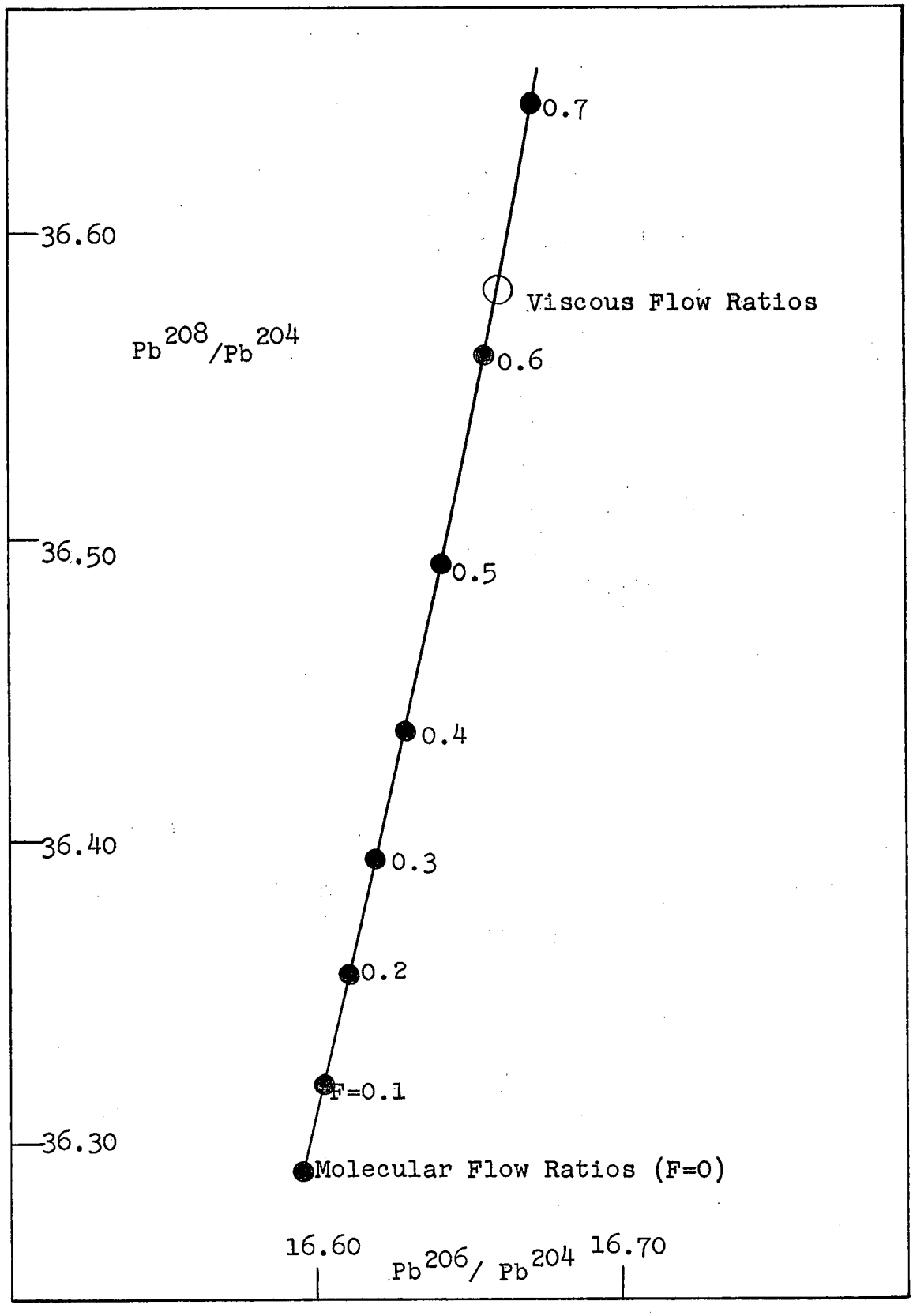

Diagram 2.5. Theoretical Flow Models .Viscous Flow and Molecular Flow at Various Depletions:II.

Table 2.2 The measured Lead Isotope Effects of Molecular Flow on Small Samples

Sample	Analyses	Sample Line Pressure * (cm. Hg)	Type of Flow	Max. Total Depletion *	$\frac{Pb(206)}{Pb(204)}$	$\frac{Pb(207)}{Pb(204)}$	$\frac{Pb(208)}{Pb(204)}$
Sullivan 324	A	3.8	Viscous	.308	16.661	15.670	36.581
	B	.4	Molecular	.792 (.484)**	16.606	15.577	36.414
Sullivan 325	A	.5	Molecular	.104	16.523	15.488	36.210
	B	.8	Molecular	.448	16.622	15.608	36.510
Sullivan 322	A	.7	Molecular	.254	16.582	15.538	36.242
	B	.7	Molecular	.521	16.669	15.678	36.685
Sullivan 320	A	1.0	Viscous	.063	16.645	15.662	36.675
	B	0.9	Viscous	.215	16.635	15.635	36.599

* See Table 2.1

** Depletion under molecular flow conditions.

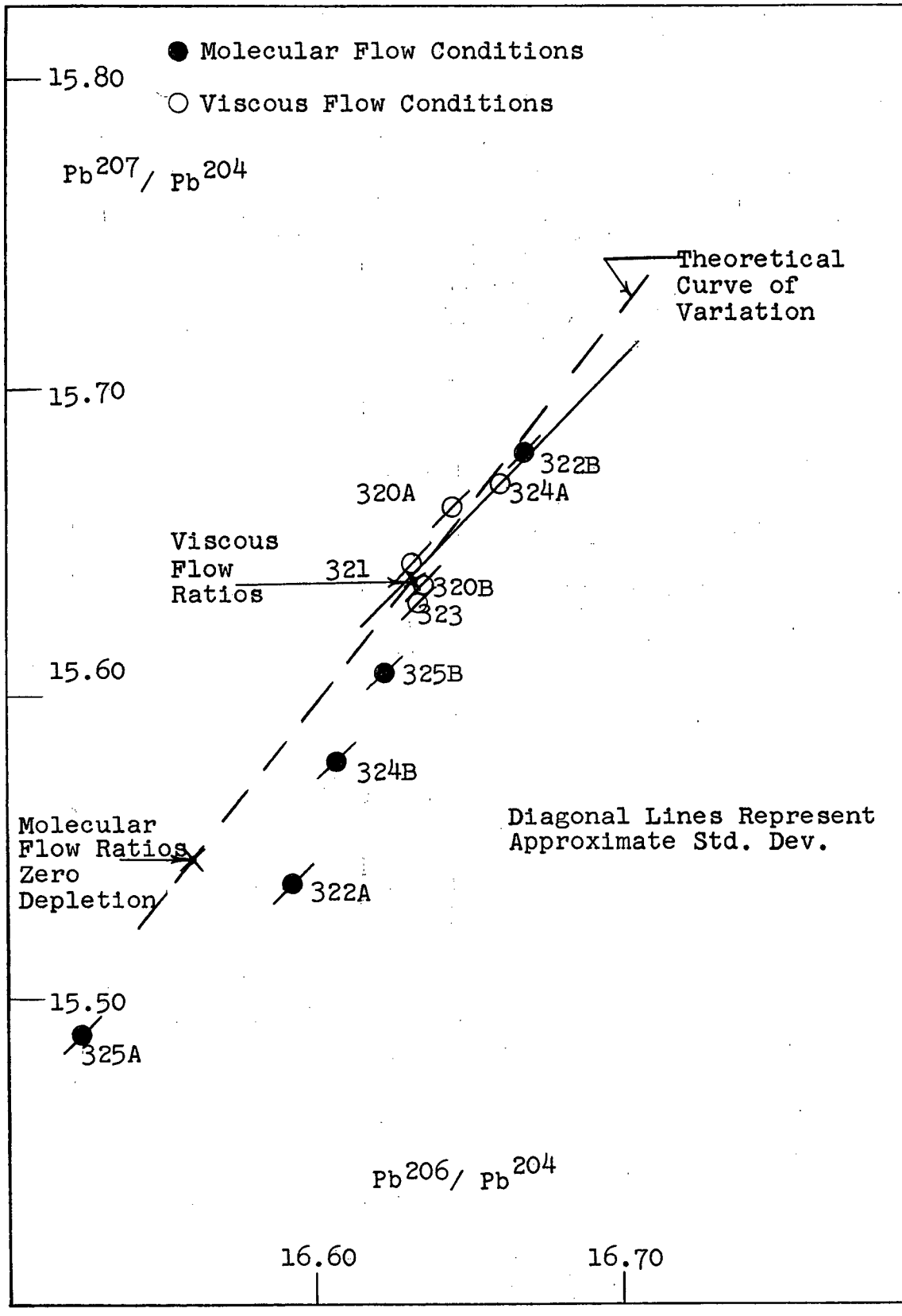

Diagram 2.6.Experimentally Observed Lead Isotope Fractionation at Low Pressures:I.

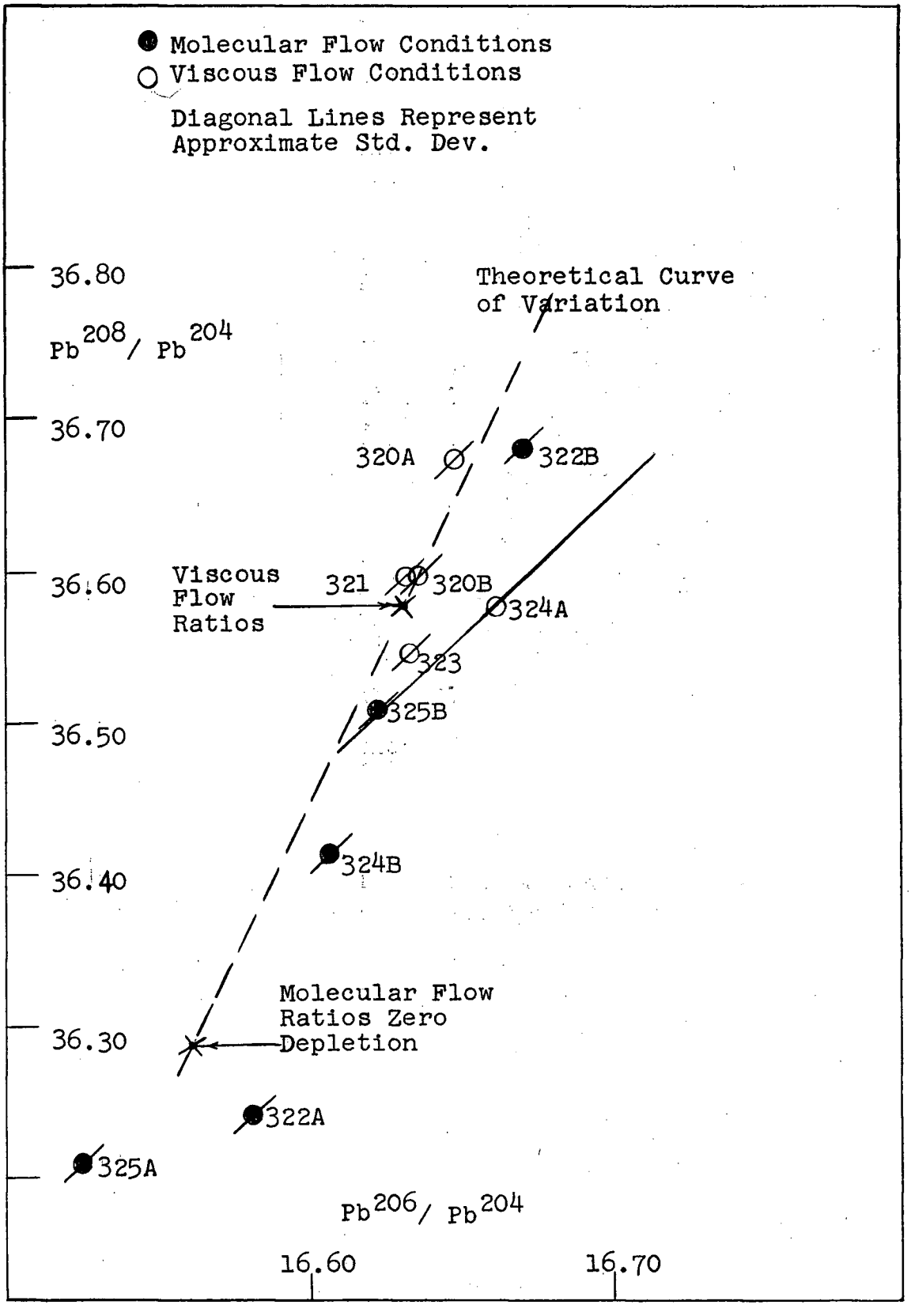

Diagram 2.7. Experimentally Observed Lead Isotope Fractionation at Low Pressures:II.

Grignard reaction and analysed under viscous conditions (A.J. Sinclair - personal communication). The average of these two samples is used as the reference point (Viscous Flow Ratios). Also shown are the expected initial (no depletion) Molecular Flow Ratios, and the curve that would result if the sample were progressively depleted under molecular flow conditions. The small samples lie closely along this curve.

All of the small samples (324, 325, 326, and 320) were prepared by the micro-lead technique. Sample 324 was first analysed at high pressure and low sensitivity (A analysis) then purified and run at a low pressure (B analysis). Since the sample was depleted significantly the B analysis should, and does, lie above the expected molecular flow ratios of 324A. Samples 325 and 326 were not run in the viscous region so the expected molecular flow ratios cannot be computed. These samples do, however, fit the molecular model in that the ratios of the B runs have increased (greater depletion) relative to those of the A runs. Sample 320 was analysed just in the viscous region. The 206/204 and 207/204 ratios do not vary significantly between the A and B runs, and the variation in the 208/204 ratio is only slightly larger than that normally observed (Table 2.1).

It was thus concluded that the molecular flow model adequately describes the observed change of lead isotope

ratios as the sample is depleted, and that no change occurs in the ratios if the flow is viscous. This means that, particularily when analysing small samples, the sample line pressures must not fall below about 1.0 cm. Hg. If the sample is too small (less than approximately 500 micrograms) a carrier of some sort should be added or else the sample should only be partially purified.

The following section describes a simple method devised by the present writer to determine the viscous and molecular regions of a given leak.

2.1.4 Determination of Leak Characteristics

The procedure used to outline the viscous and molecular pressure regions of the present mass spectrometer leaks is similar to, but simpler than, that recommended by Nerkin (1956) who measured the rate of flow into a known volume.

The present experiments involved measuring the pressure of a known volume of tetramethyllead as it decreases with time (e.g. with the depletion of the sample as it is pumped out through the leak). The expected pressure vs. time relationship can be readily derived (Appendix A.1) for the two types of leaks. For a molecular leak, assuming it approximates a long circular pipe:

$$\ln\left[\frac{P_o}{P}\right] = \left[\frac{Cmt}{V}\right] \qquad (2.7)$$

where: P = pressure at time t, in sample line.

P_o = initial sample line pressure.

V = volume of sample line, constant.

and the molecular conductance:

$$Cm = \frac{1}{6}\sqrt{\frac{2\pi kT}{m_o}}\ \frac{D^3}{L}$$

where: D = diameter of a circular pipe

L = length of pipe

T = temperature, °K

k = Boltzmann's constant

m_o = mass of gas molecule

For a viscous leak, and long circular pipe:

$$\frac{1}{P} = \frac{C_V t}{2V} + \frac{1}{P_o} \qquad (2.8)$$

where $PC_V/2$ = viscous conductance C

and $C_V = \frac{\pi D^4}{128nL}$

n = viscosity of gas flowing through the leak.

Within the validity of these models for tetramethyllead it should be possible to distinguish the type of leak by observing the relation of P to t and comparing it to equations (2.7) and (2.8). The results for one of the present mass spectrometer leaks are shown in Diagrams (2.8) and (2.9).

For pressure greater than about 1.0 cm. Hg (e.g. times less than 6 hours) the results indicate viscous flow; that is, they best fit a straight line on the 1/P vs. t plot. Below 0.8 cm. Hg (times greater than 7 hours) the molecular model gives the best fit to a straight line. These results agree, in the main, with those of the preceding section.

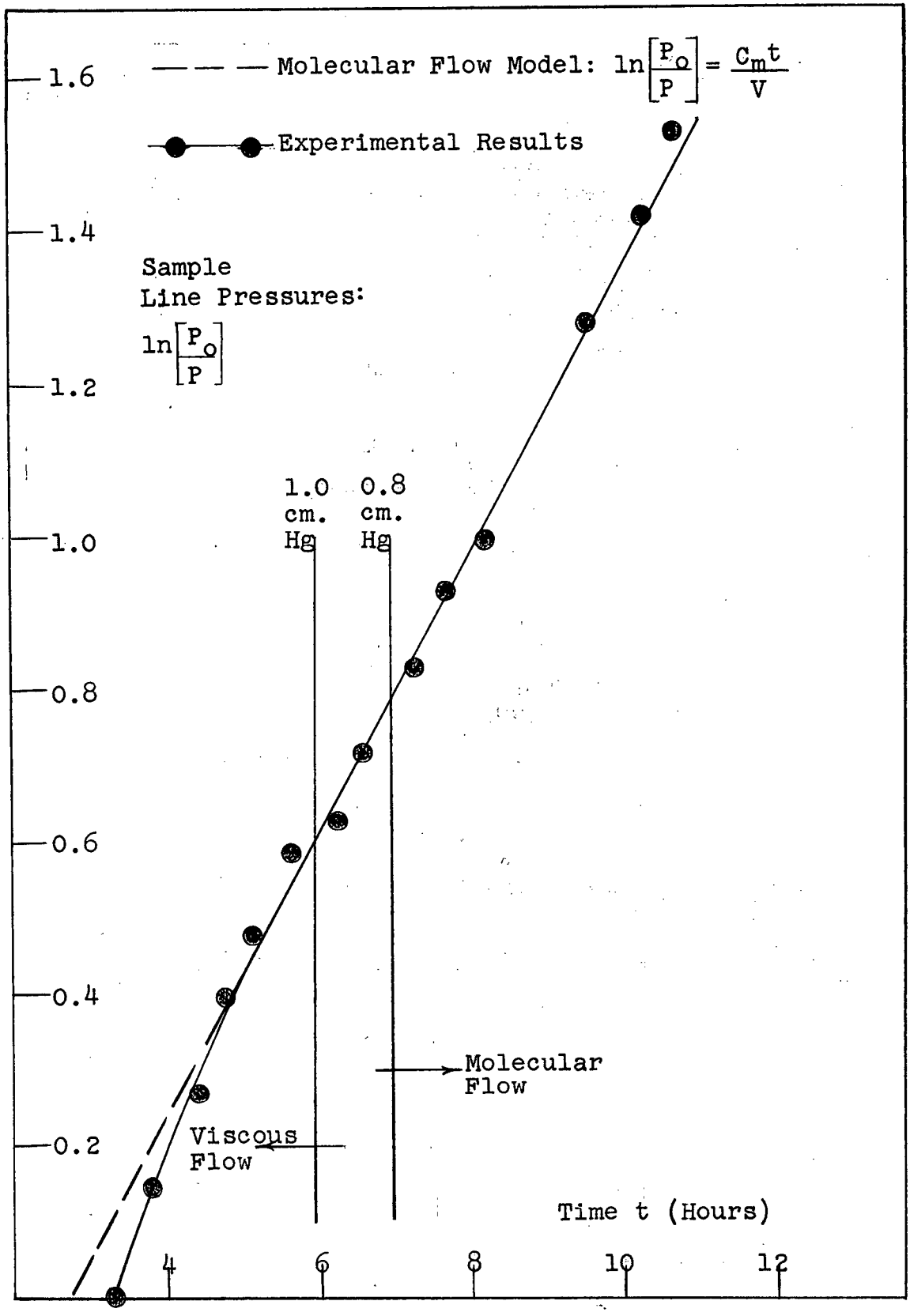

Diagram 2.8. Molecular Flow Model and Leak Characteristics

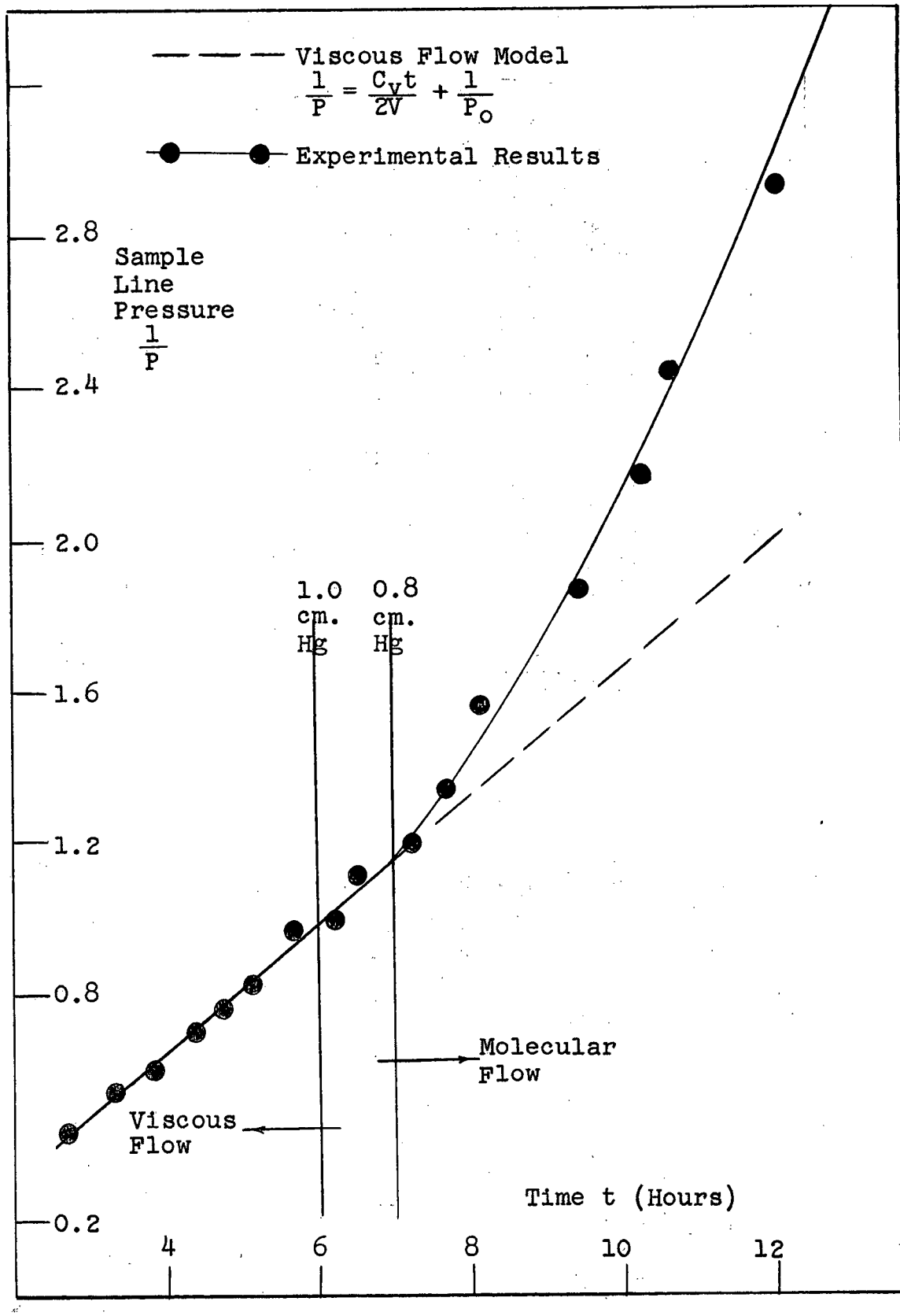

Diagram 2.9.Viscous Flow Model and Leak Characteristics

2.1.5 Intercomparison of Samples

The present work on fractionation also raises an interesting point concerning the intercomparison techniques used in this laboratory. These techniques involve a comparison of a standard (Broken Hill#1) to the sample, and its isotope ratios are then computed in comparison to the assigned ratios of the standard (Ostic, 1963). Hence if we let

$(R_t)_i$ = true isotope ratio a/b, (e.g. partial pressures ratios in sample line) of sample i,

$(R_v)_i$ = measured isotope ratio (viscous leak) of sample i,

then in intercomparing samples A and B we essentially compute the difference

$$(R_v)_A - (R_v)_B$$

Since we really want the true ratio difference

$$(R_t)_A - (R_t)_B$$

and since

$$(R_v)_i = \sqrt{\frac{M_A}{M_B}}\ (R_t)_i$$

then we should compute the difference as

$$(R_t)_A - (R_t)_B = \sqrt{\frac{M_A}{M_B}}\left[(R_v)_A - (R_v)_B\right]$$

although this corresponds to a 0.4% systematic error it does not seem too important at the present time.

2.2 Asymmetrical Pressure Scattering Correction

2.2.1 Empirical Correction

As the trimethyllead ions leave the ion source slit system and pass through the magnetic field to the collector they encounter gas molecules of various kinds that are mostly the result of decomposition reactions in the hot source region, or of impurities in the sample. A portion of the ions in the ion beam are thus scattered from the central beam; this is the main cause of "tailing" in the mass spectrum (Diagram 2.10). Hence measurements, of peaks above a given base line, will be too large by a value depending upon the size of tailings from adjacent peaks. The size of the tailings will depend mainly upon the pressure at which the sample is analysed and the resolution of the mass spectrometer.

Over the past several years investigators in the U.B.C. Geophysical laboratory have developed an empirical method of calculating the tailing values and correcting the measured peak heights (Kollar, 1960; Ostic, 1963). Two basic assumptions were involved:

(1) the tailings were symmetrical; e.g., equal at equal distances on either side of the peak; and,

(2) the tailing was observed only up to two mass units away from the peak.

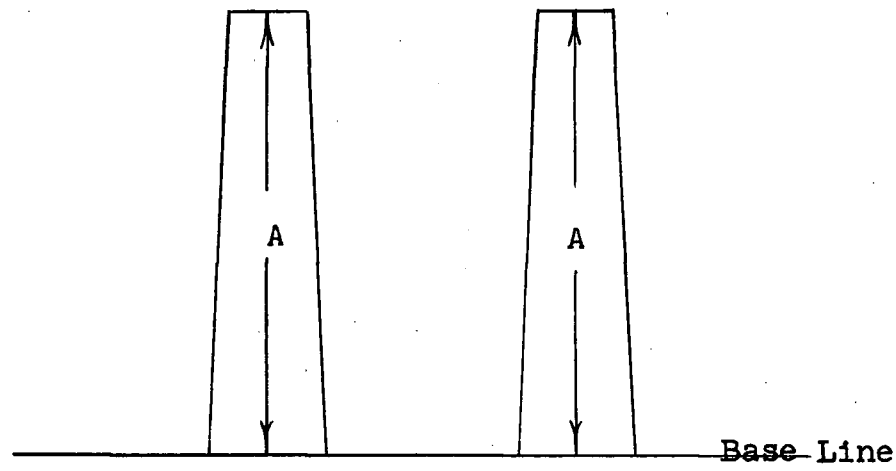

(a) Idealized Spectral Peaks, No Scattering

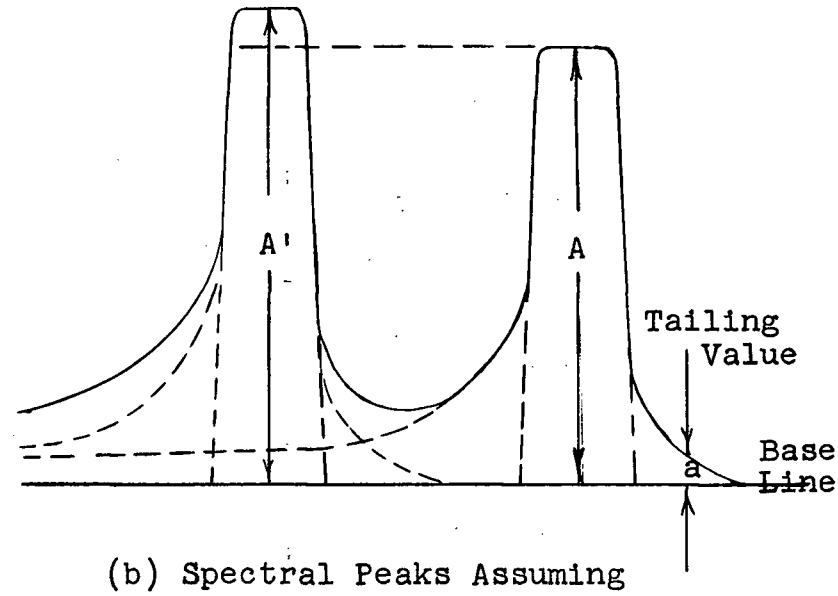

(b) Spectral Peaks Assuming Asymmetrical Pressure Scattering

Diagram 2.10. The Effect of Pressure Scattering on Idealized Spectral Peaks

Some discrepancies in the computations appeared so that the assumptions were not strictly adhered to, and the method of measurement of the tailing coefficients was adjusted to give the best results. This correction was found to be quite satisfactory for the larger column-purified samples analysed at pressures in the order of $1 - 2 \times 10^{-6}$ mm. Hg. Since the present writer had to carry out the analyses with small and relatively impure samples at pressures of $1 - 5 \times 10^{-6}$ mm. Hg, a greater understanding of the scattering had to be obtained.

2.2.2 Experimental Tailing Characteristics in the 250 Mass Range

The basic study of tailing characteristics was carried out using $Bi(CH_3)_3$ since its spectrum is relatively simple, and is in the same mass range as $Pb(CH_3)3^+$. Twenty-one $Bi(CH_3)_3^+$ spectrum were obtained and the tailing values (distance from base line to spectrum= a, in Diagram 2.10) were measured and averaged. "Tailing coefficients" (or "pressure scattering coefficients") were then calculated:

$$\text{tailing coefficient} = \frac{\text{tailing value}}{\text{peak height}} = \frac{a}{A}$$

The tailing coefficients for different mass units away from the main peak (A=1) are illustrated in Diagram (2.11). Thus ld represents the tailing coefficient one mass unit away, down mass and lu, one mass unit up mass, etc.

The tailing is distinctly asymmetrical dropping

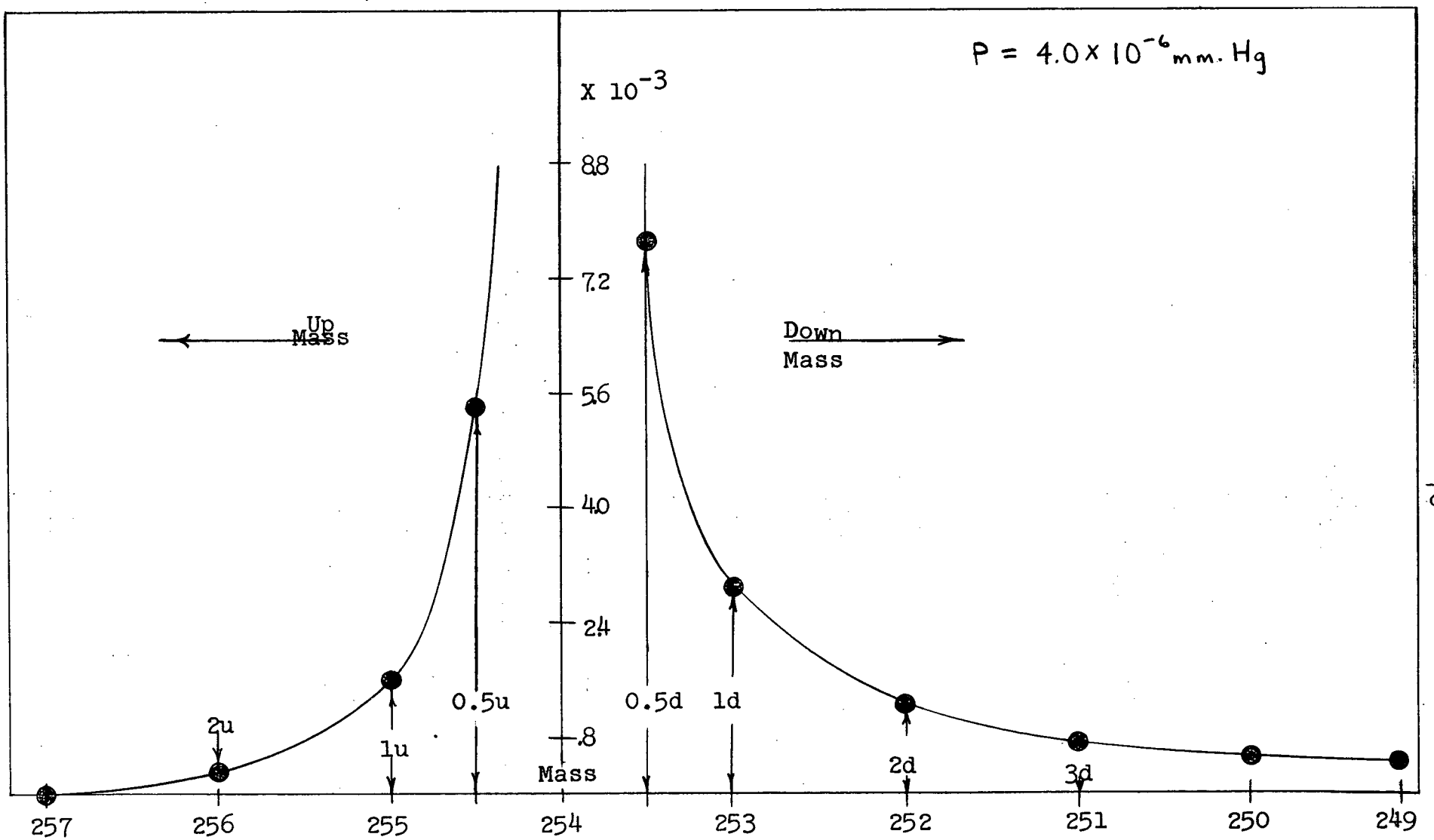

Diagram 2.11. Average Pressure Scattering Coefficients for the 250 Mass Range

essentially to zero at three mass units up mass of the peak but extending and leveling out several mass units below. This latter feature explains the upward shift of the base line below mass 248 in the $Pb(CH_3)_3^+$ spectra (Ostic, 1963). On the basis of the present work it is apparent that this increase is the result of superimposing the down mass tails of masses 251, 252, and 253.

2.2.3 Asymmetrical Pressure Scattering Correction for Trimethyllead Spectrum.

The asymmetrical tailing coefficients are derived from the $Pb(CH_3)_3^+$ spectra (Diagram 2.12) in the manner discussed in Appendix A.2. One large sample was analysed at a number of different pressures and the corresponding tailing coefficients calculated. The results are illustrated in Diagram 2.13. Although the ratios of the coefficients remain the same within a few percent, the coefficients themselves vary non-linearly with the vacuum gauge pressure. The cause of the non-linearity is not known but it may be due to non-linearities in the operation of the vacuum(ion) gauge.

The spectral peak heights must be corrected for the tailing of adjacent peaks. This correction is applied as follows. If A denotes the measured peak height and A^o that corrected for tailing, then:

$$A^o_{249} = A_{249} + (0.5u)\, A_{249}$$

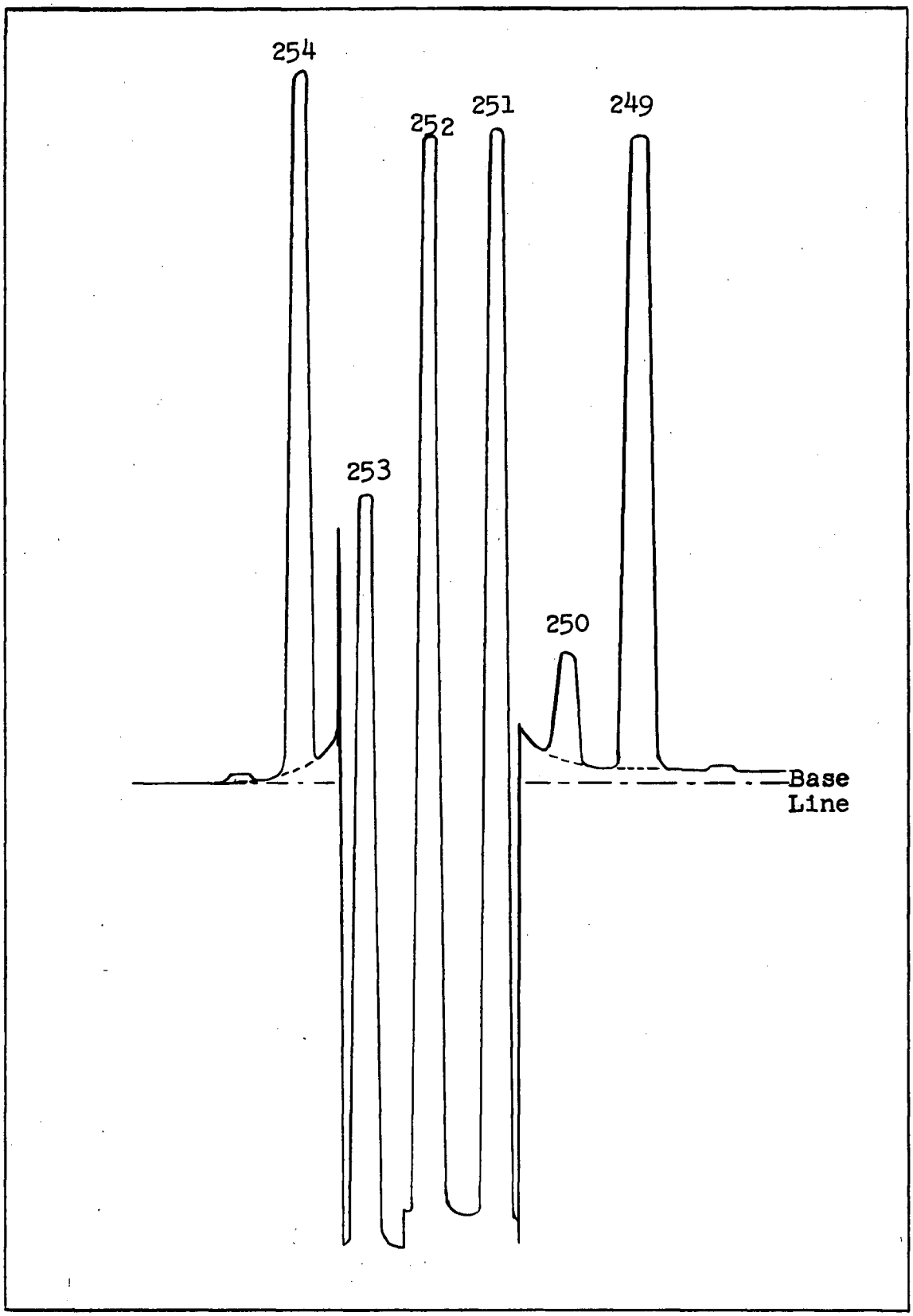

Diagram 2.12. Normal Amplitude Trimethyllead Spectrum

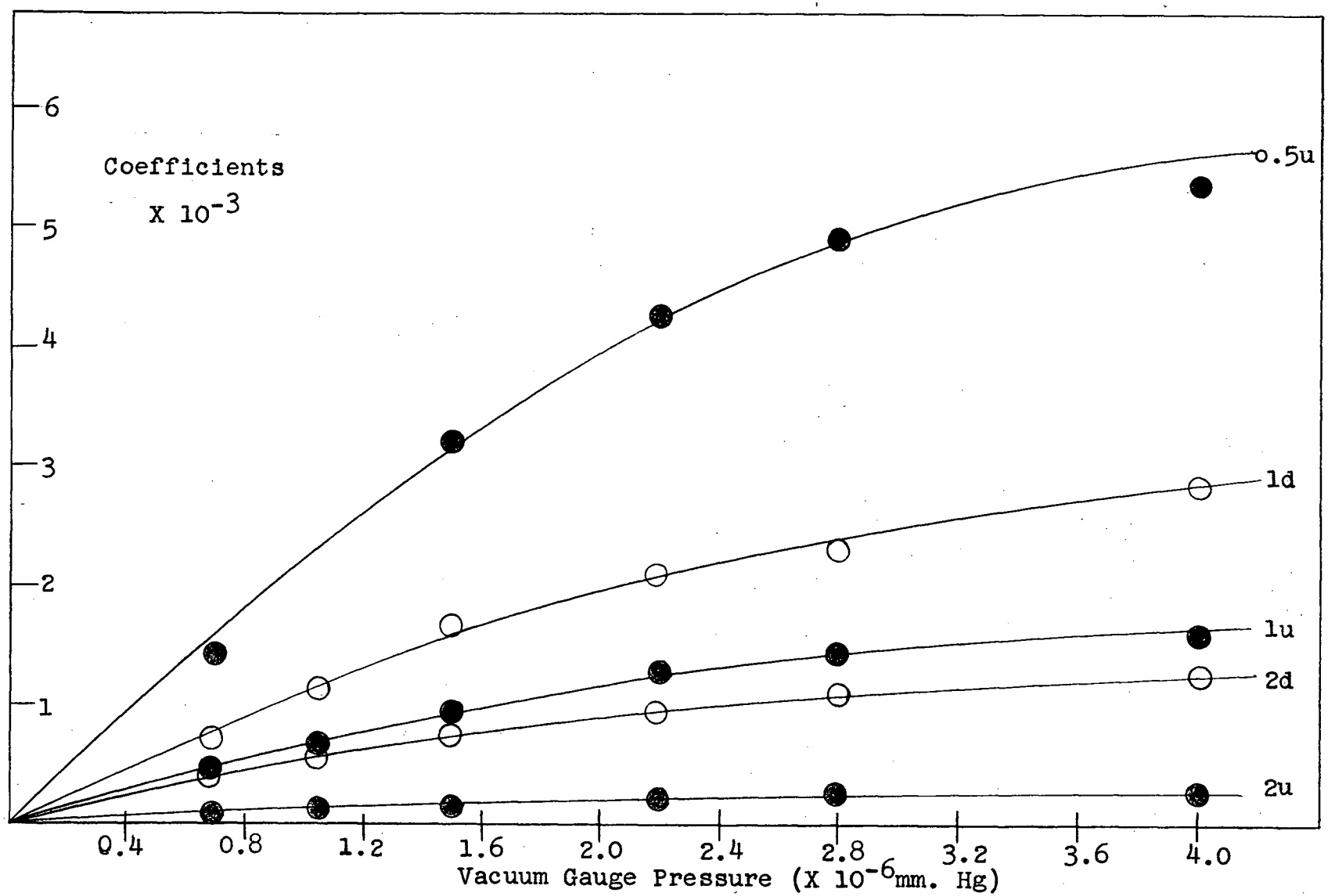

Diagram 2.13. Pressure Scattering Coefficients from the Trimethyllead Spectrum

$$A^{o}_{250} = A_{250}$$

$$A^{o}_{251} = A_{251} - (1d)\, A_{252} - (2d)\, A_{253}$$

$$A^{o}_{252} = A_{252} - (1u)\, A_{251} - (1d)\, A_{253} - (2d)\, A_{254}$$

$$A^{o}_{253} = A_{253} - (1u)\, A_{252} - (2u)\, A_{251} - (1d)\, A_{254}$$

$$A^{o}_{254} = A_{254}$$

The contributions from some of the smaller peaks (249, 250, and 254) are negligible in some of the corrections. Masses 250 and 254 are measured from the curved base line and no correction need be applied. In measuring the A_{249} the lowest points on either side were averaged and the peak height determined using this average as the base line. Measurements showed that this average corresponded to measuring the base line one-half a mass unit up mass (tailing coefficient = 0.5u). This meant that the 249 peak measurement was too small by this factor and the correction had to be added.

A comparison between the asymmetrical and empirical types of correction was obtained by analysing one sample at two different pressures. The tailing coefficients were calculated from the spectra and the corrections applied; the results are illustrated in Diagram (2.14) and (2.15). On the Pb^{207}/Pb^{204} vs. Pb^{206}/Pb^{204} plot the uncorrected ratios for the two pressures differed by about 0.5%. When corrected the ratios were essentially identical (0.05%). The asymmetrical correction gave a greater reduction in the difference between the analyses at different

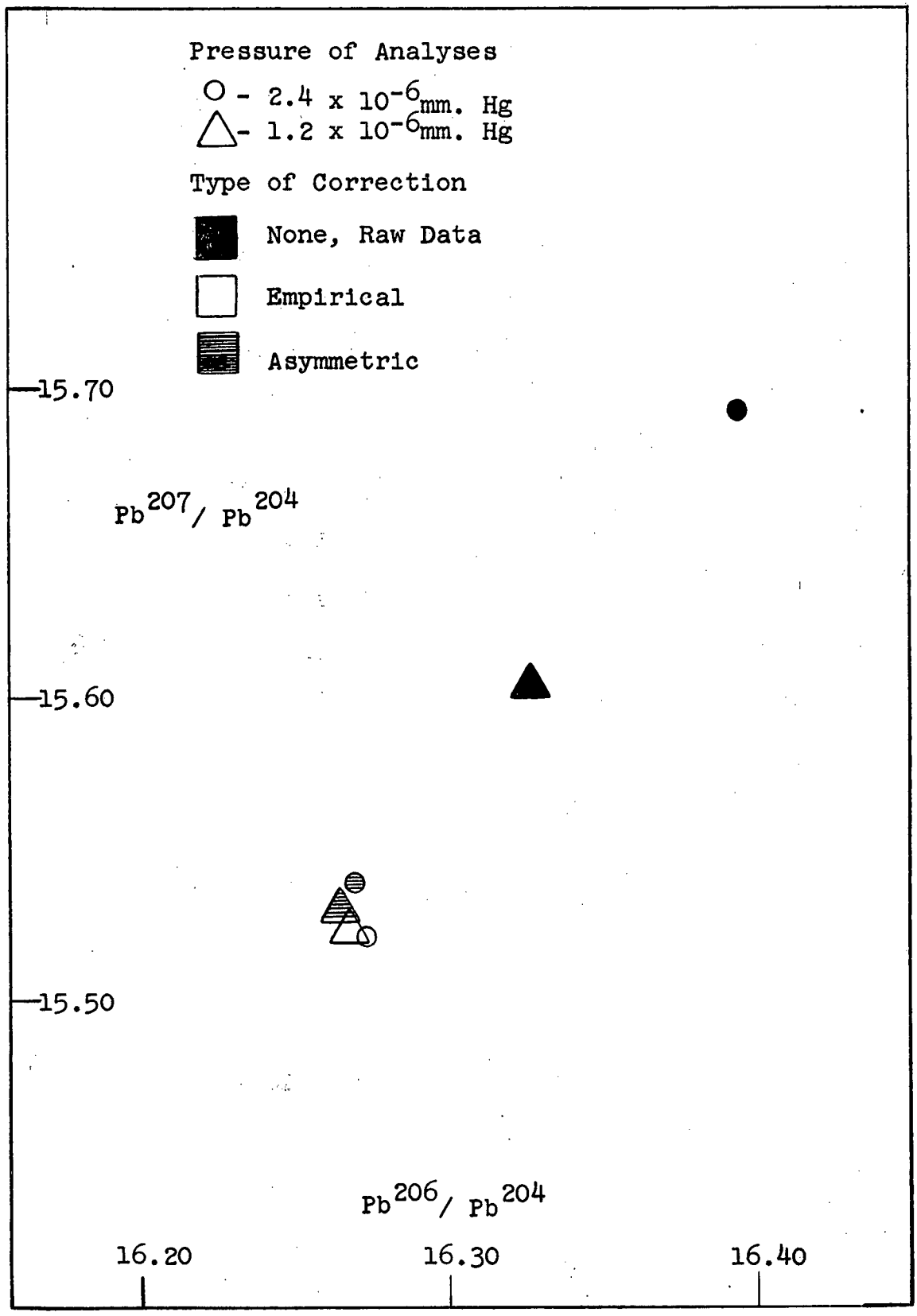

Diagram 2.14. Comparison of Pressure Scattering Corrections I

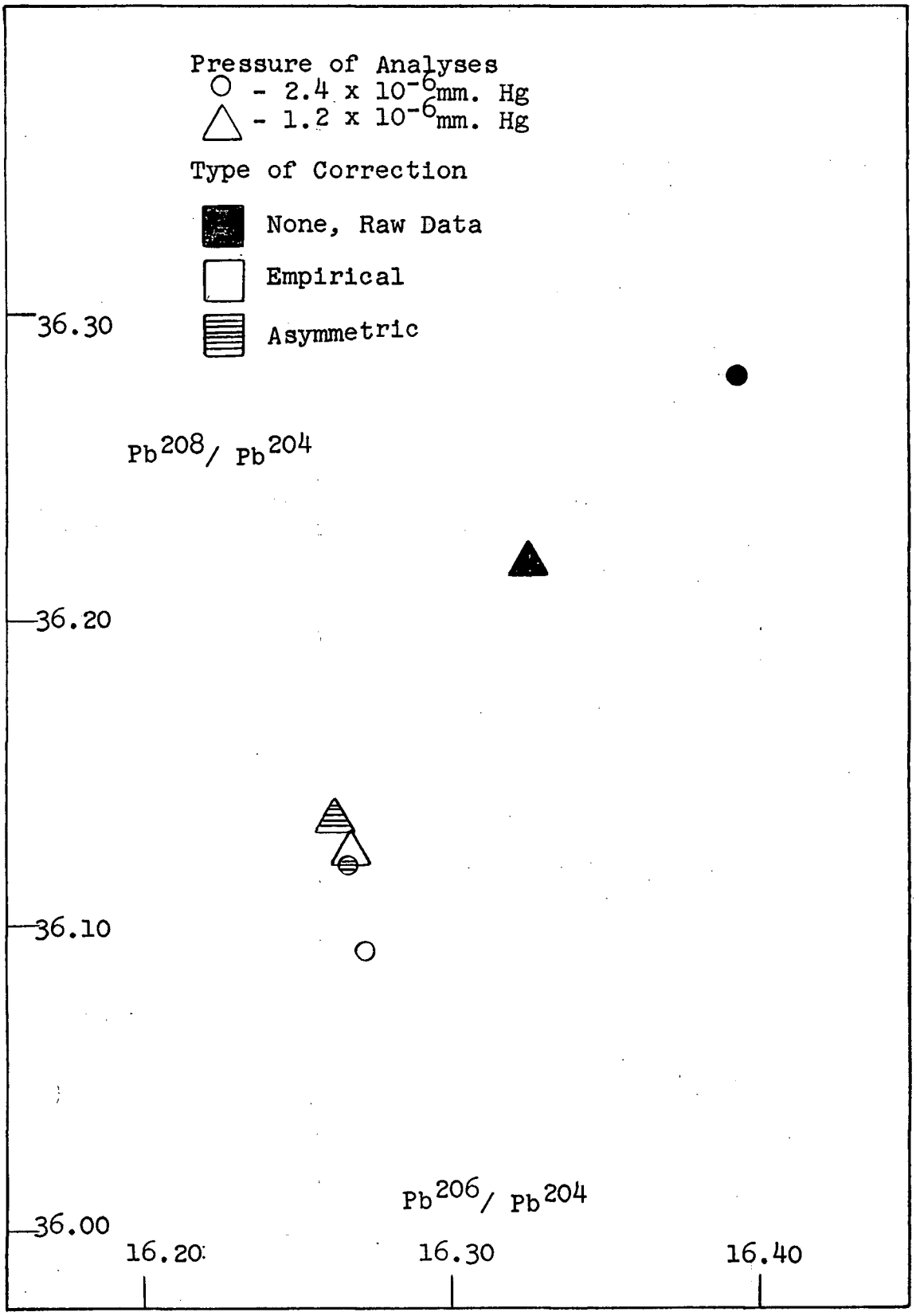

Diagram 2.15.Comparison of Pressure Scattering Corrections II

pressures on the Pb^{208}/Pb^{204} vs. Pb^{206}/Pb^{204} plot, than the empirical correction. This appears to be the result of the assumption of symmetry in the empirical correction.

To apply the asymmetrical correction to the smaller micro-lead samples it was necessary to determine the tailing coefficients graphically (from Diagram 2.13) since the sample ion amplitude was too low to permit measurements.

The cause for the asymmetry observed in this work is not clearly understood. It appears to be partially due to the passage of the ions through a magnetic field.

2.3 Precision and Reproducibility

2.3.1 Precision

Lead isotope ratios are computed from six of the spectral peaks of trimethyllead (Diagram 2.16 and 2.12). Those of masses 249, 251, 252, and 253 are most important; peaks of mass number 250 and 254 are used mainly to calculate the H^+ loss, and C^{13}/C^{12}, factors.

The precision of measurement refers to the standard deviation of the mean of a set of measurements of peak heights (extrapolated to zero time) due to one mass. (Since the peak heights decay with time, a cubic equation is first fitted to the peak measurements and then the individual peaks are extrapolated back to zero time). Thus, if a second analyses were completed under identical conditions

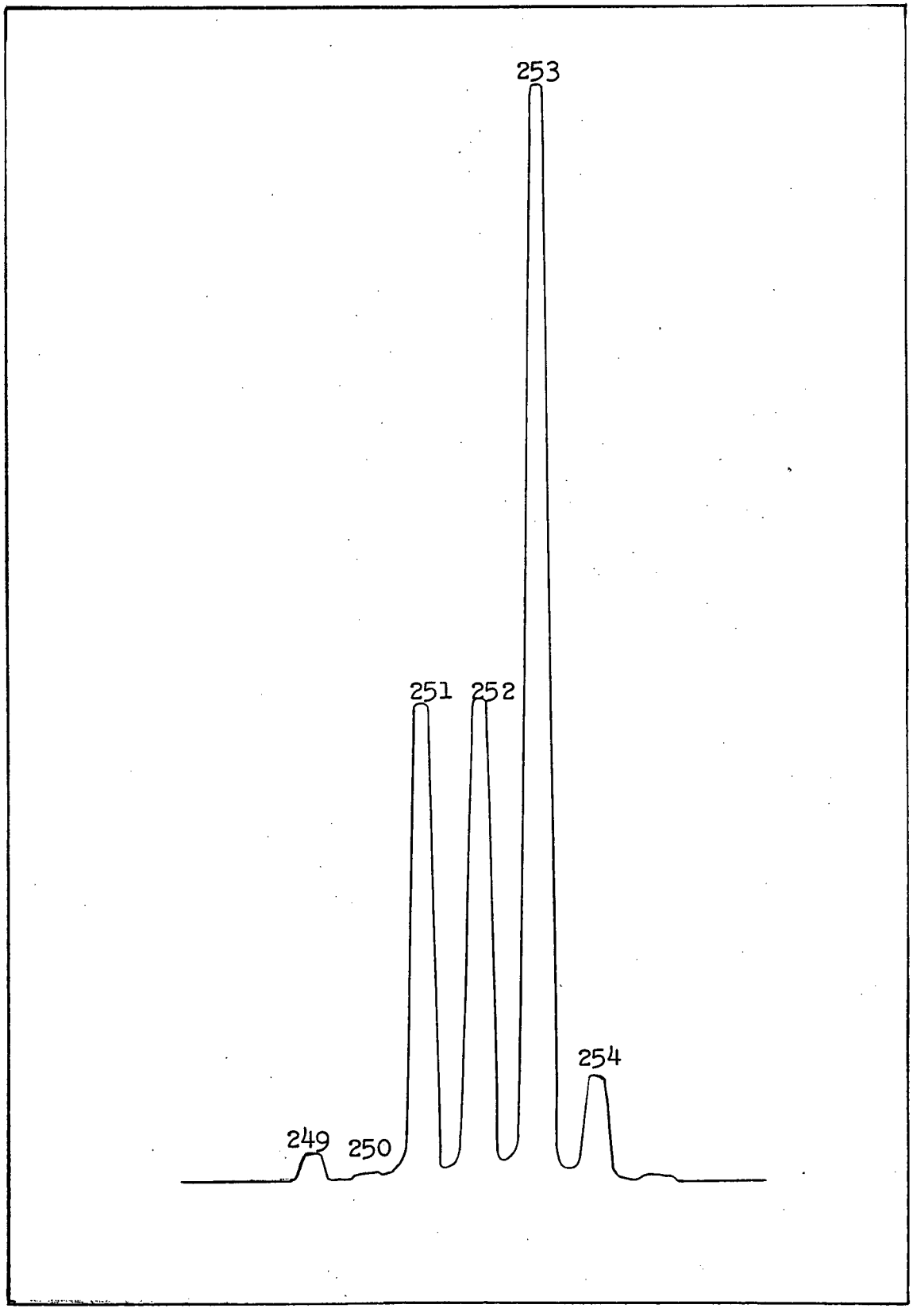

Diagram 2.16. Micro-Lead Mass Spectrum

to the first, there is a 2/3 probability that the mean, ± standard deviation, of the second analysis would fall within the range defined by the mean, ± standard deviation, of the first. This must not be confused with the reproducibility of the same sample run at different times. Changes in mass spectrometer operating conditions can cause changes in the mean isotope ratios larger than those quoted for a single analysis.

In the present work the precision of the isotope ratios relative to the Pb^{204} abundance was always better than 0.4% for samples of 30-60 micrograms of lead. This compares to 0.04% precision for samples of 500 micrograms or larger (Table 2.3). This decrease in precision is the result of a decrease in signal amplitude, since 300-500 micrograms corresponds to the smallest size that can be analysed with normal ion signal amplitude.

2.3.2 Reproducibility

For samples of 500 micrograms or larger it appears necessary to use intercomparison techniques to reproduce a sample ratio to within the precision of measurement. For a discussion of this technique one is referred to Ostic (1963). At the levels of signal amplitude and precision available with the smaller samples analysed in this work intercomparison techniques are of little value and were not used.

Table 2.3. Micro-Lead Precision

Trimethyllead Mass Number	249	251	252	253
Lead Isotope	204	206	207	208
Std. Dev. at approximately 30 micrograms lead	0.35%	0.02%	0.02%	0.02%
Std. Dev. at greater than 500 micrograms lead	0.037%	0.015%	0.015%	0.007%

Table 2.4. Estimation of Micro-Lead Reproducibility. Samples from Sullivan Mine, Kimberly, B.C.

Sample	Pb^{206}/Pb^{204}	Pb^{207}/Pb^{204}	Pb^{208}/Pb^{204}
320	16.640±0.005*	15.646±0.005*	36.638±0.01*
321	16.632±0.005	15.643±0.005	36.599±0.01
323	16.633±0.005	15.633±0.005	36.555±0.01
324A	16.66±0.05	15.67±0.05	36.58±0.10

* Estimated standard deviations.

The reproducibility was estimated by comparing the analyses of samples from the Sullivan Mine, Kimberly, B.C. The isotope ratios of micro-lead samples 320 and 324A were compared to two large Grignard-prepared samples 321 and 323 (A.J. Sinclair, personal communication) from the same deposit. Sample 320 (a galena) was of sufficient size to be analysed at normal signal amplitude and was compared to the Broken Hill #1 standard, as were 321 and 323. 324A, a pyrrhotite, was analysed at low signal amplitude (Diagram 2.16). The Sullivan deposit appears to be uncontaminated primary lead so the isotope ratios of the samples were assumed to be identical. This was found to be essentially correct to within the precision of measurement. It would thus appear that the micro-lead analyses are reproducible to within 0.4% for the smallest samples, 0.04% for those of normal signal amplitude (Table 2.4).

2.4 Summary

The present writer has observed the first reported occurrence of lead isotope fractionation. Such fractionation appeared if the sample passed from the sample line into the mass spectrometer under conditions of molecular flow. This unexpectedly limits small sample analyses to sample line pressures of not less than about 1.0 cm. Hg with the present facilities.

Thus small samples (<500 micrograms of lead) cannot be analysed as pure tetramethyllead; if they are initially purified a carrier must be added to bring the pressure up above the molecular range. The pressure scattering under these conditions is distinctly asymmetrical, with the spectral peaks exhibiting an extreme down mass tailing. A correction for this scattering has been devised and is shown to result in more reproducible analyses.

The sample reproducibility appears to be within the precision of measurement.

Chapter 3: ISOTOPIC RESULTS AND SAMPLE DESCRIPTIONS

"In some way, our journey may be said to end ---."
R.L. Stevenson in An Inland Voyage

3.0 Introduction

This chapter reports the lead isotope analyses obtained during the present research, and briefly describes the samples. It has been divided into two sections.

The first section deals with those samples prepared by the micro-lead technique described in the first two chapters of this thesis. The analyses of the fractionated samples are not reported here.

The second section lists the isotope ratios of a number of galenas. These were analysed early in the present research program as part of the study of single stage leads. These results are of interest in the present work since it is necessary to find the model which most adequately fits those crustal leads having the simplest history, before one can interpret leads which are the result of two or more tectonic events.

3.1 Micro-Lead Samples

Table 3.1 lists the lead isotope results.

1. Sullivan Mine, Kimberly, B.C.

These samples were donated by R.M. Thompson, Department of Geology, University of British Columbia.

Table 3.1 Lead Isotope Data for Samples Prepared using the Micro-lead Technique.

Sample, Location	ppm.* (estimated)	$\frac{206}{204}$	$\frac{207}{204}$	$\frac{208}{204}$	Maximum Std. Dev.**
320, Sullivan Mine Galena Kimberly, B.C.		16.640	15.646	36.638	0.04%
324A Sullivan Mine Kimberly, B.C.	100	16.66	15.67	36.58	0.4%
471, Hope, B.C.	1	17.8±0.5	15.3±0.5	37.8±1.0	2%
465, Stillwater Complex, Montana	10	16.36	15.79	36.71	0.4%
466, Stillwater Complex, Montana	10	15.89	15.83	36.31	0.4%
460, Mt. Isa Australia	10	16.44	15.69	36.22	0.4%
463, Mt. Isa Australia	15	16.49	15.67	36.36	0.4%

* Assumes a 60% yield (Section 1.3.4)
** For the relative Pb^{204} abundance. Those for Pb^{206}, Pb^{207}, and Pb^{208} relative abundances are about 1/5 to 1/10 this value.

#320 - Cummings suite. Mixed galena and sphalerite. Micro-lead preparation ML-110.

#324A - Jewett suite. Pyrrhotite. Micro-lead preparation ML-111.

2. Hope, B.C.

Several samples were obtained with the permission of Giant Mascot Mines Ltd.

Located about 7 miles north of the town of Hope, the ore occurs as stock-like bodies entirely within an irregular northerly plunging mass of ultrabasic rock (approximately two square miles in area). The ultrabasic intrusive consists of a core of olivine pyroxenite or peridot, surrounded by pyroxenite (Aho, 1956).

#471 - Obtained from a fault zone in Brunswick #7 orebody, 3253 drift. Host mineral primarily chalcopyrite in talc schist. Micro-lead preparation ML-102.

3. Stillwater Complex, Montana.

H.H. Hess donated these samples, which had been collected earlier by Peoples (1932). The specimens are from small prospects of massive sulfides along the base of the complex.

#465 - Host mineral mainly pyrrhotite. Peoples' number 463-J-X66. Micro-lead preparation ML-101.

#466 - Host mineral mainly chalcopyrite with some pyrrhotite. Peoples' number 463-J-3. Micro-lead preparation ML-99.

4. Mt. Isa, Australia.

These samples were obtained from Mount Isa Mines Limited by J.R. Richards.

#460 - Host mineral predominantly chalcopyrite. Mine coordinates: 4325N, 1728E, level 10, 500 orebody. Micro-lead preparation ML-104.

#463 - Host mineral predominantly chalcopyrite in silicous dolomite. Mine coordinates: 6674N, 1542E, level 13, 500 orebody. Micro-lead preparation ML-106.

3.2 Grignard - Prepared Galenas.

Table 3.2 lists the lead isotope ratios. All the samples were converted to tetramethyllead by Grignard reaction, and the spectra interpreted in a manner similar to that of Diebler and Mohler (1951), Collins, Freeman and Wilson (1951), or Collins, Farquhar and Russell (1954). Each sample has been intercompared to Broken Hill #1. In all the analyses, the standard deviations were less than 0.05%.

1. Broken Hill, Australia.

#1 - From the main lode. This sample and the isotope

Table 3.2 Lead Isotope Data for Grignard-Prepared Galenas

Sample	Location	$\frac{Pb^{206}}{Pb^{204}}$	$\frac{Pb^{207}}{Pb^{204}}$	$\frac{Pb^{208}}{Pb^{204}}$
1	Broken Hill, Australia *	16.116	15.542	36.068
264	Ivigtut, Greenland	14.682	14.810	34.899
124	Kankaapää, Finland	15.605	15.431	35.562
125	Viitasaari, Finland	15.674 15.671	15.419 15.429	35.504 35.542
126	Pithipudas, Finland	15.633	15.325	35.381
127	Aijala, Finland	15.764	15.470	35.607
128	Korsnäs, Finland	15.808	15.471	35.654
129	Pernaja, Finland	15.738 15.723	15.413 15.415	35.567 35.530
130	Attu, Finland	15.797	15.476	35.635
131	Orijärvi, Finland	15.817	15.496	35.674
132	Pakila, Finland	15.759	15.485	35.634

* Kollar et al (1960). University of British Columbia Geophysical Laboratory standard.

ratios listed are used as the University of British Columbia Geophysical Laboratory standard.

2. Ivigtut, Greenland.

#264 - A galena with chalcopyrite, cryolite, and weathered siderite. Analysed in cooperation with E.R. Kanasewich.

3. Southern Finland.

All of these samples were sent by O. Kouvo, Outokumpa Company, Outokumpa, Finland. Two of the samples were analysed twice (#125 and #129). The first set of ratios shown in Table 3.2, were obtained in May, 1962; the second in Feburary, 1964.

#124 - Vertuunjärvi, Kankaapää.

#125 - From a garnet-bearing mica gneiss near Kärnä school, Viitasaari parish. According to Kouvo and Kulp (1961 - sample 15) this non-economic deposit has to be considered epigenetic. The mineralization belongs to the western border of the Savo-Schist zone.

#126 - Ritovuori region south of Pithipudas Church. According to Kouvo and Kulp (1961 - sample 16) the mineralized zone cuts volcanic schists and is rich in quartz veins and tourmaline breccia.

#127 - Aijala sulfide deposit, Kisko.

#128 - Korsnäs Mine, Korsnäs.

#129 - From some sulfide veins, Koskenkylä, Pernaja (Pb-235, Kouvo and Kulp, 1961).

#130 - From a small sulfide mineralization in Attu. (Pb-233, Kouvo and Kulp, 1961).

#131 - Orijärvi sulfide deposit, Kisko. (A-67, Kouvo and Kulp, 1961).

#132 - From a small galena mineralization found at Pakila near Helsinki. (Pb-175, Kouvo and Kulp, 1961).

Chapter 4: INTERPRETATION

"-useful as such models are for the purpose of developing language and concepts and clarifying elementary ideas, the ideas they illustrate must be explored systematically, critically, and in detail in a real context."

-Herman Kahn in
Thinking About the Unthinkable
(p.142)

4.0 Introduction

The main aim of this chapter is to interpret the lead isotope abundances obtained in this research (those listed in Chapter 3). The present writer was directly interested in the single-stage lead models, those describing crustal leads that have had the simplest histories, and in obtaining evidence which could be used to define more clearly the characteristics of primary leads. However, while many of the results are of considerable importance in this matter, the simple models are not sufficient to explain all of the results obtained. It is necessary to define and apply models which describe the growth of leads in several different systems - the "multi-stage" lead models. On the basis of such models it is possible to interpret the lead isotope patterns of the Stillwater Complex sulfides, the galenas and chalcopyrites of Mt. Isa, and the galenas of southern Finland.

A preliminary study is also made on lead isotope fractionation in nature, and the possible effects of such fractionation on interpretation and lead isotope

models.

4.1 Lead Isotope Fractionation in Nature

Since the present writer has been able to show that lead isotopes can be readily fractionated in the laboratory, the question naturally arises as to the possibility of similar fractionation in nature. Very little work has been directed to this end, and since the expected effects are fairly small much of the published lead data is of little use. Some studies of fractionation of the lighter elements might, however, provide a guide.

4.1.1 Diffusion

Senftle and Bracken (1955) have discussed this problem theoretically. These authors consider solid-state diffusion, the diffusion of atoms through a crystal lattice, along grain boundries or over surfaces, to be of minor importance in isotopic fractionation. In particular, they note that "to obtain significant changes in the isotopic abundance ratio for a given element a relatively large fraction of this element must have diffused out of the original crystal leaving a small remaining fraction enriched in the heavy isotopes". The diffusion of molecules, ions, or atoms in static fluid solutions held intergranulary in saturated rocks is likely to be more effective than solid diffusion. However, again it appears that little isotopic fractionation can be expected until the concentration of the diffusing material drops to less than 0.1 of the

concentration of the source material; e.g. it will only be important on a low concentration diffusion front and the effect will again be evident only in a small amount of material. Senftle and Bracken thus conclude it is "improbable that a large body exists in which a major constituent is isotopically enriched by diffusion processes."

The experimental evidence supports these conclusions. Silverman (1951) had suggested that O^{18}/O^{16} measurements taken across the contact of a gabbro and intruding granophyre were indicative of diffusive fractionation; however, Clayton and Epstein (1958) later pointed out that the observed variation was more likely due to isotope fractionation during magnetic differentiation. Friedman (1953) had suggested hydrogen diffusion as an explanation of the isotopic uniformity of the hydrogen in ice samples which showed changes in the oxygen isotopes. Other writers (Ault and Kulp, 1960) have questioned the validity of the oxygen analyses. Sulfur isotope analyses were obtained by Ault and Kulp (1960) for samples from a ZnS halo around an ore body. This particular example should have indicated the effectiveness of diffusion in fractionation, since the concentration of sulfides in the halo were less than 10^{-3} of that in the ore body, and the deposit appeared to have undergone regional metamorphism which would have produced elevated temperatures for a

considerable length of time. No evidence of fractionation was observed. The same authors noted also that there existed considerable irregular variations (1%) in the sulfur isotope ratios of a single crystal of galena which were not erased by diffusion. Similar variations have been noted in the lead isotope ratios by Austin and Slawson (1961). Wanless et al (1960) have studied gold-quartz deposits of the Yellowknife District and suggested that diffusion was the main cause of the sulfur isotope differences that were observed. The sulfide ore bodies were considerably heavier in S^{34} than the surrounding country rocks, and the ratios increased gradually to this latter value. The authors considered the preferential diffusion of S^{32} as the probable answer. It would seem to the present writer that chemical contamination of the neighbouring rock by the ore (enriched in S^{34}) is an equally probable explanation. In any case the difference between ores and country rock is quite small (0.14%) when considered as an average. Let us assume that the expected lead isotope fractionation will be less by the amount indicated by the difference between the square root of the masses:

$\sqrt{34/32}$	$\sqrt{208/204}$	$\sqrt{207/204}$	$\sqrt{206/204}$
1.031	1.010	1.006	1.004

Hence if the fractionation of the sulfur isotopes is x%, that for the 208/204=x%/3, 207/204=x%/5, and 206/204=x%/8. If the above mentioned average variation of 0.14% is due

to diffusion, the corresponding variation for the lead isotopes would be below the limits of detection (±0.05‰).

It is thus concluded that lead isotope fractionation due to diffusive processes in nature, is not likely to be greater than the present level of precision.

4.1.2 Weathering

Ault and Kulp (1959) have looked for sulfur isotope fractionation due to oxidation during surface weathering. They conclude that the process is "essentially a quantitative one which does not allow isotopic fractionation."

4.1.3 Crystallization

If an element is carried in solution in one chemical form, then deposited in another form, fractionation can occur (Ault and Kulp, 1960; Jensen, 1959; Tudge and Thode, 1950; Dechow, 1960); for example, the exchange process

$$S^{32}O_4^{=} + PbS^{34} = S^{34}O_4^{=} + PbS^{32}$$

can result in a difference of 7‰ at 25°C., under equilibrium conditions, between the sulfur isotope ratios of the PbS and the sulfate. The effect on the lead isotope ratios will be considerably less. Adamson (quoted in Russell and Farquhar, 1960) has calculated the expected equilibrium constants for reactions envolving lead isotopes, and his results suggest that even at low temperatures the lead isotope fractionation will be less than 0.05‰.

4.1.4 Biological Processes

It has been conclusively demonstrated that very significant sulfur isotope fractionation can take place in the bacteriological reduction of sea water sulfates to H_2S. If this H_2S is responsible for the deposition of metallic sulfides, their sulfur isotope ratios will reflect this fractionation and any changes in its extent. Such changes have been shown to result from differences of temperature, variations of organic material, rate of H_2S production, etc. These variations are characteristic of bacterial reduction and can range up to 2% for samples of native sulfur (Harrison and Thode, 1958) and 1% for sedimentary pyrites from a core (Thode et al, 1960).

Nothing is known about the fractionation of lead isotopes in bacterial processes but there is good evidence that lead is at least involved in these processes (Tatsumoto and Patterson, 1963). If we assume the relations between the sulfur and lead isotope fractionation suggested earlier, sea water leads might be expected to show variations of about:

$$\triangle(208/204) = \pm 0.05 \text{ to } \pm 0.10$$
$$\triangle(207/204) = \pm 0.02 \text{ to } \pm 0.03$$
$$\triangle(206/204) = \pm 0.01 \text{ to } \pm 0.02$$

Such variations are close to the limits of reproducibility presently obtained for the larger samples, but might be detectable with intercomparison techniques. It is an interesting possibility.

4.2 Single Stage Lead Models

The models discussed in this section consist of sets of equations which are developed, according to certain assumptions, to relate the changes in lead isotope ratios to the time and the relative proportions of lead, uranium, and thorium. The presentation is essentially pictorial and the mathematical derivations will be left to appendix A.3.

Diagram (4.1) illustrates the basis of our models. We assume that at the beginning of geologic time, t_o years ago, all lead had a unique composition (primordial lead):

$$\begin{aligned} a_o &= (Pb^{206}/Pb^{204})_{t_o} \\ b_o &= (Pb^{207}/Pb^{204})_{t_o} \\ c_o &= (Pb^{208}/Pb^{204})_{t_o} \end{aligned} \qquad (4.1)$$

Assuming that the radioactive decay law applies, and that the changes in lead composition are due only to the decay of uranium and thorium

$$\begin{aligned} {}_{92}U^{235} &= {}_{82}Pb^{207} + 7He^4 + \text{energy} \\ {}_{92}U^{238} &= {}_{82}Pb^{206} + 8He^4 + \text{energy} \\ {}_{90}Th^{232} &= {}_{82}Pb^{208} + 6He^4 + \text{energy} \end{aligned} \qquad (4.2)$$

then one can derive the variations of Pb^{206}/Pb^{204}, etc., with time. The Pb^{204} abundance is considered constant. The resulting relationships between Pb^{206}/Pb^{204} and

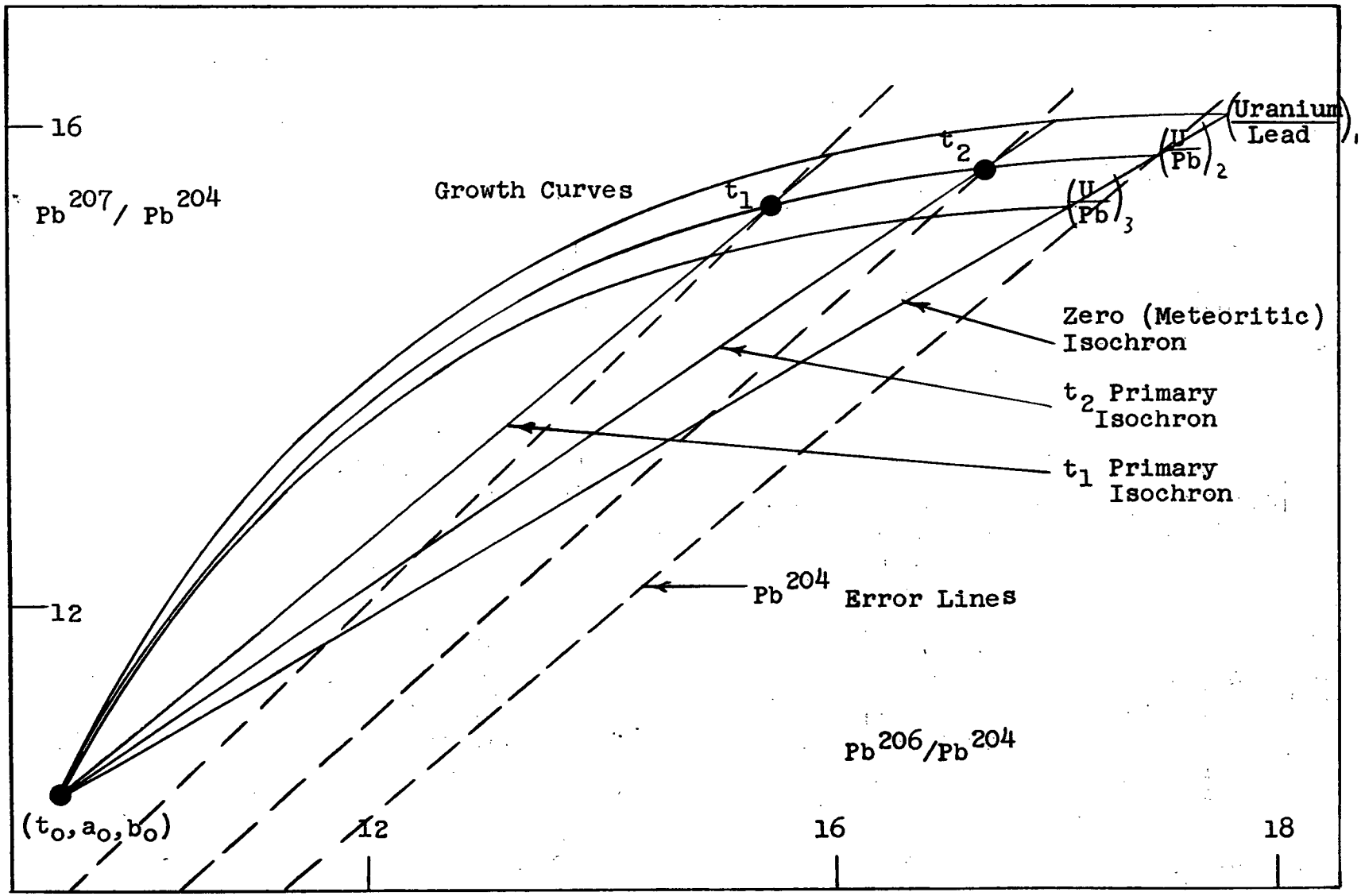

Diagram 4.1. The Isochron Model, and the Relation of Primary Isochrons to Pb^{204} Error Lines

Pb^{207}/Pb^{204} are shown in diagram (4.1). The isotope ratios will grow from the primordial values along a curve depending upon the uranium to lead ratio of the closed system in which the lead is developing. Two single stage models have been proposed.

4.2.1 Isochron Model.

Gerling (1942), Holmes (1946) and Houtermans (1946) constructed the first single stage lead model on the assumption that leads developed in a series of locally closed systems. Hence the ratios would grow from the primeval values along a series of growth curves similar to those shown in Diagram (4.1). If the leads were extracted from the various closed systems at the same time t_1, and separated from uranium and thorium, they would be linearly related and lie along the t_1 "primary isochron".

4.2.2 Primary Lead Model and Possible Primary Lead Characteristics.

Collins, Russell and Farquhar (1953) postulated that all single stage leads have evolved from one closed system having essentially constant uranium - lead and thorium - lead ratios. This system was assumed to be deep in the earth - the lower crust or upper mantle. On the basis of the primary lead hypothesis one might expect primary leads to possess the following characteristics.

(1) They should have lead isotope ratios which lie

closely along a single, unique growth curve in the Pb^{206}/Pb^{204} vs. Pb^{207}/Pb^{204} plot. This will reflect their identical uranium-lead ratios at any given time.

(2) Since the primary lead system is postulated to be deep in the earth, reducing conditions are likely to exist, and uranium and thorium will geochemically be similar. One might thus expect that primary leads will fit a unique growth curve in the Pb^{206}/Pb^{204} vs. Pb^{208}/Pb^{204} plot.

(3) Primary leads, to the extent they are uncontaminated on their passage from depth, should be isotopically uniform throughout a deposit or even throughout a district. This assumes that they are emplaced at the same time and separated from uranium and thorium.

(4) If the primary lead is uncontaminated the sulfur isotope ratios should be fairly constant and close to the meteoritic value. This assumes that the primary lead system has the meteoritic sulfur isotope ratios, and that the temperatures of deposition are high enough to prevent significant fractionation. It is also necessary to postulate the same lead and sulfur source. The validity of these assumptions is indicated in analyses of ultrabasic deposits, which are generally assumed to have come from considerable depth. The average of 15 samples from the magmatic sulfide ores of Sudbury, the Stillwater Complex, and the Insizwa

Sill is S^{32}/S^{34} = 22.21 ± o.o5 and Thode et al (1961) suggest "that there is no significant difference in isotope ratios between sulfur of magmatic sulfides, associated with ultrabasic rocks, and meteorites" (meteoritic value S^{32}/S^{34} = 22.225 ± 0.005). It must be noted, however,that the variations of the sulfur isotope ratios in basic and ultrabasic rocks are found to be larger than those in meteorites, and also that some fractionation of the sulfur isotope ratios occurs during the crystallization in magmatic processes (Thode et al, 1962).

This characteristic would not apply if the leads have had contact with the sea, since significant mixing and fractionation is then probable.

The primary lead model seems to be the most adequate in describing the observed isotope ratios of single stage leads, and there appears to be no good evidence that primary isochrons exist. This point will be more fully developed in the following section.

4.3 Single-Stage Leads.

4.3.1 The Elusive Isochron

Since one cannot reconstruct the events leading up to the formation of a deposit it is not possible to test the two single stage lead models by experimentation. Rather, one must study a large number of analyses and look for evidence which supports one particular theory. In this

sense it is impossible to disprove either of the two models to the point where it can be said that one theory is wrong. The data should, however, indicate that one model more adequately describes the observed isotope ratios than does the other.

What, then, is the evidence for the existence of primary isochrons? Although there was the difficult question of how the series of closed systems postulated for this model could remain closed over the period of geologic time involved (Burlings, 1952), several sets of published data seemed to illustrate the existence of primary isochrons. These included galenas from Southwestern Finland, Ivigtut Greenland, Bluebell B.C., and St. Magloire Que. However, it appeared that these results could be due to errors in measuring the relative Pb^{204} abundance; such errors would cause variations very similar to those expected on the isochron model ("204 Error Lines", Diagram 4.1). These Pb^{204} errors are attributed to interlaboratory differences, the presence of contaminants, analytical measuring errors, and pressure scattering. E.R. Kanasewich and the present writer reinvestigated the deposits for which primary isochrons were postulated and were able to report that these isochrons are either very short or else non-existant (Kanasewich, 1962a; Whittles, 1962).

1. Ivigtut, Greenland.

Diagram (4.2) compares the results of the Ivigtut

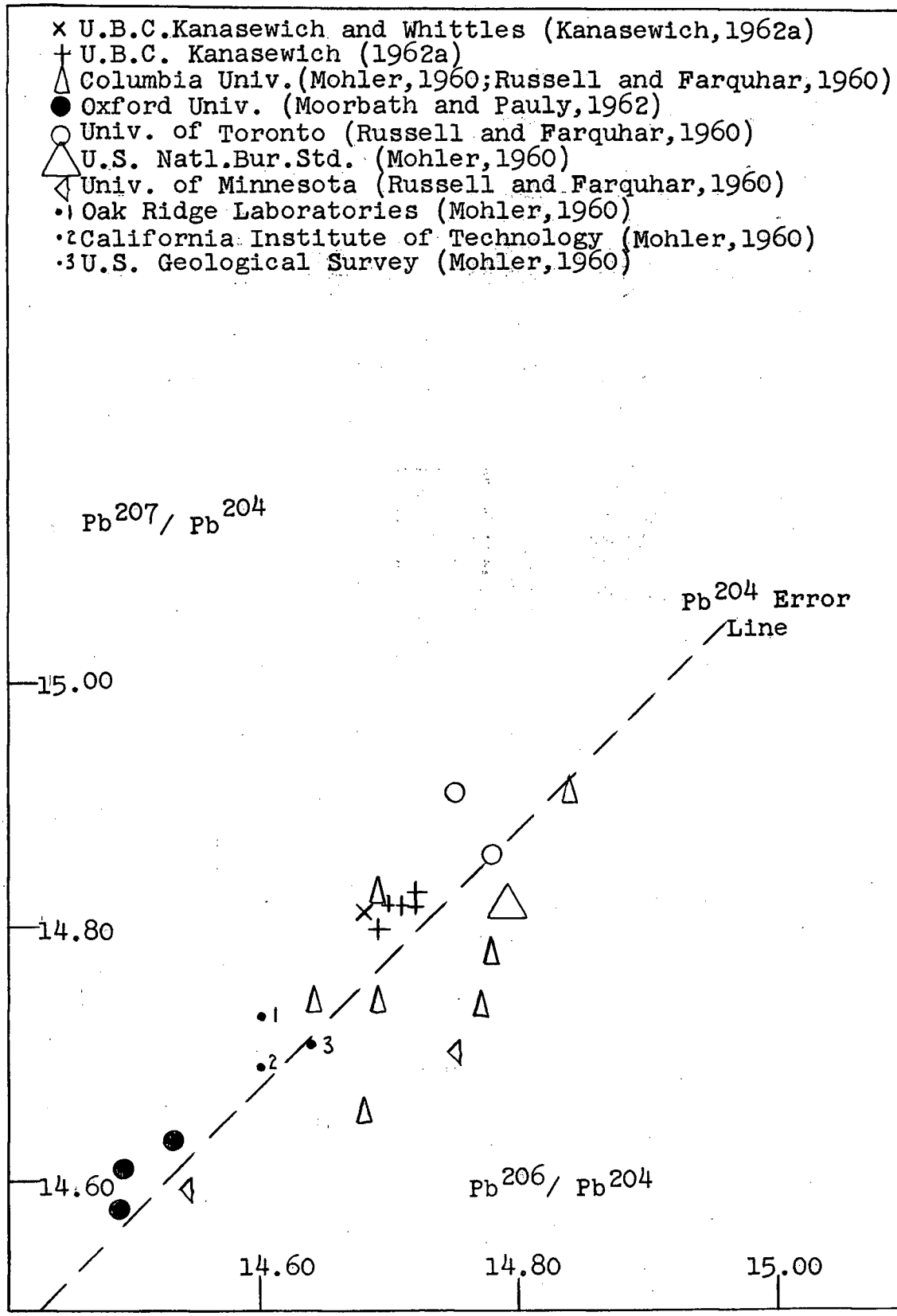

Diagram 4.2.Analyses of Ivigtut Galenas
(Kanasewich and Slawson,1964)

analyses to those of other laboratories. The variations are clearly along a Pb^{204} error line and have been reduced to the small cluster at the center of the group. The same result is seen on the Pb^{208}/Pb^{204} vs. Pb^{206}/Pb^{204} plot.

2. Southwestern Finland

Samples from the Svecofennian deposits along the coast of Finland had been reported as supporting the isochron model (Schütze, 1962); in fact, this area apparently provided one of the best examples of a primary isochron. However, the present writer's analyses now show that most of the previously observed variations were due to Pb^{204} errors. Diagram (4.3) illustrates five of the nine Finnish galenas analysed by the present writer. The remaining samples have isotope ratios that are more easily explained on the basis of multi-stage growth, and will be discussed in a later section. The variations observed previously have been reduced by a factor of ten, and no primary isochron appears to exist. This is given added support on the Pb^{208}/Pb^{204} vs. Pb^{206}/Pb^{204} plot (Diagram 4.4). Further confirmation is received from sulfur isotope analyses (Vaasjoki and Kouvo, 1959; Kouvo and Kulp, 1961) of samples of the same deposits. The S^{32}/S^{34} ratios range from 22.17 to 22.27, averaging 22.226. This compares favorably with the meteoritic average of 22.225 ± 0.005 (Thode et al, 1961). Finally, as shown later in Diagrams (4.5) and (4.6), these new analyses lie directly on the primary growth curves (as defined in the following section)

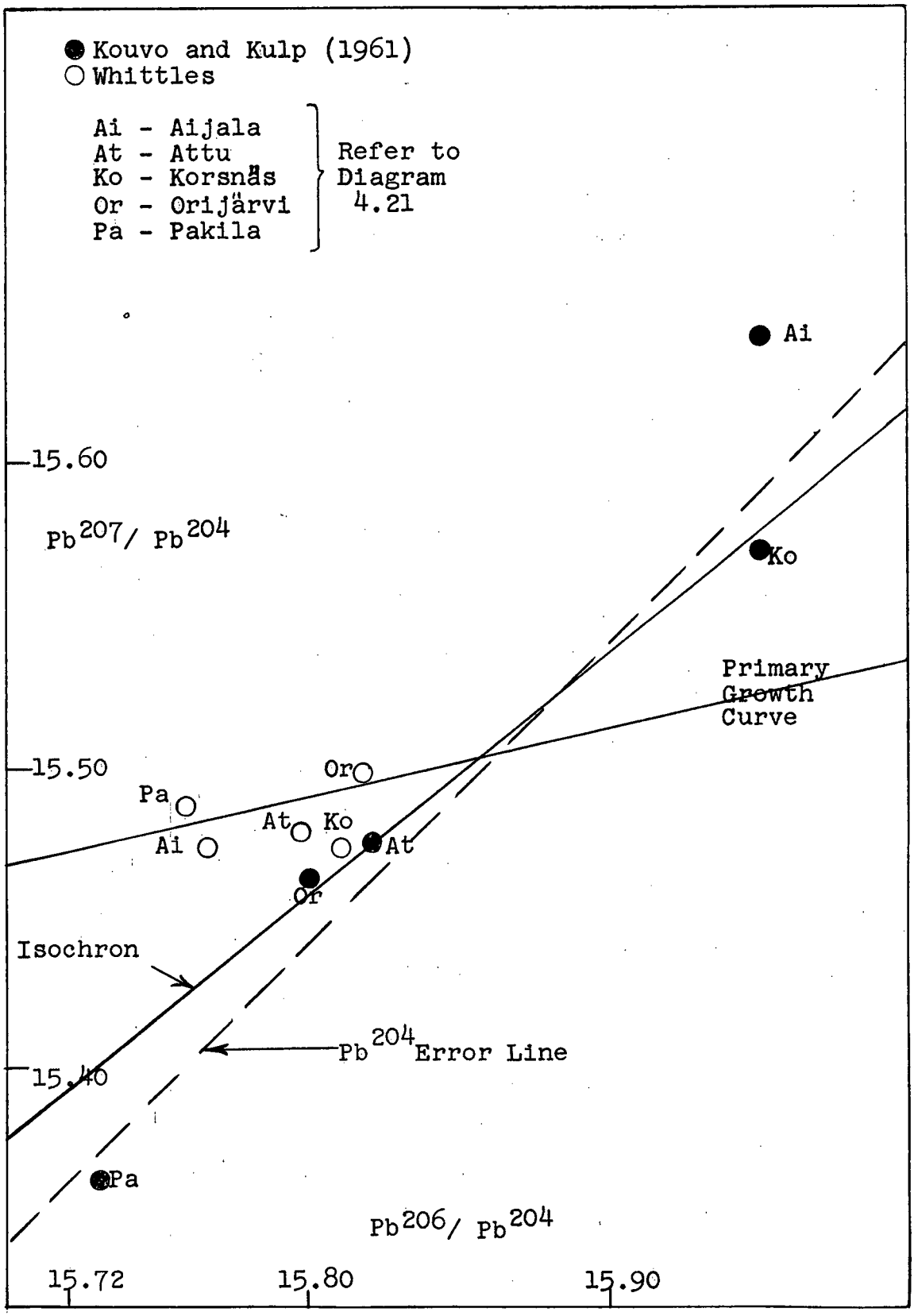

Diagram 4.3. Galenas from the Coast of Southwestern Finland I

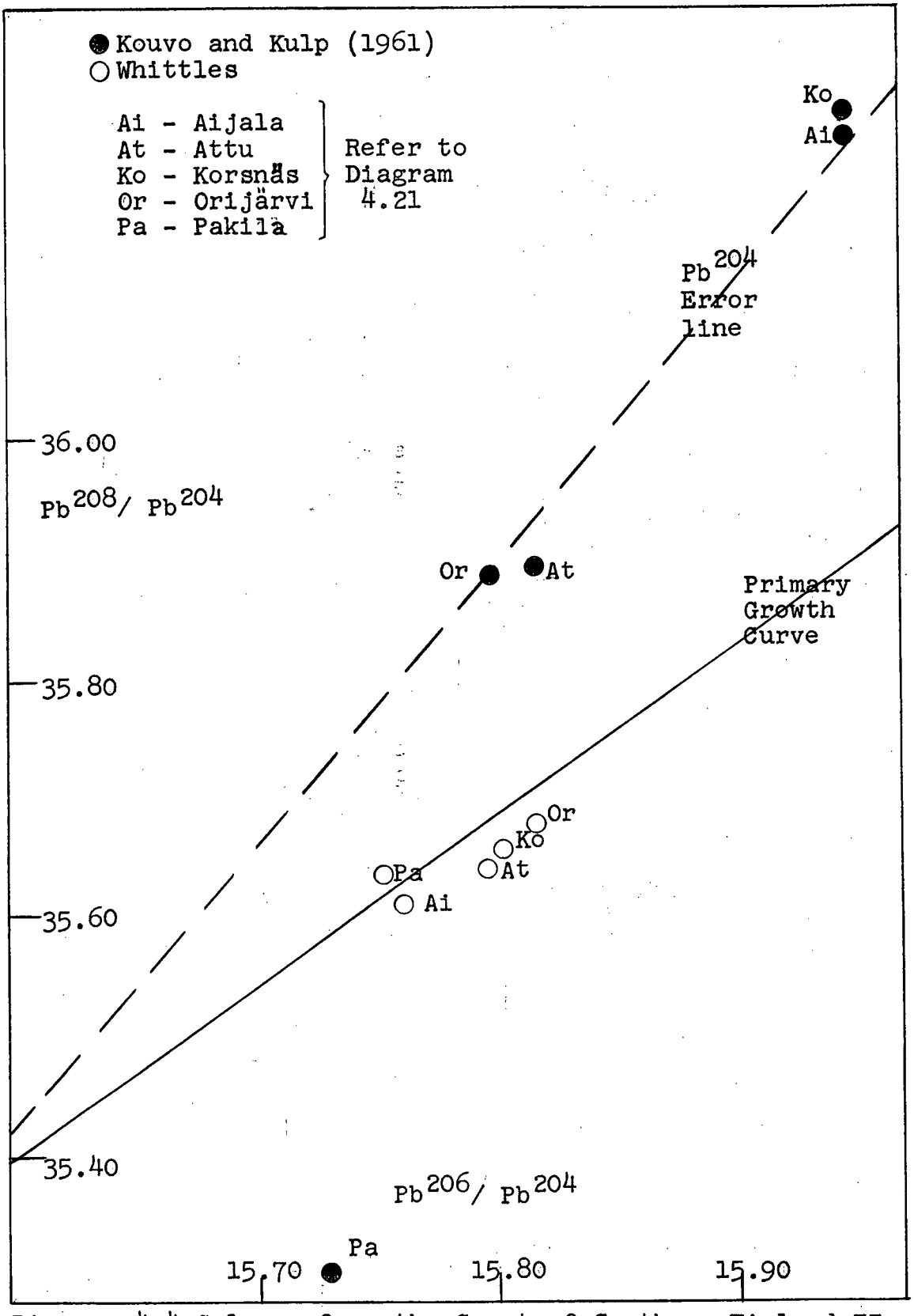

Diagram 4.4.Galenas from the Coast of Southern Finland:II.

on both of the lead isotope plots.

It is apparent that the primary lead model much more adequately describes these samples than does the isochron model.

3. Other Areas

Analyses of samples from Bluebell, B.C. and St. Magloire, Que. (Kanasewich, 1962a) have shown that the previously reported variations were also due to errors in estimating the relative Pb^{204} abundances.

In summarizing the available data, one can say that no good examples of primary isochrons exist, and that the isochron model does not adequately describe the observed lead isotope ratios.

4.3.2 Possible Types of Primary Lead.

According to R.L. Stanton the leads of two types of deposits were expected to fit most closely the primary lead model (Stanton and Russell, 1959).

(1) Orthomagmatic deposits in mafic rocks derived from beneath the continental crust.

(2) The sedimentary (conformable) deposits derived from depth by basalt-andesite volcanism along or at some distance from the continental margins, and quickly isolated in volcanic sediments.

It was argued that since both types would have only limited contacts with the crust neither would suffer significant radiogenic contamination. Ostic (1963) analysed a large number of samples from conformable massive lead-zinc deposits and showed that many of these deposits fitted the primary lead model, although not all did. These results, and those of other research workers, suggest that primary leads have formed in a region for which there are very narrow limits of ± 0.6% and ± 0.8% variation in the U^{238}/Pb^{204} and Th/U ratios. The curves defined by these leads, and assumed to be the primary growth curves in this work, are illustrated in Diagrams (4.5) and (4.6). Some of the conformable deposits are shown, as well as the locations of the supposed primary leads of South-western Finland and Sullivan Mine, Kimberly, B.C.

Part of the present writer's research program involved the analyses of ultrabasic sulfides and conformable chalcopyrites using the micro-lead technique discussed earlier. The lead isotope ratios of samples from the conformable chalcopyrite deposits of Mt. Isa were found to be significantly different from those of the massive lead-zinc deposits, and do not appear to be primary. It also appears that ultrabasic sulfides are not necessarily primary. Samples from the Stillwater Complex do not have the proposed characteristics of primary leads, and the lead in these samples appears to have developed in at

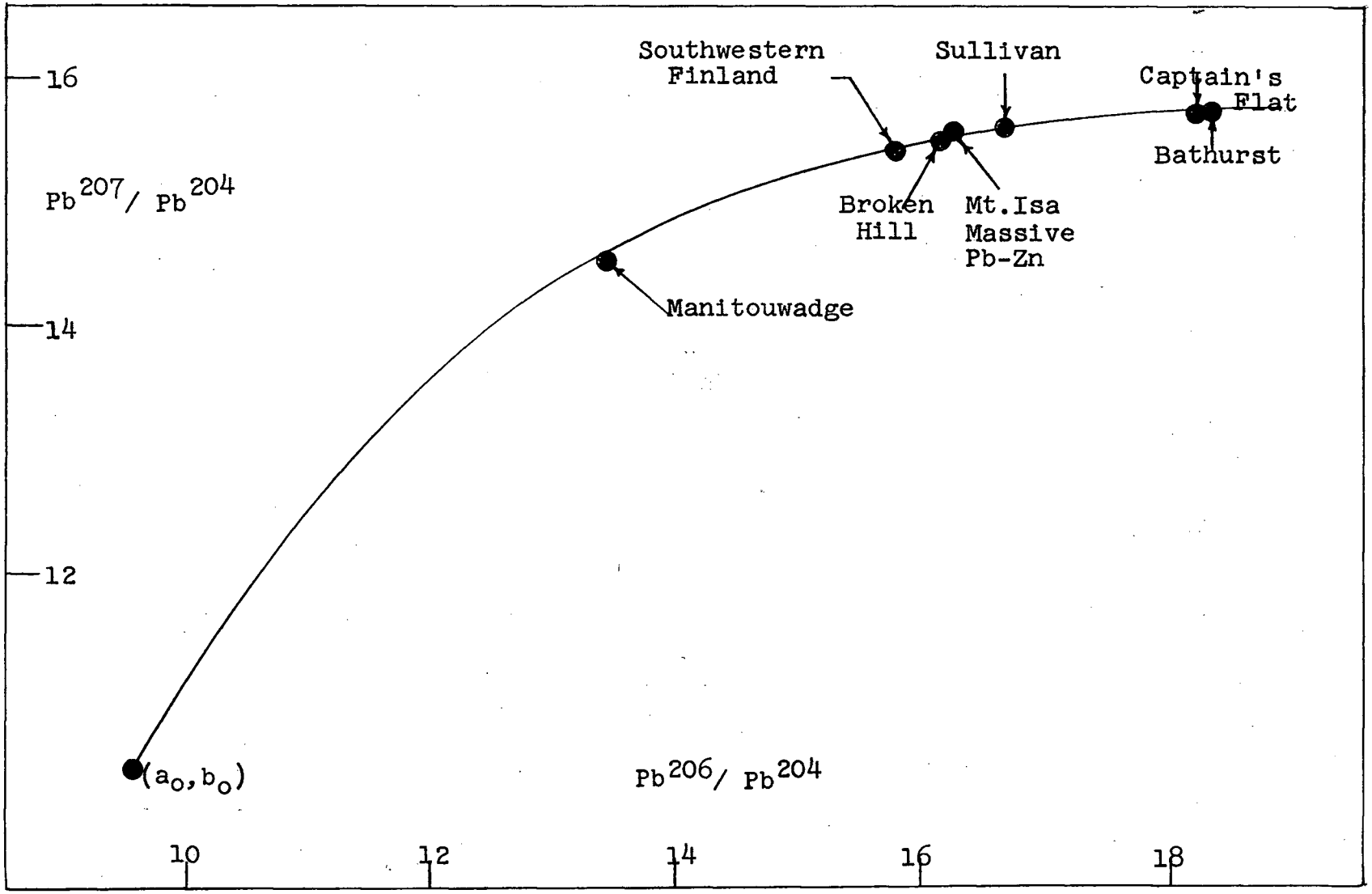

Diagram 4.5.Proposed Primary Growth Curve (Ostic, 1963)
(a_o = 9.56, b_o = 10.42, t_o = 4.55x 10^9yrs.,U^{238}/Pb^{204}=9.2)

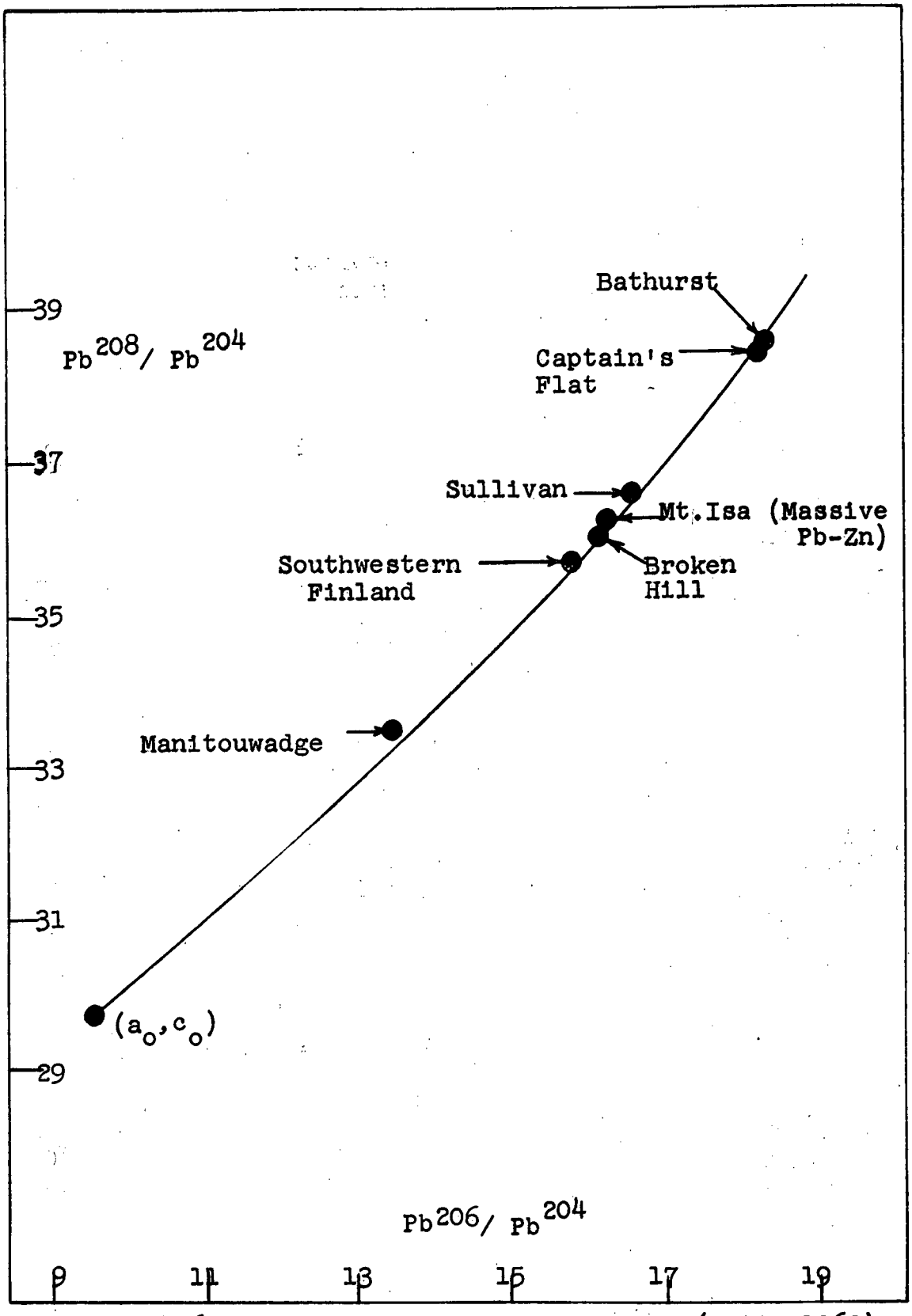

Diagram 4.6. Proposed Primary Growth Curve (Ostic, 1963) (a_o = 9.56, c_o = 29.71, t_8 = 4.55 x 10^9 yrs., U^{238}/Pb^{204} = 9.2, Th/U = 4.1)

least two crustal systems. The Mt. Isa and Stillwater samples will be discussed in more detail in a later section on multi-stage leads.

Several samples were obtained from the nickeliferous ultrabasic deposit 7 miles north of Hope, B.C. The lead content was too low for even fair isotopic analyses and only one sample was analysed (#471). The results, reported in Chapter 3, are rather imprecise and can be used only as an approximate guide; however, they do agree roughly with the supposed geologic age (approximately Cretaceous: see Aho, 1956). The lead in this deposit may be primary. A considerable increase in mass spectrometer sensitivity is required before more useful analyses can be carried out at this level of lead concentration.

It should be noted that other leads may be primary (but not conformable or ultrabasic) provided they are extracted from the deep source and emplaced in the crust without significant contamination. The leads from south-western Finland appear to be one example. Those of the Sullivan Mine, Kimberly, B.C. may also be primary. The samples from both locations lay close to the primary growth curves in the Pb^{207}/Pb^{204} vs. Pb^{206}/Pb^{204} and Pb^{208}/Pb^{204} vs. Pb^{206}/Pb^{204} plots. The sample isotope ratios are identical to within the precision of measurement. No sulfur isotope data are available for the Sullivan samples.

4.4 Multi-stage Lead Models.

The mathematical models for multi-stage leads are constructed by assuming that the uranium-lead and thorium-lead ratios are functions of time and place. Kanasewich (1962a, 1962b) proposed that these ratios would change discretely at the time of tectonic activity, and remain constant until the next event. In this way, the leads develop in a series of steps or stages; such development is called "multi-stage" growth.

The following presentation is, as before, essentially pictorial; the interested reader is referred to Appendix A.3 for the mathematical derivations.

4.4.1 Primary Lead Mixtures

The primary lead mixture is, as the name implies, a mixture of two primary leads brought to the surface at two different times. In this sense, it can be called a special "two stage" lead model. Referring to Diagram (4.7) we suppose that lead was extracted from the primary system at time t_1 and emplaced in the crust essentially free of uranium and thorium. When a second period of tectonic activity (t_2) occurs more primary lead is extracted, some of which mixes with that of the first event t_1. The isotope ratios will lie along a line joining t_1 and t_2 on the growth curve. These leads will have three features that distinguish them from general two stage leads.

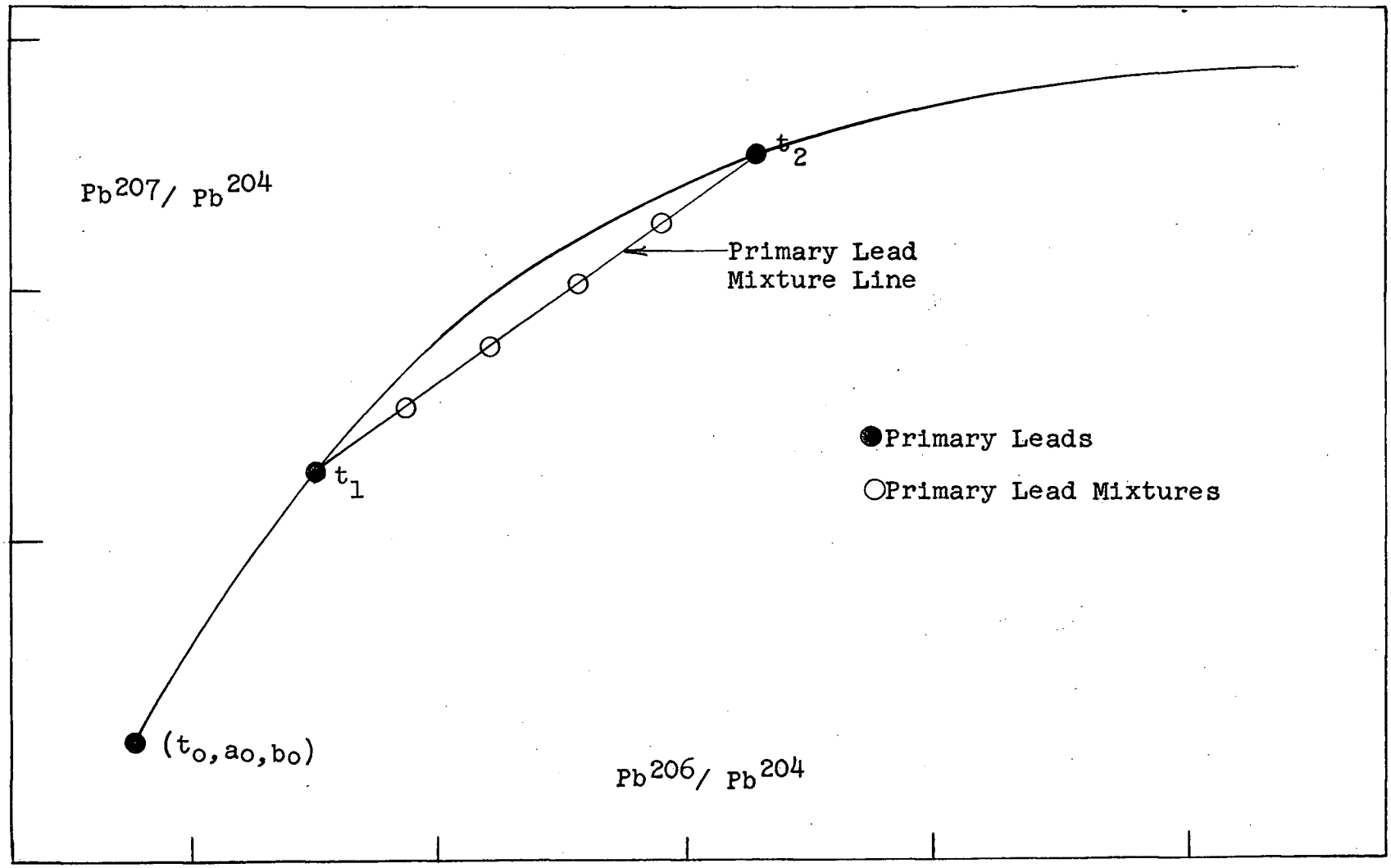

Diagram 4.7. Development of Primary Lead Mixtures : I.

(1) The primary lead mixtures will lie along a line on the Pb^{207}/Pb^{204} vs. Pb^{206}/Pb^{204} plot, joining t_1 and t_2, but not extending beyond t_2.

(2) The leads will lie along a similar line (Diagram 4.8) in the Pb^{208}/Pb^{204} vs. Pb^{206}/Pb^{204} plot as well.

(3) The sulfur isotope ratios should be close to the meteoritic value for all the samples. General two stage leads are likely to have considerable sulfur isotope variations.

Primary lead mixtures could be expected along the boundaries of two geological provinces.

4.4.2 General Two Stage Lead Model

The first step represents the growth in the primary system, with the lead being extracted at some time t_1. This lead is, however, then placed in crustal systems having varying uranium-lead and thorium-lead ratios. If these leads are then removed during a second event at t_2, they will have isotope ratios which lie along a line from t_1 and passing through t_2 (Diagram 4.9). Some of the resulting ratios are likely to lie on the line extending beyond t_2, since crustal systems often have a higher uranium-lead ratio than the primary one. The Pb^{208}/Pb^{204} ratios do not yield an independent equation of the times t_1 and t_2, and the leads from the various

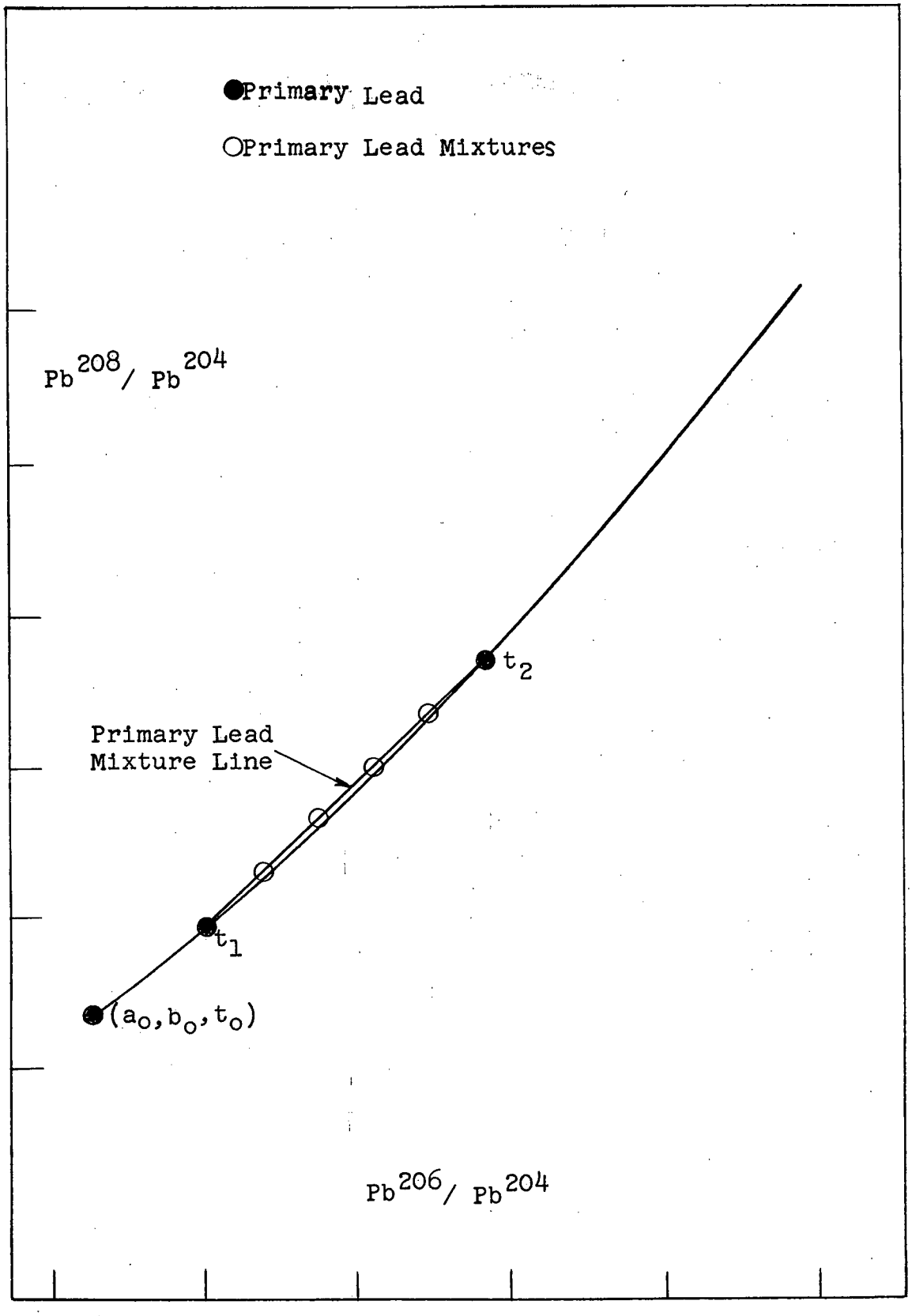

Diagram 4.8. Development of Primary Lead Mixtures:II.

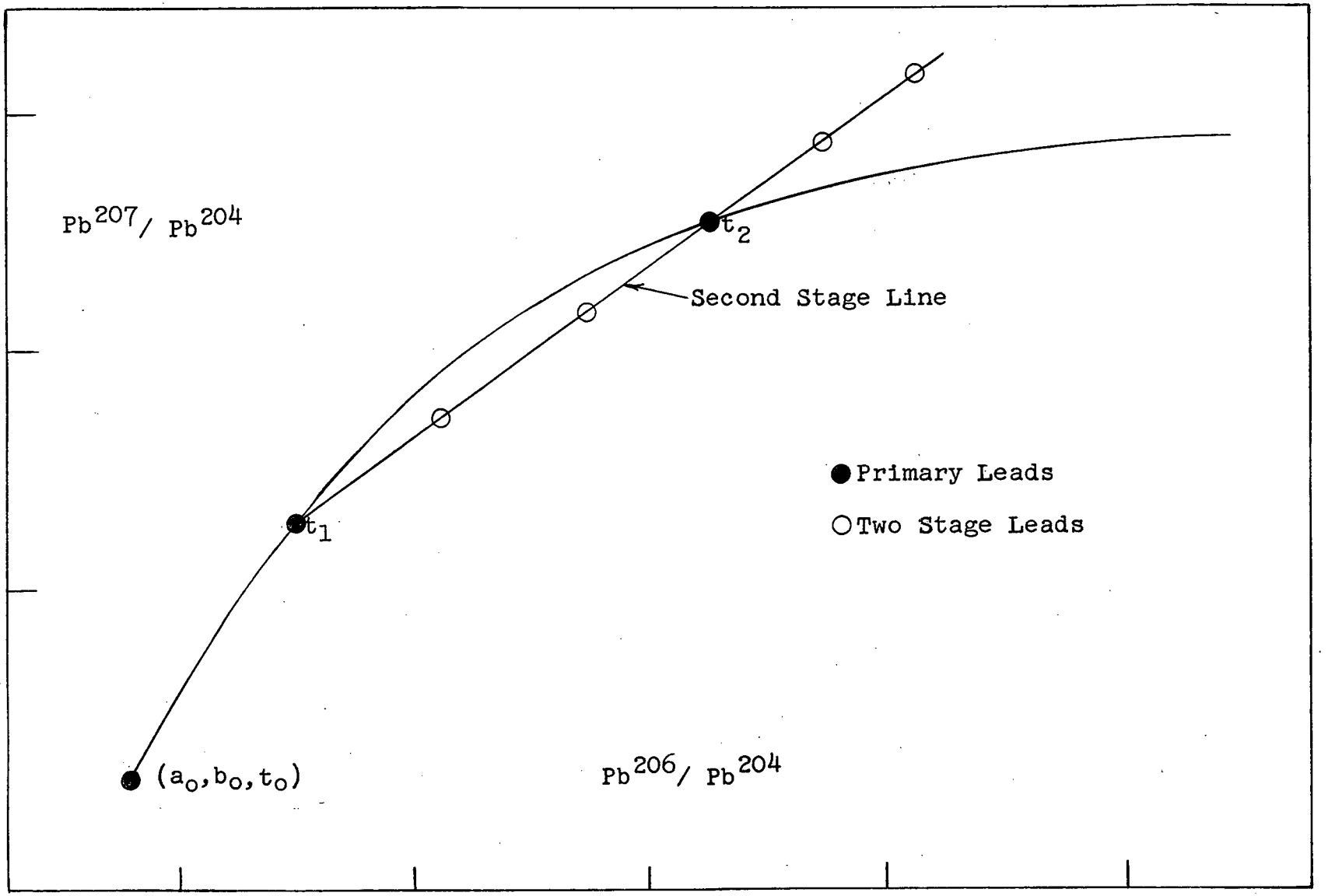

Diagram 4.9. The Development of Two Stage Leads

crustal systems may, or may not, be linearly related on the Pb^{208}/Pb^{204} vs. Pb^{206}/Pb^{204} plot. The primary growth curve in this plot results from the uranium-thorium ratio being constant at any given time. This would suggest that the uranium and thorium are chemically similar (both in the tetravalent state) in the primary system. In a crustal environment some of the uranium will oxidize to the hexavalent state while the thorium remains in the tetravalent state; hence, there may be no direct relationship between the amounts of uranium and thorium in the systems representing the second or later stages.

4.4.3 Sea Water Lead Model

Numerous present day sea water lead isotope analyses have been published (Chow and Patterson, 1959, 1962; Chow and Johnstone, 1963). Wampler (1963) has completed a study of leads in sedimentary pyrites. In most cases, a general two stage model has been used to interpret these results. For sea water leads the t_1 will be interpreted as above with t_2 being the time of extraction, due to weathering processes, and transportation to the sea. The lead is then precipitated as a trace element in pyrites, manganese nodules, and clays.

R.D. Russell and W.F. Slawson have suggested a slightly different approach. In this model t_2 is held

to be the same for all the sea water leads (the average time of leaching and deposition is likely to be less than 1 million years according to Chow and Patterson, 1959) and the uranium-lead ratio is also assumed to be fairly constant for the rocks of one area. If we then leach the lead from the source rocks of different ages (i.e. vary t_1) the resulting lead isotope ratios will lie along a curve (Diagram 4.10). We will call this the "sea water lead model". As noted above, if leads develop in a series of systems of varying uranium-lead ratios, during the second stage, a straight line results. With the sea water lead model the isotope ratios will lie along a curve A B C D if the uranium-lead ratio in the crustal systems are larger than that in the primary system. If this is not true the ratios could lie along the curve A B'C'D', below the primary growth curve. Other curves result if a different uranium-lead ratio (crustal system) is used.

This model does not apply directly to the modern sea water leads which result from weathering of areas which are different in both t_1 and the uranium-lead ratio. It also does not allow for the possibility of isotopic fractionation, and incomplete mixing, which would result in an appreciable scatter about the proposed curve. It would most probably apply to a partially enclosed bay or sea which drains areas of similar rock assemblages

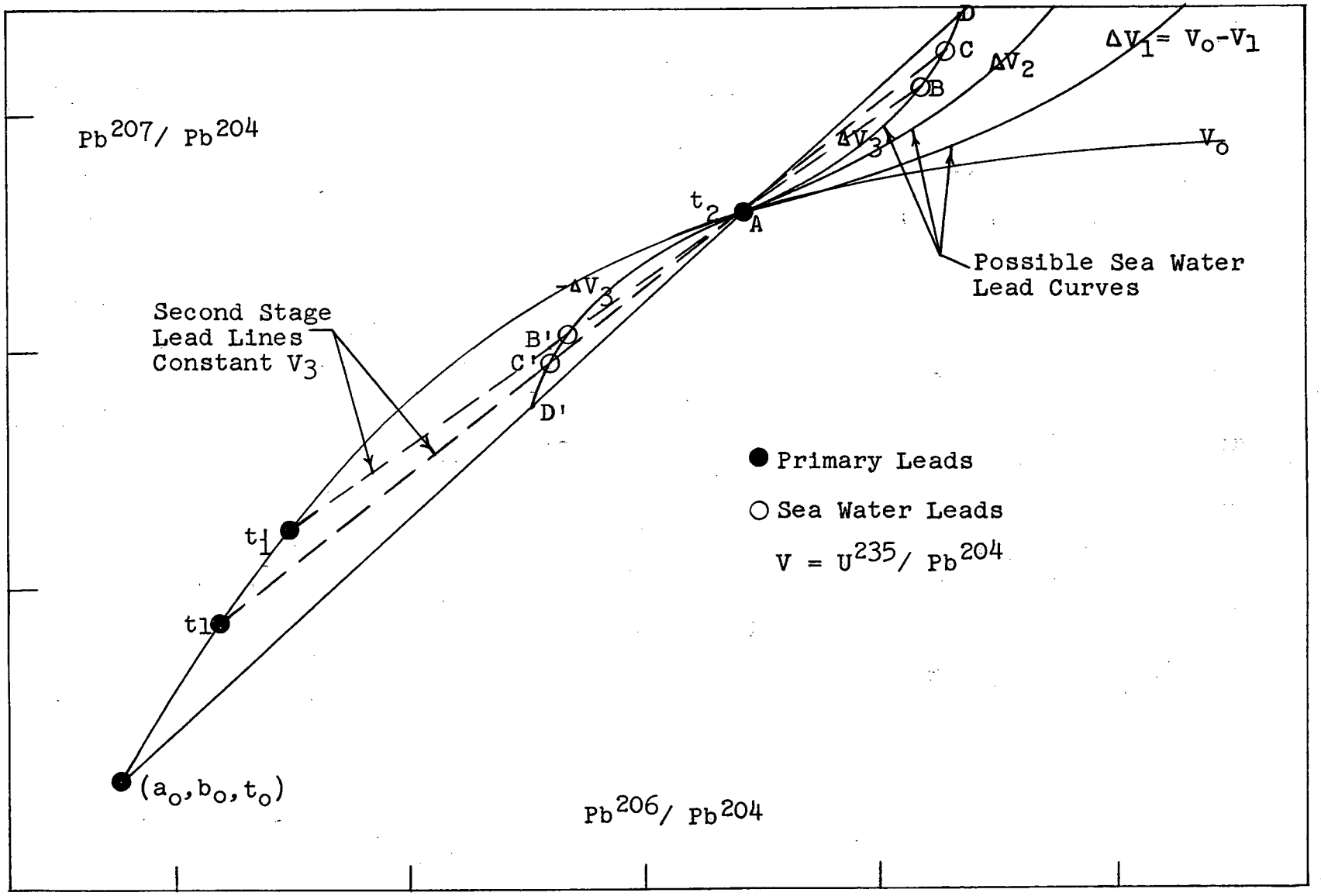

Diagram 4.10. Development of Sea Water Lead Model

but of different ages.

4.4.4 Three Stage Lead Model

If more than two events have occurred the lead isotope relationships are not likely to be simple unless extreme homogenization took place. It is possible, however, to predict certain processes that could be involved in the third stage. One of these could be the mixing of primary lead of age t_3 with two stage leads lying along the two stage line (Diagram 4.11). A family of mixing lines could thus result. This might give rise, in a special case, to a line with a negative slope, a possibility that has not been reported previously. If this actually occurs, a line should also appear on the Pb^{208}/Pb^{204} vs. Pb^{206}/Pb^{204} plot, passing through the t_3 position on the primary curve, regardless of the position of the second stage point on this plot (Diagram 4.12). The Stillwater comples analyses fit this model remarkably well.

A second process could involve the mixing of second stage leads with radiogenic lead developed between t_2 and t_3. This would result in a family of lines parallel to that joining t_2 and t_3 on the growth curve on the Pb^{207}/Pb^{204} vs. Pb^{206}/Pb^{204} plot (Diagram 4.13). In this case, no linear relationship is expected on the Pb^{208}/Pb^{204} vs. Pb^{206}/Pb^{204} plot since uranium and

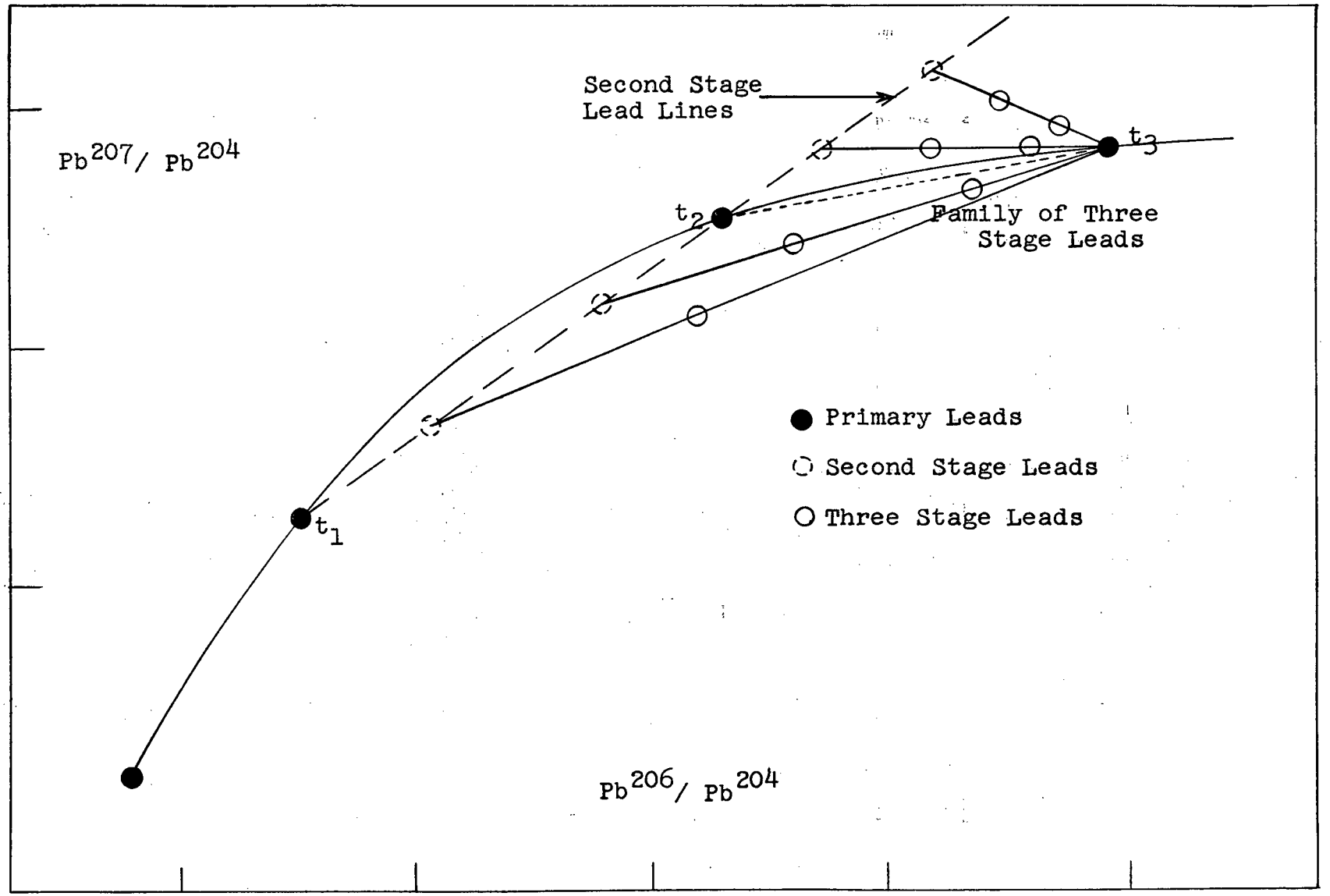

Diagram 4.11.Third Stage Leads as a Mixture of Second Stage Leads and Primary Lead of Age t_3:I

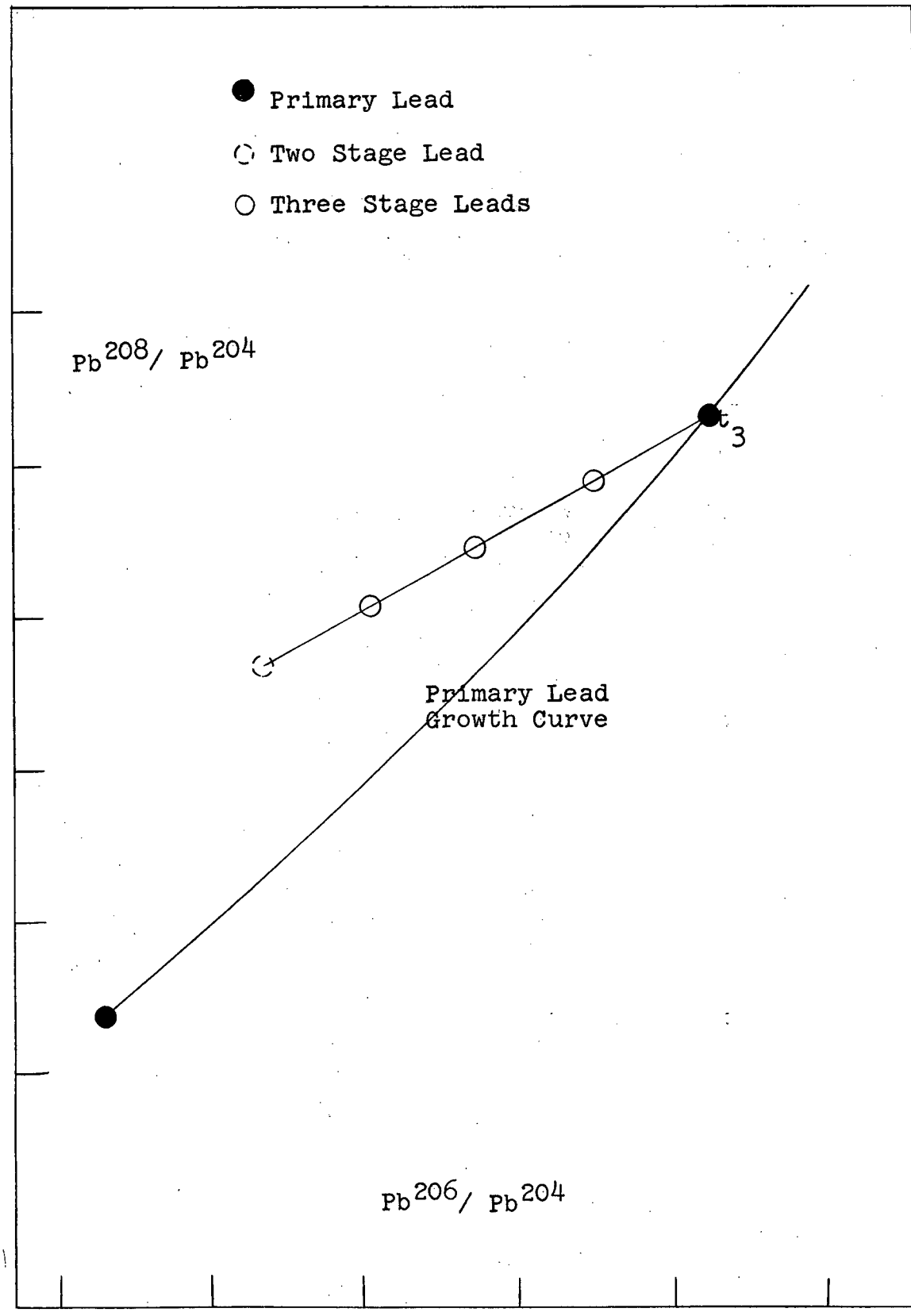

Diagram 4.12. Third Stage Leads as a Mixture of Second Stage Lead and Primary Lead of Age t_3:II

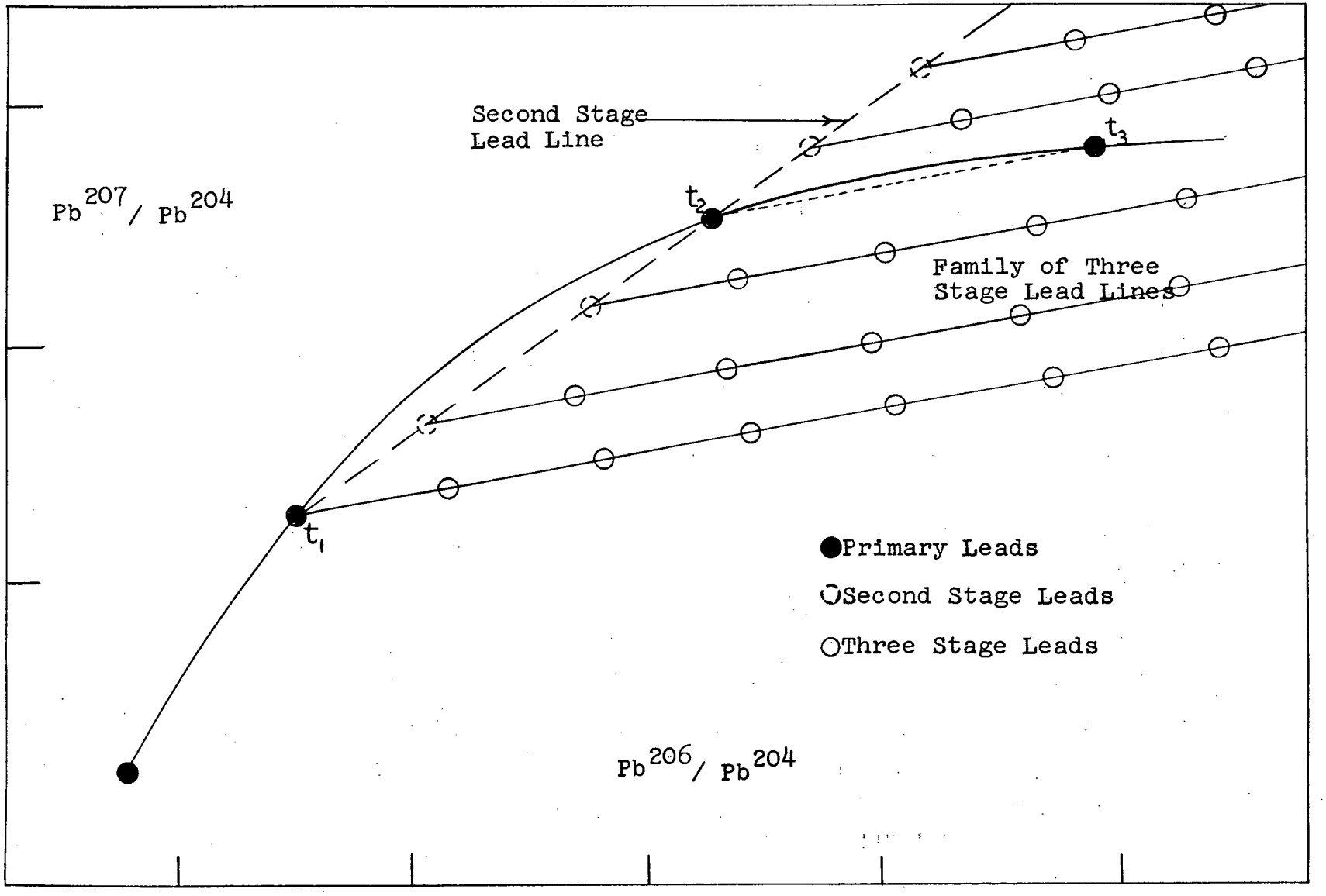

Diagram 4.13. Third Stage Leads as a Mixture of Second Stage Leads and Radiogenic Lead Generated Between Times t_2 and t_3

thorium differ geochemically in a crustal environment. If the lines due to these two processes do exist they are likely to be observed in samples collected in localized areas; over a larger region, the results could lie anywhere in the 3rd stage area shown in Diagram (4.14).

It might be noted that if a line is obtained on the Pb^{207}/Pb^{204} vs. Pb^{206}/Pb^{204} plot as the result of either of these processes, the intersection of this line and the primary growth curve (if such an intersection exists) would represent a minimum time for t_1.

4.5 Examples of Multi-Stage Leads

4.5.1 Stillwater Ultrabasic Complex, Montana

A geological map of this area is given in Diagram (4.15) showing the relation of the Stillwater Complex to the Beartooth Mountains. The probable history of events in this region has been discussed by Eckelmann and Poldervaart (1957), Catanzaro (1961), and Kulp et al (1963b).

(1) Deposition of Archean sediments (source rocks greater than 3140 my.).

(2) Folding, mafic and ultra-basic plugs, dykes and sheets.

(3) Metamorphism and granitization (2700 my.).

(4) Uplift.

(5) Peneplanation

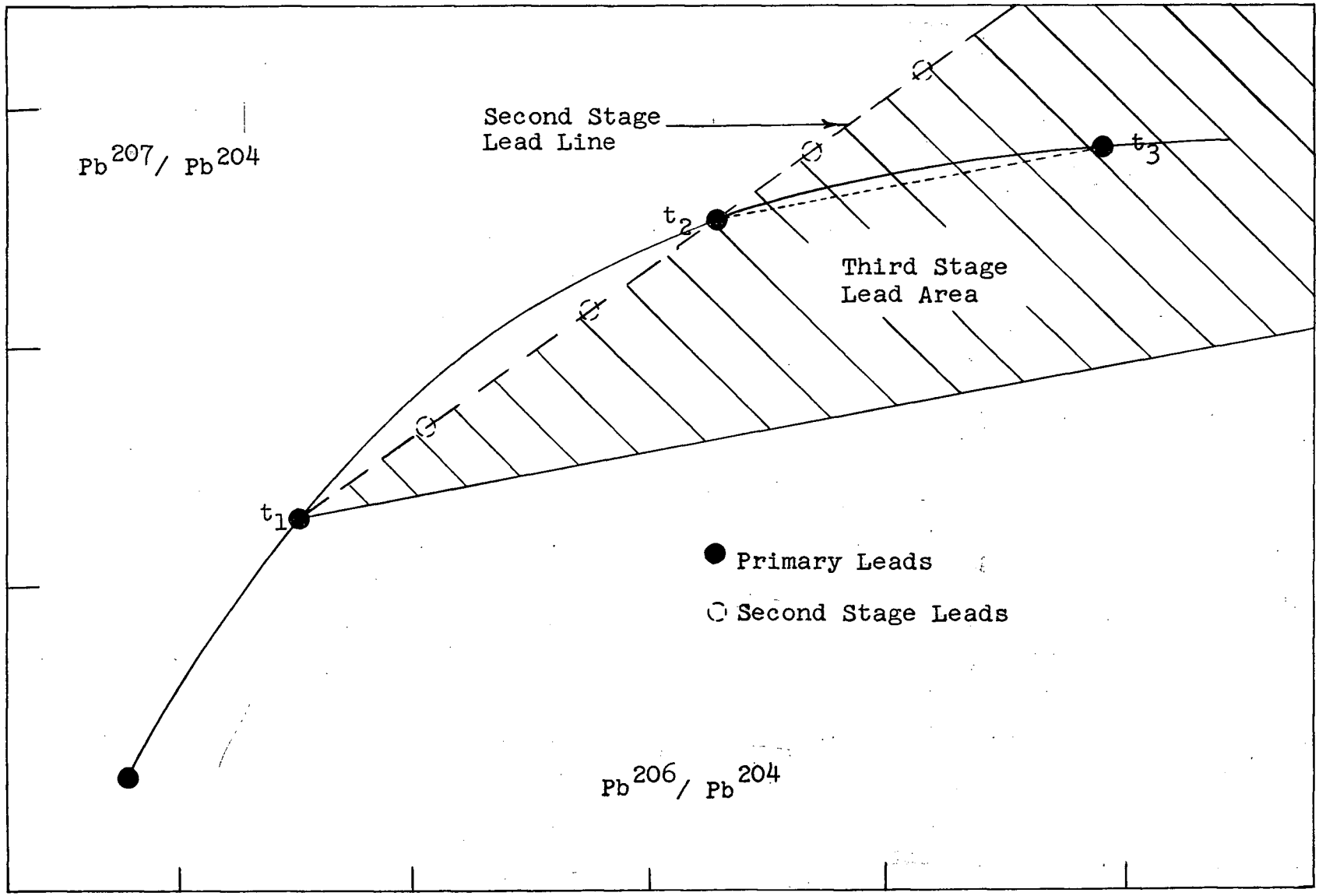

Diagram 4.14.Possible Location of Three Stage Leads on the Pb^{206}/ Pb^{204} vs. the Pb^{207}/ Pb^{204} Plot

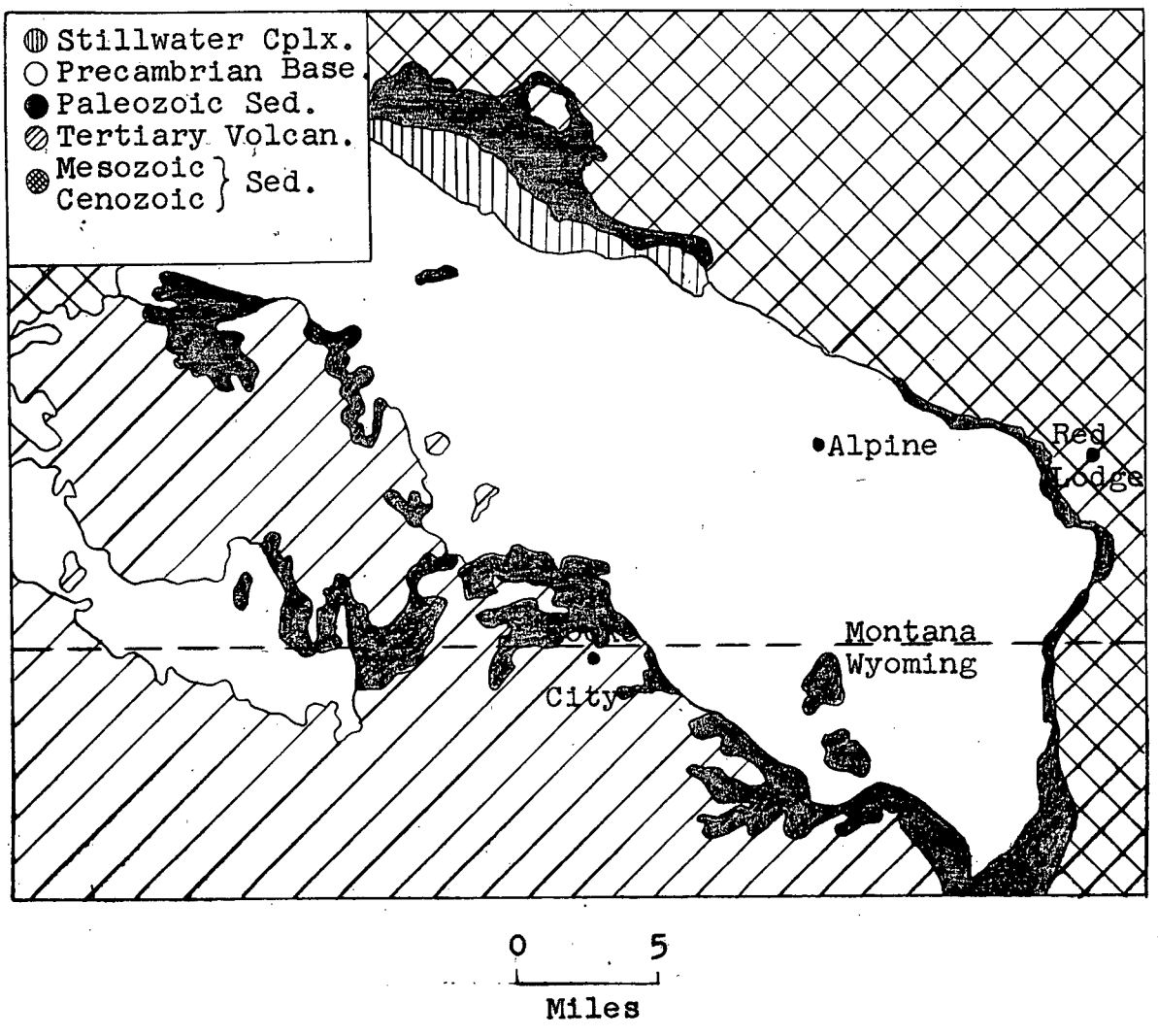

Diagram 4.15.Geological Map:Beartooth Mountains and the Stillwater Complex (Harris Jr.,1959)

(6) Deposition of Paleozoic and younger sediments.

(7) Uplifting, thrusting, emplacement of felsic porphyry dykes (120 my.?).

Hess (1960), Bucher et al (1934) and Foose et al (1961) have also discussed the geology. The 2700 my. event is well documented by Rb-Sr, and K-A analyses (Gast et al, 1958). It is believed that the Stillwater Complex was emplaced before this event.

Catanzaro (1961) analysed a number of zircons from this area and found that the results could best be explained by episodic lead loss. By this hypothesis the zircons are greater than 3140 my. old; during the 2700 my. event they lost varying amounts of radiogenic lead and younger zircon material (overgrowth) was formed. All the samples were then thought to have lost some radiogenic lead at 120 my. when the Laramide porphyries were formed. Catanzaro suggested that "the 120 my. episodic loss in the Little Belt and Beartooth mountains might have been due to leaching of radiogenic lead from the zircons by alkaline ground water solutions which were heated and given increased circulation during the Laramide Revolution".

The present writer's analyses of lead in sulfides associated with the Stillwater Complex, fit nicely into the suggested sequence of events. These leads can be explained readily as three stage leads, with the first event at $t_1 > 3000$ my. At this time primary lead was extracted from depth and emplaced in a crustal system.

At the t_2=2700 my. event two possibilities arise. Firstly, the leads could be extracted from the first crustal system and placed in a second one; if such leads were remobilized during the Laramide Revolution (t_3) and isolated in the sulfide, they could lie along lines parallel to the "Third Stage Lead Model II" line in Diagram (4.16). Or, alternately, the leads could be extracted at t_2, and separated from the uranium and thorium; at t_3 they could have mixed with primary lead of age t_3 (Third Stage Lead Model I, Diagram 4.16). This latter possibility is given added weight by the linear relationship observed in Diagram (4.17). As noted earlier the mixing model requires just such a relationship in both of these plots. Since this appears to be the first reported suggestion of such a model, additional analyses from the Stillwater Complex could be of considerable interest.

4.5.2 Mt. Isa Area, Australia

1. Geological Considerations

The ores of Mt. Isa have well developed banding parallel to the bedding of the enclosing sedimentary rocks and are generally conformable with one particular unit of the sediments. According to J. Richards (personal communication) the area may have been a partially enclosed bay at the time of formation of the sediments. The mode of formation of the ore deposits is a matter of considerable

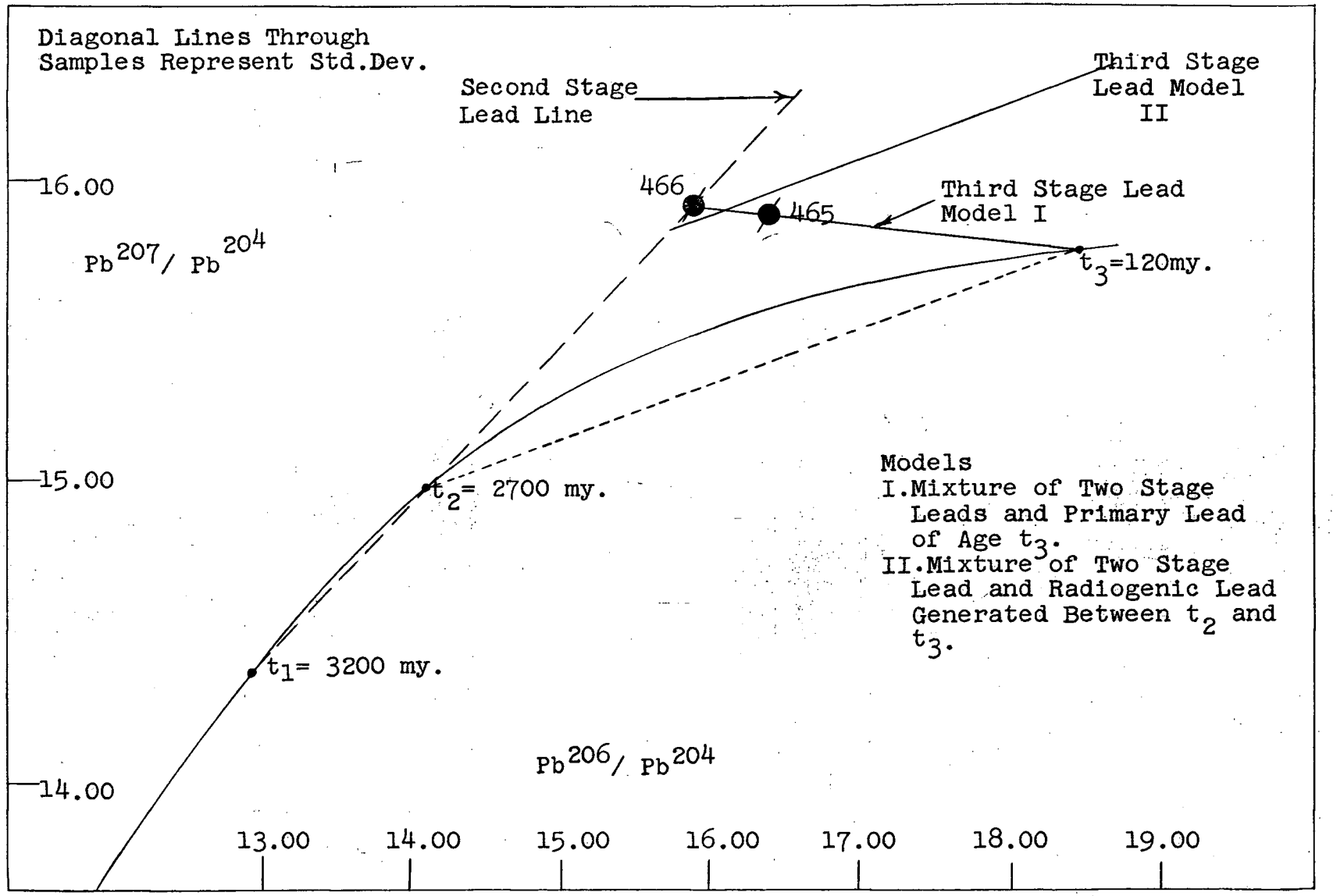

Diagram 4.16. Stillwater Complex Sulfides: I.

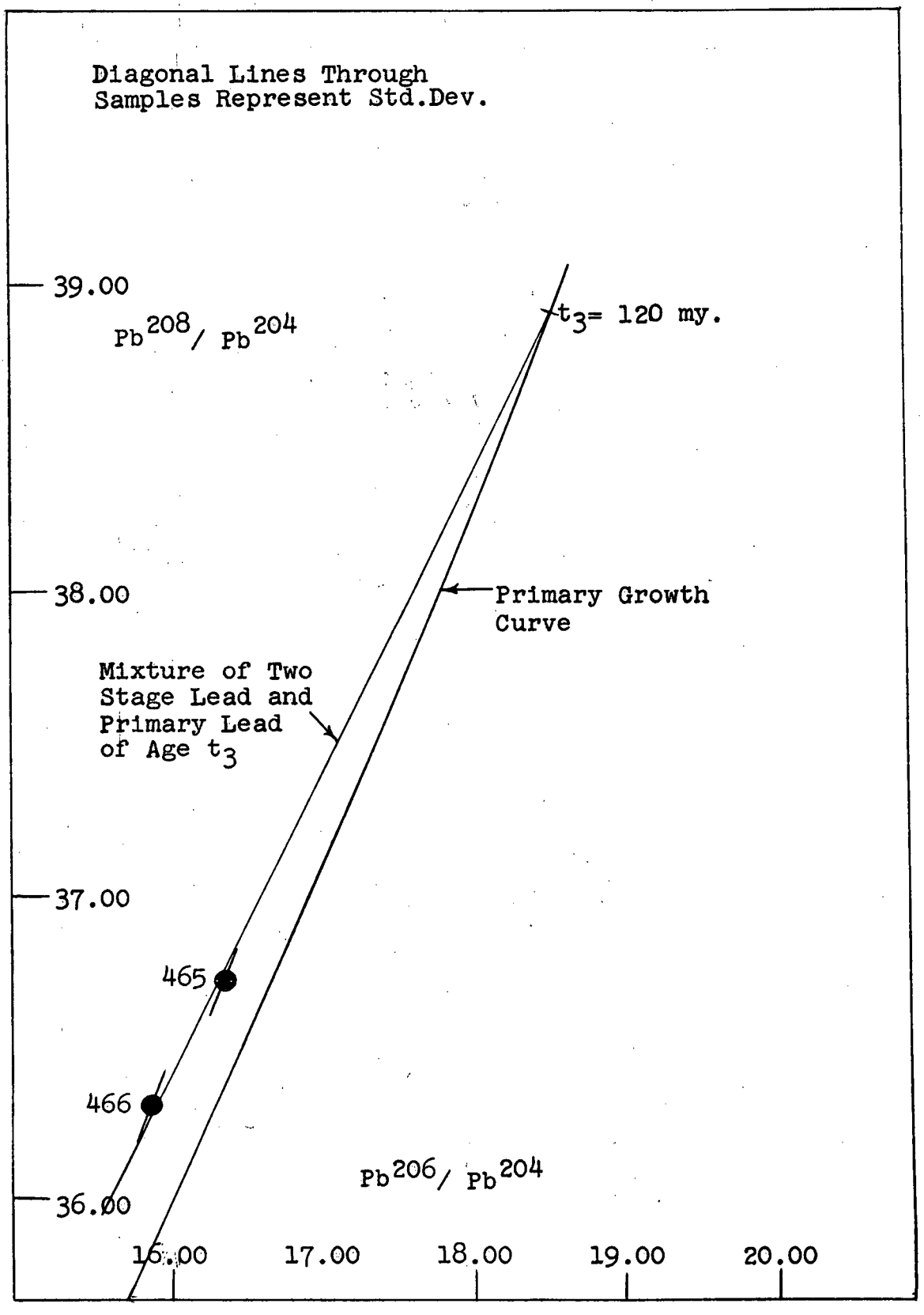

Diagram 4.17. Stillwater Complex Sulfides:II.

controversy.

Grondijs and Schouten (1937), Blanchard and Hall (1942) maintained that the ore bodies are primarily epigenetic (metasomatic replacement). This point of view does not rule out the possibility that some of the first generation pyrite may be of syngenetic origin; in fact, Love and Zimmerman (1961) have given strong evidence of this being so. Love (1962) later noted, however, that it was "not argued that the other ore bodies now formed were in the original sediment." Davidson (1962) has particularily stressed the low concentration of copper in sea waters, too low to seem an acceptable source of the conformable chalcopyrite bodies.

Stanton (1960, 1955) has forcefully argued in favor of a syngenetic origin, suggesting submarine volcanic activity as the source of the conformable deposits metals. The association of these deposits with basic volcanic tuffs, tuffaceous shales, etc. is well known. Williams (1960) and Dunham (1964) have suggested that the conformable deposits could form in enclosed basins with very slow sedimentation and hydrothermal mineralization in progess at many places below or within the drainage of the lagoon. Such a process is particularily attractive when considering the formation of some of the base metal deposits in Europe which extend over extremely large areas more or less conformable with a single zone; it is difficult to decide whether or

not it could apply to the smaller scale conformable deposits like Mt. Isa.

2. Lead and Sulfur Isotope Ratios

Analyses by Kollar (1960), Ostic (1963), and by J. Richards (personal commumication) have shown that the Mt. Isa lead-zinc ore bodies have a uniform lead isotope abundance; however, two Mt. Isa chalcopyrite samples and a galena from a neighbouring region were found to be different. The high uniformity of the main lead deposits and their primary nature would tend to rule out direct sea water deposition. Sea water leads are quite variable in isotopic ratios and tend to appear younger (isotopically) than the enclosing sediments (Chow and Patterson, 1962; Wampler, 1963). If the lead were remobilized sea water leads, or hydrothermal replacements, it is unlikely that the lead isotope ratios would be uniform with the sulfur isotope ratios varying as significantly as they do. (Love and Zimmerman, 1961).

On the other hand, if hydrothermal solutions entered a bay and contributed a high concentration of lead (at a given stage) and sulfur, one would expect a considerable bacterial sulfur isotope fractionation, and much less or no lead isotope fractionation. Because of the hydrothermal contamination, the sulfur isotope ratios should be enriched in S^{32} over that of sea water sulfates and

tend toward the meteoritic value. The lead would be primary to the extent that it was uncontaminated on its passage from depth, and uncontaminated with sea water lead. The latter contamination would depend mainly upon the relative concentrations of hydrothermal and sea water lead; certainly, as the lead content of the hydrothermal solutions decreased, sea water lead contamination would increase. This could result in later depositions (visualized here as being rich in copper) having significantly different lead isotope ratios. In addition, since copper is "notoriously lethal to life" (Davidson, 1962) we might expect these later stage sulfides to have a narrower range of sulfur isotope ratios.

This suggested sequence of events seems to agree with the isotopic analyses. The sulfur isotope data are reported in Love and Zimmerman (1961). The pyrites believed to be syngenetic by these authors had sulfur isotope ratios of $21.77 \leqslant 32/34 \leqslant 21.97$; the average was 21.88. The sulfides believed to have been deposited later are significantly lighter - eleven samples gave ratios ranging from 21.77 to 22.16 with the average being 22.05. No sulfur analyses are available for the chalcopyrites.

The lead isotope data is given in Diagrams (4.18) and (4.19). A variation of the lead isotope ratios of the main lead-zinc deposits of Mt. Isa does exist and is of the order estimated for biological fractionation; however,

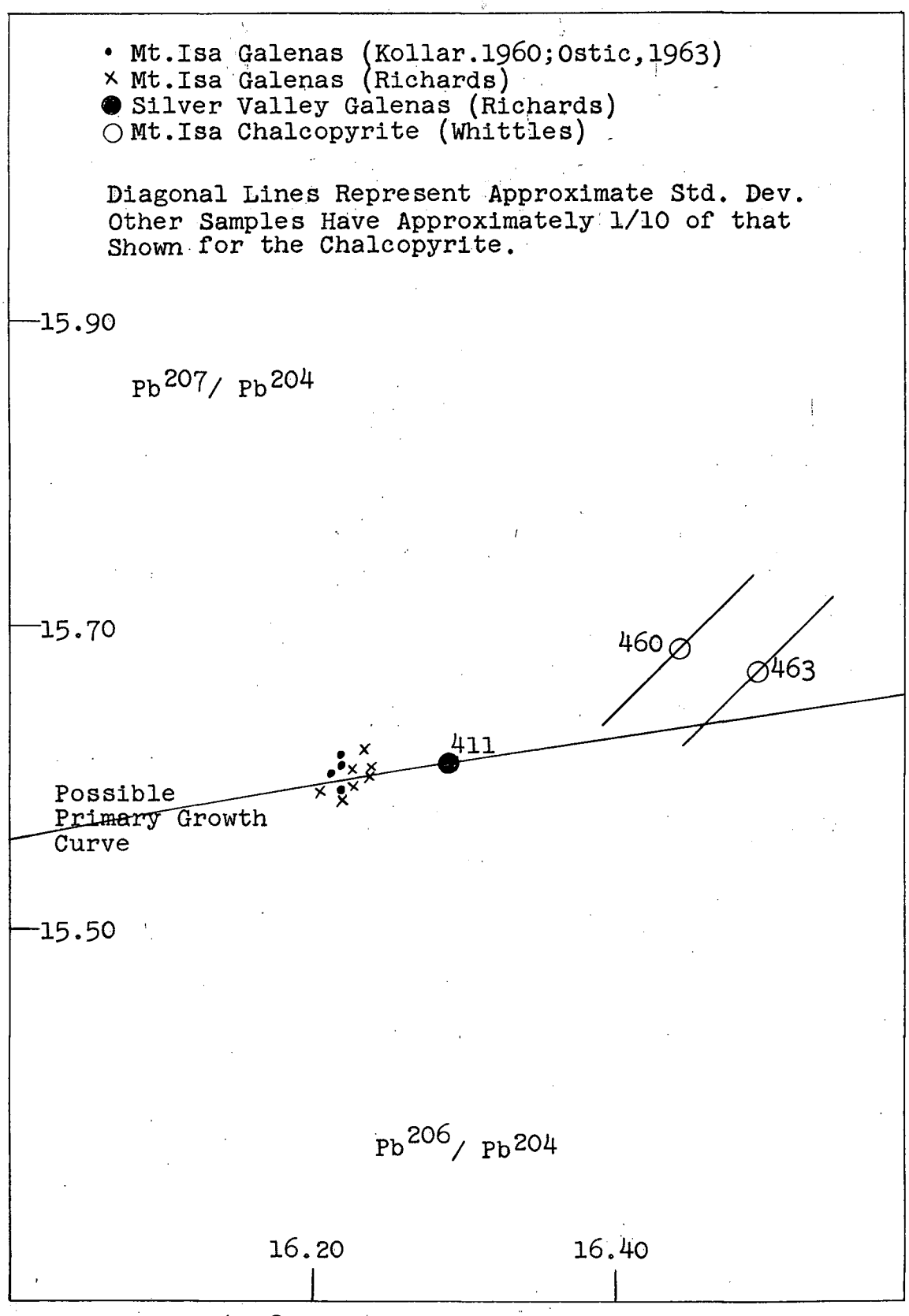

Diagram 4.18.Mt.Isa Area Leads : I.

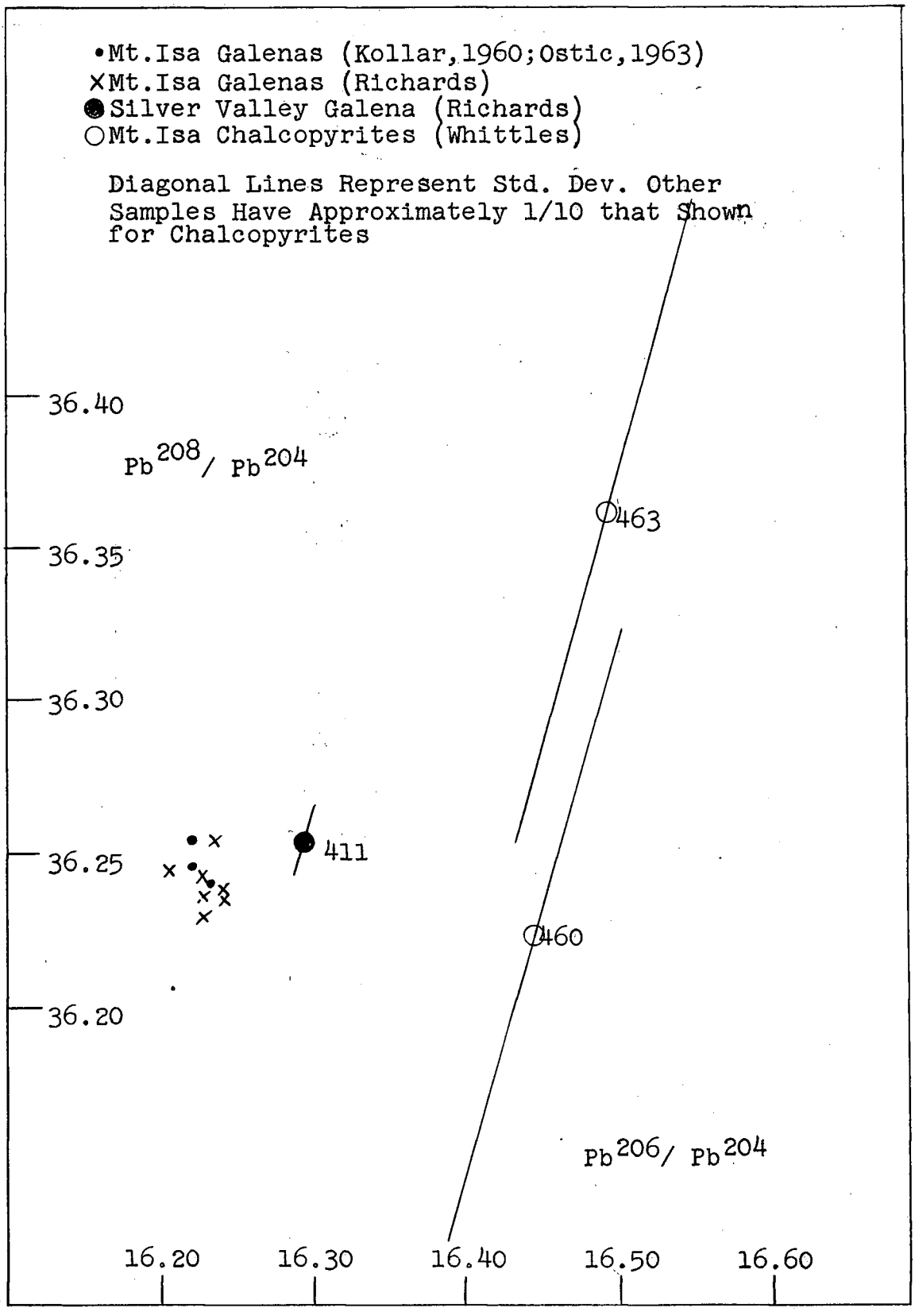

Diagram 4.19. Mt. Isa Area Leads : II.

this may be due to measurement errors. A galena sample from Silver Valley (7 mi. N.E. of Mt. Isa) is significantly different from the Mt. Isa lead-zinc samples and could represent a later development of the hydrothermal-syngenetic sequence. The chalcopyrite samples from Mt. Isa contained only small amounts of lead (=10ppm.) and the lead isotope ratios are quite different from the main lode deposits. An approximate lead isotope model is illustrated in Diagram (4.20). Several sea water lead curves are shown for different t_2, t_1, and $\Delta \frac{U^{238}}{Pb^{204}}$ values. A curve which assumes the main cluster to be primary (e.g. t_2= 1600 million years) and $\Delta \frac{U^{238}}{Pb^{204}}$= 1, seems to fit reasonably well. This model suggests that the U^{238}/Pb^{204} ratio of the source rocks was about 10.2, compared to the primary source ratio of 9.2. The age (t_1) of the source rocks could vary up to 2800 million years. This seems somewhat larger than the maximum reported for this area (2000-2200 million years) by Richards (private communication.) These values are by no means unique since t_2, $\Delta \frac{U^{238}}{Pb^{204}}$, and t_1 can be varied in several ways to give a good fit to the data.

The results do, however, indicate the suggested model is not unlikely. The deposition of the lead, wholly or mainly from dissolved sea water lead, or from remobilized sea water lead, does not fit the isotope data.

4.5.3 Southern Finland

On the basis of the present writer's precise analyses

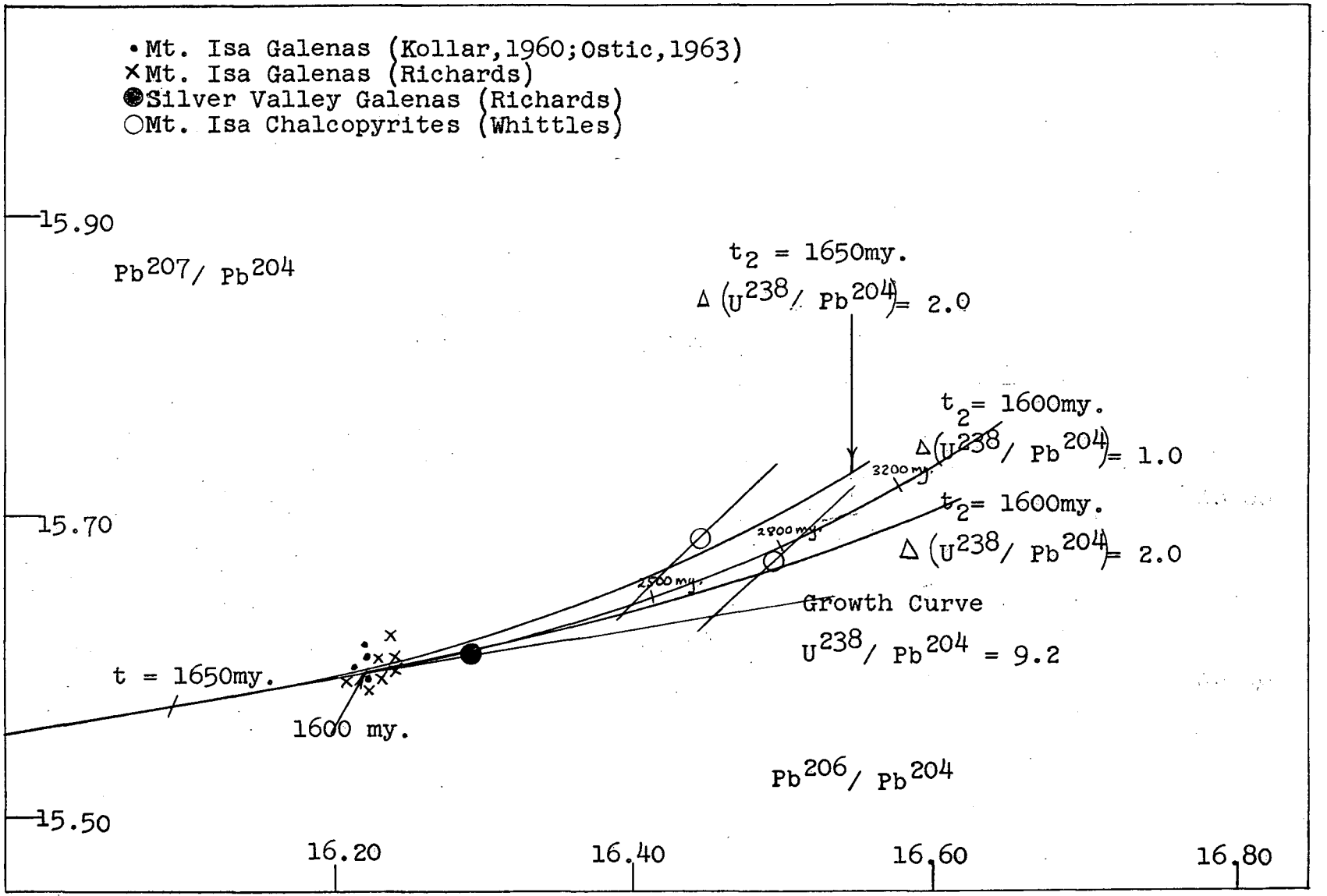

Diagram 4.20. MT. Isa Area Leads Interpreted as Primary Lead - Sea Water Lead Mixtures

of nine galenas from Finland it is possible to re-evaluate previous lead isotope data and correlate it more meaningfully with the results obtained by other means.

1. Geological Considerations

The geology of S.W. Finland is illustrated in Diagram (4.21). Detailed references may be found in the reports of Vaasjoki and Kouvo (1959), Kouvo and Kulp (1961), Wetherill et al (1962) and Wampler (1963). Four major units are of interest.

(1) Pre-Karelian (Saamian) granite gneiss basement. The zircon, microcline, muscovite and galena samples date from 2600 to 2800 my. In contrast the biotite ages give about 1800 my. by either K-A or Rb-Sr methods, reflecting a reworking of these rocks during the Karelian orogeny.

(2) Karelian belt of metasediments and plutonic rocks separated from the Saamian basement by an erosional unconformity. Kouvo and Kulp had reported lead isotope ages of 2100 my., but the single stage model used apparently is not valid for these leads. Moreover, it now appears that the Karelian plutonic rocks are contemporaneous with those of the Svecofennian belt, and the two represent two different aspects of a single orogeny occurring about 1800 my. ago. The geological differences of these two belts (ultramafic bodies and quartzite associated with the

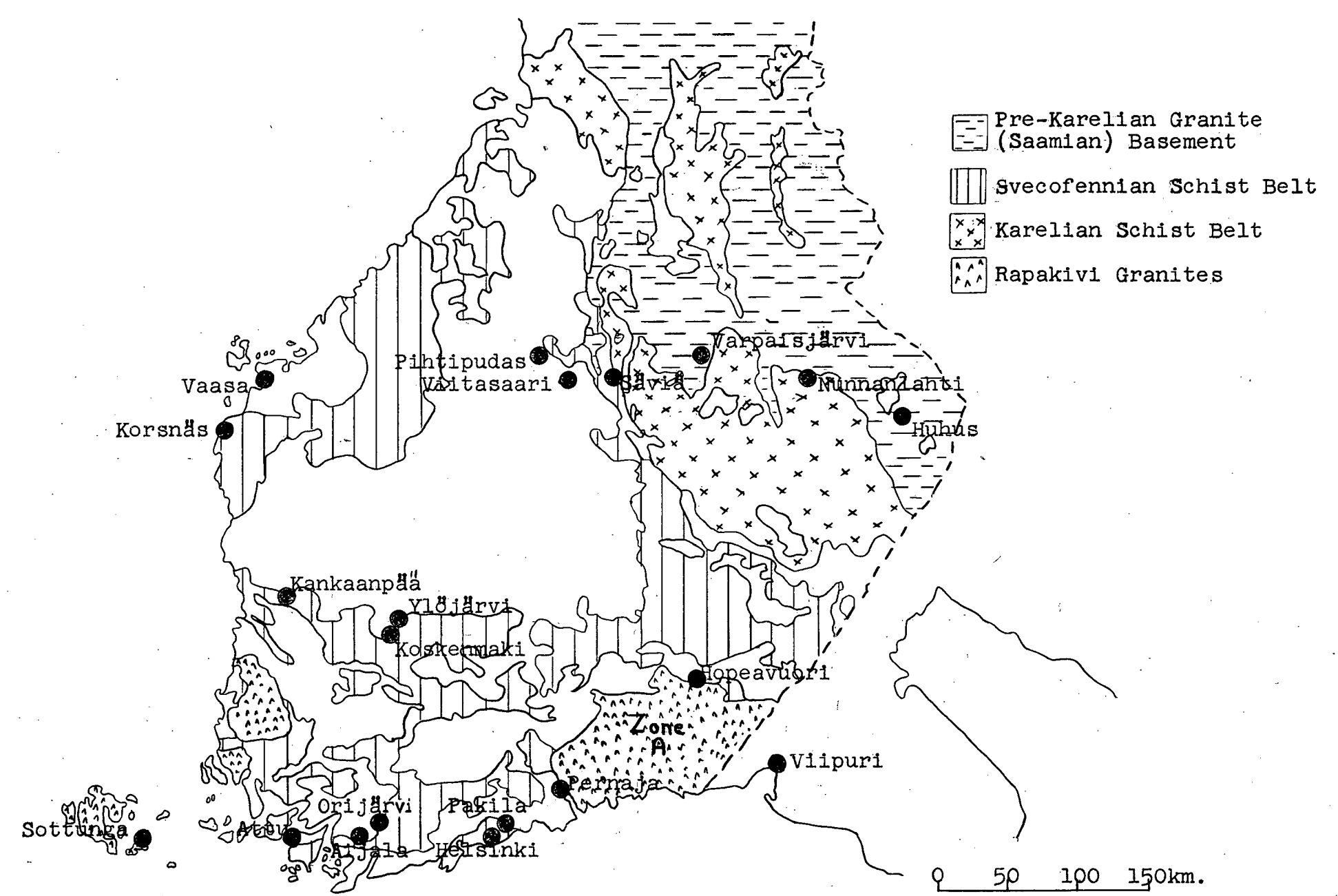

Diagram 4.21. Geologic Map of Southern Finland
(Simonen, 1960)

Karelian but not the Svecofennian rocks) were probably determined by their location with respect to the Saamian basement.

(3) Svecofennian belt of metasediments and plutonic rocks. 1800 my. ages have been obtained with all of the various dating methods.

(4) Rapakivi granites intruded about 1600 to 1650 my. ago.

(5) Later events. Although no younger ages have been reported for rocks in S.W.Finland, a later event must have occurred since sulfide veins are found cutting into the Rapakivi granites. Vaasjoki and Kouvo state that "the mineralization (e.g. the veins) as related to their Rapakivi host are undoubtedly epigenetic in character", and also that "according to the field evidence these ores occur as fissure filling and obviously are much younger than the Rapakivi host." Just when this event happened is not clear and the lead data available is not sufficiently accurate for a precise answer. The present writer has shown that the results are at least consistant with two events: the first, representing the end of the Rapakivi intrusion; the second, corresponding to the 900 to 1100 my. age values reported for Southern Sweden and Norway (Kulp et al, 1963).

2. Primary Leads

All of the new Finnish analyses obtained by the present

writer are plotted on Diagrams (4.22) and (4.23), and compared to previous analyses. Five of the samples appear to be examples of primary lead, and although they come from widely separated regions, they have practically identical isotope ratios. The remaining samples appear to represent primary lead mixtures, and three stage leads.

It is possible to interpret the Pithipudas, Pernaja, and primary samples as lying along an isochron in the Pb^{206}/Pb^{204} vs. Pb^{207}/Pb^{204} plot; however, there is good evidence that this is only accidental. Pithipudas lies close to Viitasaari (which does not fit this isochron) and both are several hundreds of kilometers from the other samples. They are also geologically different and lie close to the boundaries of the Saamian basement, Karelian Schist Belt and Svecofennian Schist Belt. Pernaja is over 400 km. from Pithipudas and lies close to a large exposure of Rapakivi granite. There is strong evidence that a similarly located sample (Hopeavuori) was affected by the Rapakivi event and it seems reasonable to assume that the Pernaja sample was also. Although more analyses are needed before a definite answer can be given, the evidence suggests that the samples in question (Pithipudas, Pernaja, and Viitasaari) are 3rd stage leads. The present writer has assumed this to be so.

3. Primary Lead Mixtures

The present writer's primary lead analyses can be

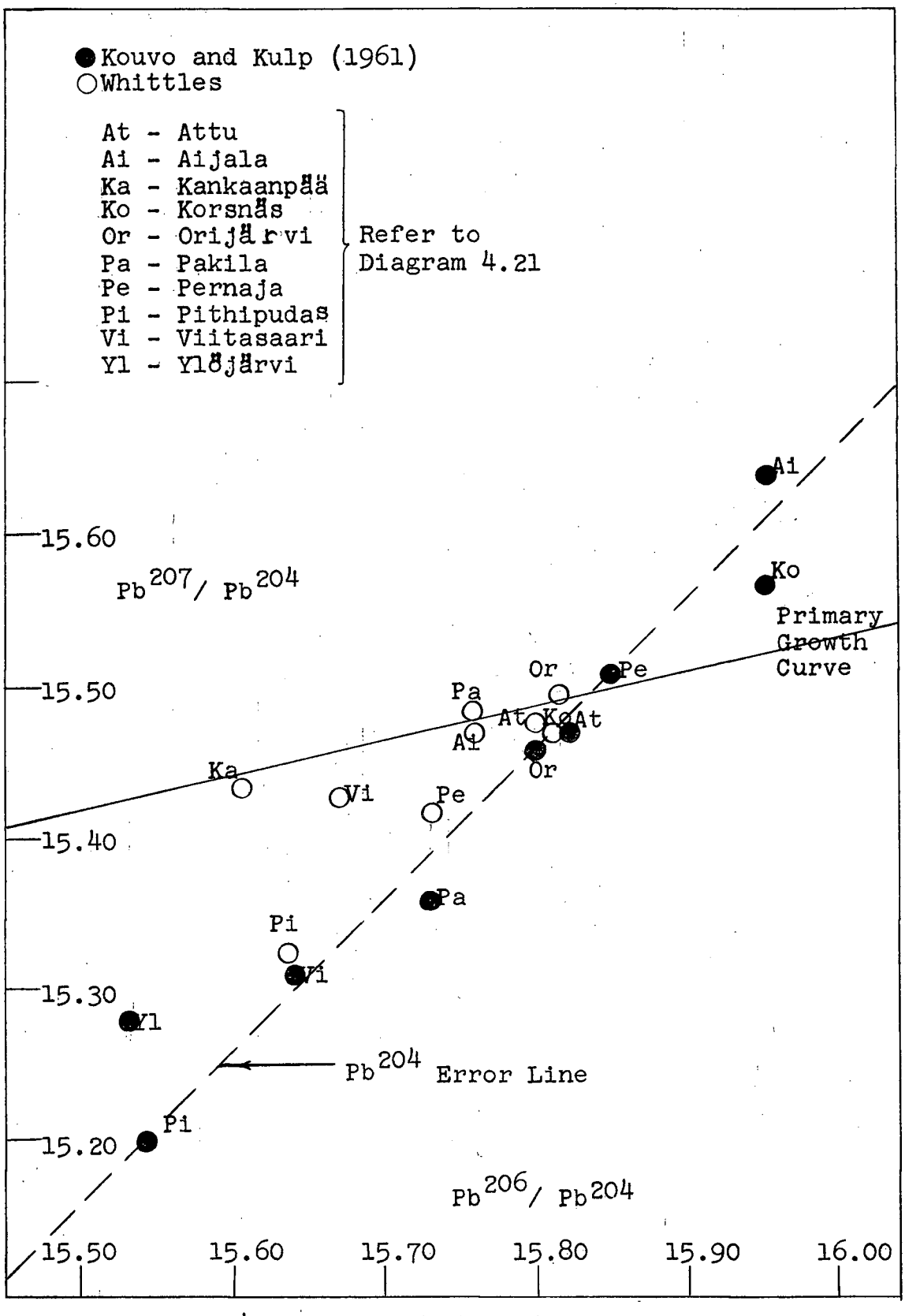

Diagram 4.22. Finnish Svecofennian Galenas:I.

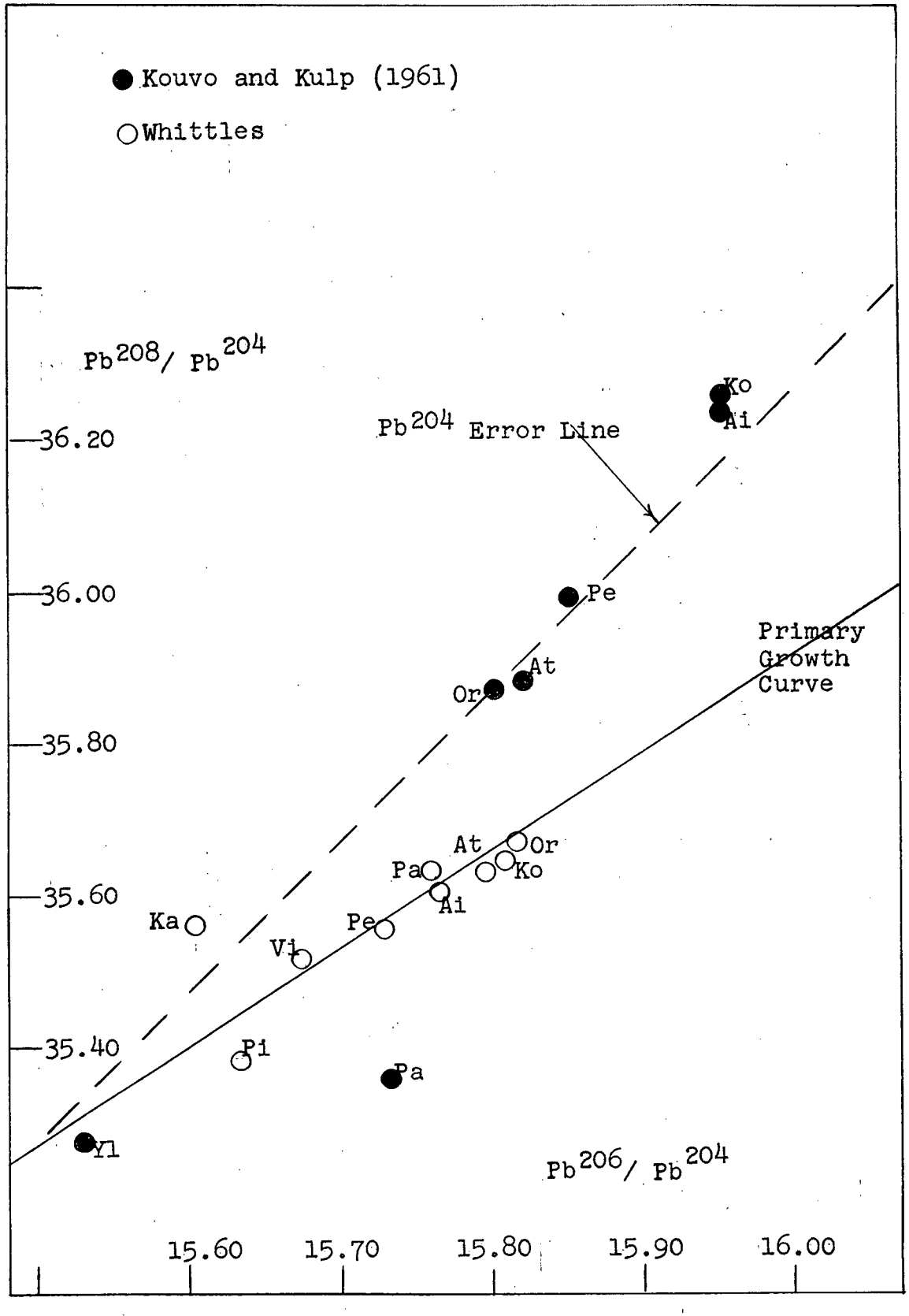

Diagram 4.23. Finnish Svecofennian Galenas:II.

used to re-interpret the lead isotope analyses of Kouvo and Kulp (1961). These analyses were averaged wherever the variations indicated Pb^{204} errors; the average Svecofennian analyses were then "assigned" isotope values the same as the average of the primary leads of the present work. The other values of Kouvo and Kulp could then be "corrected" according to their difference with Svecofennian average to remove the inter-laboratory differences (Diagrams 4.24 and 4.25).

A model that assumes the mixing of a primary lead of 2800 my. with one of 1800 my. fits the analyses quite well. Kouvo and Kulp note in particular that the "Nunnanlahti sample may represent lead sulfide remobilized from the 2800 my. basement rocks that, at this locality, may be at a very shallow depth." All of the 6 Karelian vein samples were located directly on the geological border between the Karelian rocks and ancient Saamian basement branite. 10 of the 12 Karelian ore body samples were also located on this border and the remaining two are within 75 km. Nunnanlahti, Varpaisjarvi, and Huhus lie on, or within 25 km. of the border. Since none of the analyses lie along an extension of this line beyond the 1800 my. point (Diagram 4.26) it appears that a mixing model is more adequate than the general two stage model. The Pb^{208}/Pb^{204} vs. Pb^{206}/Pb^{204} support this conclusion also. A primary lead mixture must give straight lines

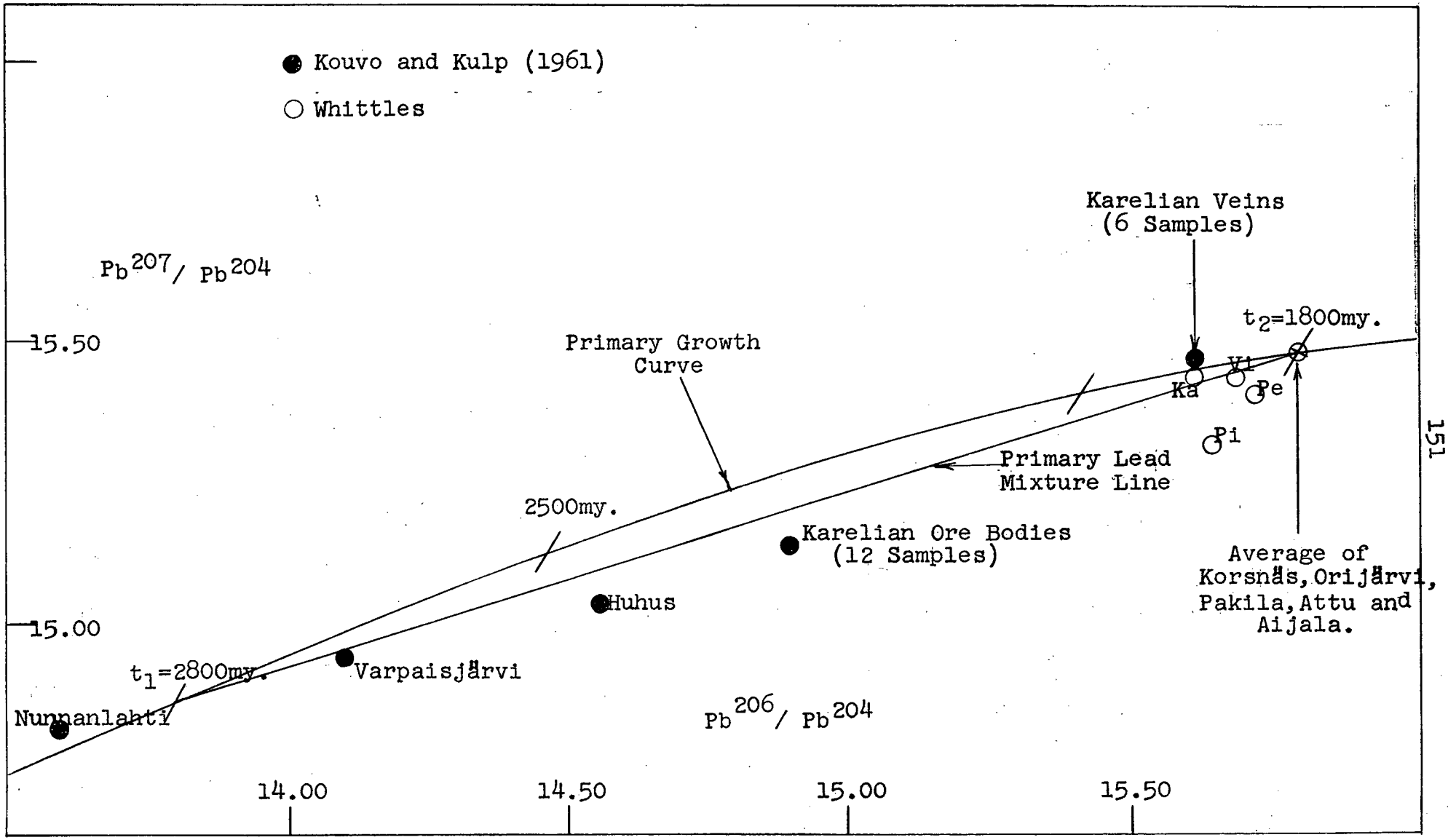

Diagram 4.24. Primary Lead Mixtures in Southern Finland:I.

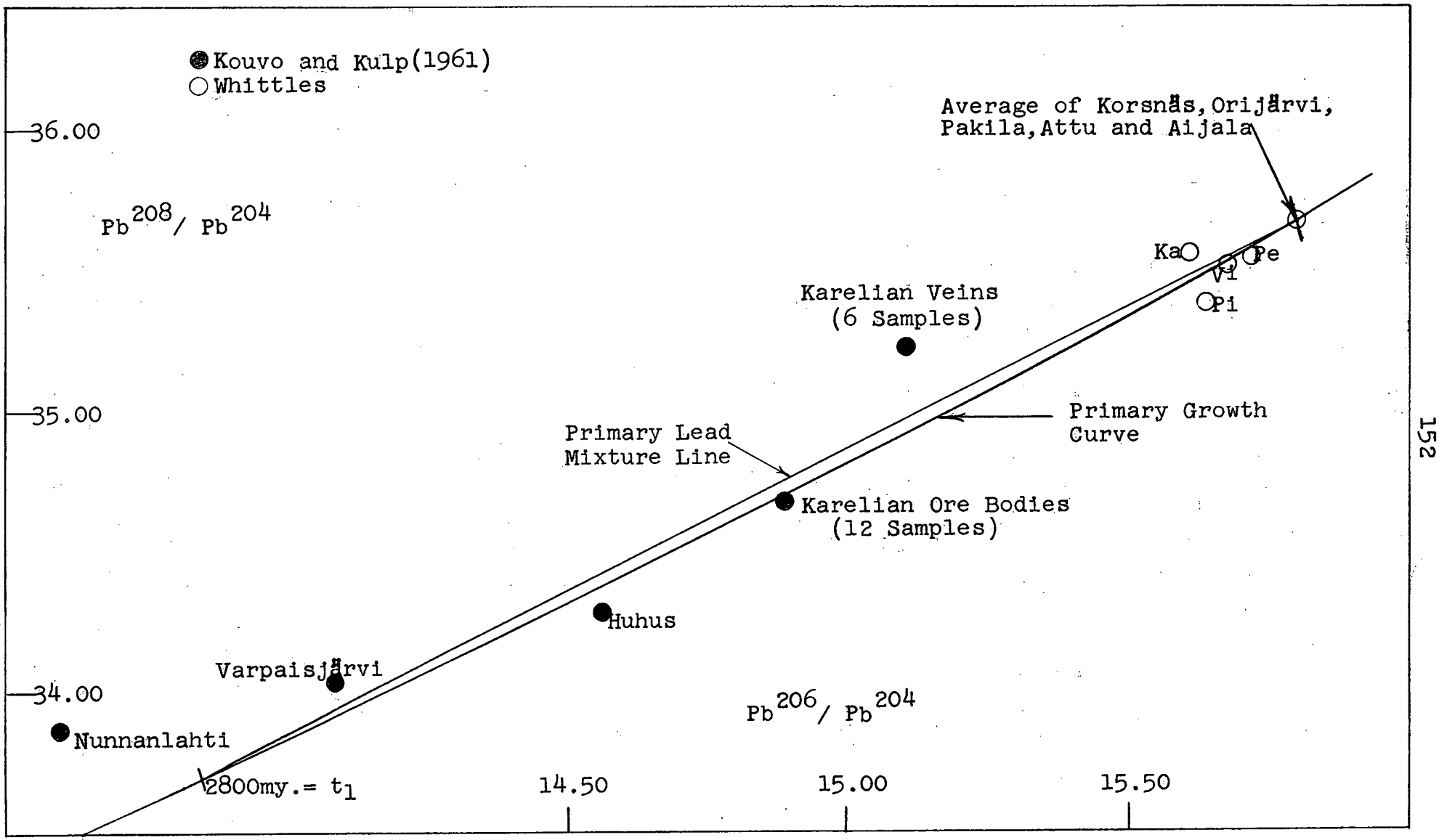

Diagram 4.25. Primary Lead Mixtures in Southern Finland : II.

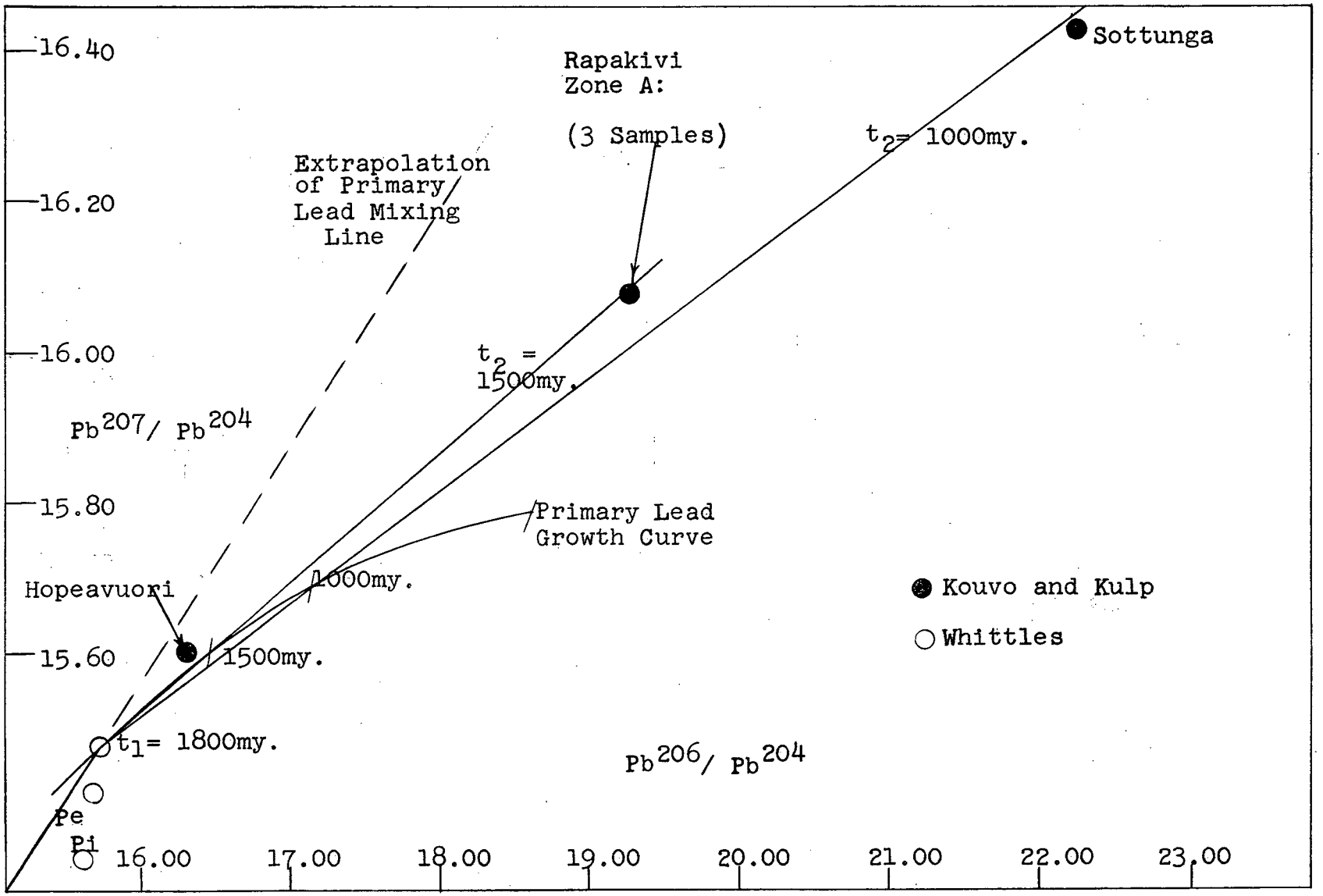

Diagram 4.26. Two Stage Leads : Southern Finland.

on both plots, whereas a general two stage lead is not likely to present this same relationship. The sulfur isotope ratios, which cluster around the meteoritic value, also indicate that most of the lead is primary.

4. Two Stage Leads.

The presence of two stage leads are also inferred in the analyses of Kouvo and Kulp (1961). Although only 4 (and another whose relationship is doubtful) samples are reported, and a considerable spread apparent, it can be shown that these analyses are consistant with the age relations of the areas. The 3 Rapakivi vein samples (Zone A, Diagram 4.21) lie along a Pb^{204} error line. They were averaged and adjusted according to the preceding standard (Diagram 4.26). The result is consistant with growth from a primary lead of 1800 my. in high uranium-lead value (crustal) systems until the close of the Rapakivi event (1600-1500 my.). The lead was then extracted at this time and isolated in the veins cutting the granite. The sulfur isotope ratios range in a group from 21.40 to 21.60, the lowest of those reported.

The Hopeavuori sample cannot be explained in terms of Pb^{204} errors. This sample was located in a small mineralization about 1/2 km. from the contact of the Rapakivi. Its sulfur isotope ratio ($S^{32}/S^{34}=21.93$) is the closest to those of the Rapakivi veins of any of the

samples reported. The lead isotope ratios are consistent with its formation at the same time as the Rapakivi veins.

Both the lead and sulfur isotope analyses, suggest that the last sample (Sottunga) is not part of the above group. In addition, a Pb^{208}/Pb^{206} vs. Pb^{207}/Pb^{206} plot shows that a Pb^{204} error does not explain its difference from the Zone A Rapakivi vein samples. The sulfur isotope ratio is 22.60, the second highest of those reported. The lead isotope ratios suggest that the lead formed from primary lead of 1800 my., and radiogenic lead formed between 1800 my. and 1000 my. (Diagram 4.26). Since Sottunga lies off the coast, midway between Finland and Sweden, this sample (from a vein in an outcropping of Rapakivi granite) may represent the effects of the 900-1100 my. event in the Gothic belt in southern Norway and Sweden.

5. Three Stage Leads.

Three of the samples (Pernaja, Pithipudas, Viitasaari) analysed in this work do not appear to be primary leads or primary lead mixtures. Although the evidence is not sufficient for a definite answer, the results suggest a three stage development (Diagram 4.27). On the basis of this model it is postulated that these samples represent primary lead mixtures that were emplaced in a uranium-thorium bearing system. They were then removed at the

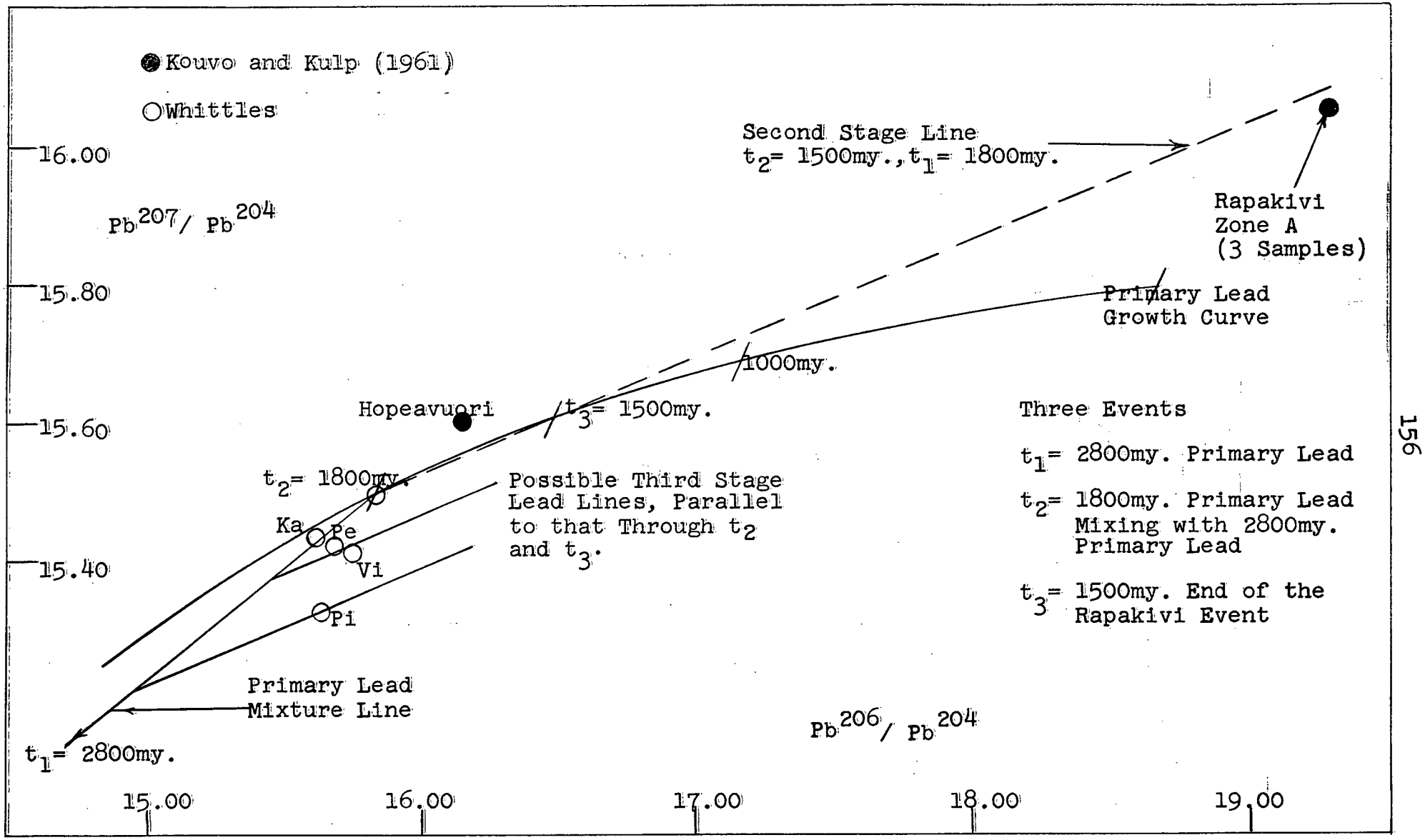

Diagram 4.27. Possible Development of Finnish Three Stage Leads.

close of the Rapakivi event and isolated from the radioactive parents. Alternately, they may represent remobilized primary lead mixtures that were mixed with radiogenic lead (generated between t_2 and t_3) at t_3=1500 my. Such leads could lie along lines which are parallel to one joining t_2 and t_3 on the growth curve. These results suggest that the Rapakivi event was not limited to the south-western coast but may have extended into the central regions.

4.6 Summary

Lead isotope fractionation in nature is likely to be rare, and at present there is no good evidence that it occurs at all.

The primary lead model more adequately describes single stage leads than does the isochron model, the primary isochrons being either very short or else non-existant. However, the primary lead model does not explain the lead isotope ratios of the conformable chalcopyrite deposits of Mt. Isa, nor those of the sulfides from the Stillwater Complex. These, and the analyses of some galenas from Southern Finland, have been interpreted using multi-stage models developed from the primary lead model.

CONCLUSIONS

"Science is a series of sucessive approximations, each of which must be valid, but none of which will ever be true."

-W.O. Davis in Analog, May, 1962

The present research contributes to all three phases of lead isotope analyses - the preparation of the tetramethyllead from a sample, the mass spectrometric analysis, and the interpretation of the results. The uniting thread of the thesis has been the attempt to prepare, analyse, and interpret samples containing only microgram quantities of lead. Analyses of galenas, using standard techniques, have also been completed to supplement the micro-lead analyses, and to justify and illustrate the lead models used in the interpretation.

A new technique has been devised based on the free radical technique reported earlier by Ulrych (1962). The success of the present writer's technique lay mainly in discovering that sample lead can be lost through its reaction with the quartz in the apparatus and the formation of the silicate $xPbO \cdot SiO_2$. Other losses can occur in the purification of the tetramethyllead. It is now possible to produce tetramethyllead from samples containing one to two orders less lead than the minimum 500-1000 micrograms reported earlier. Unfortunately, the full extent of the method cannot be utilized since it has been discovered that the present mass spectrometer sensitivity limits the most precise analyses to

samples of about 500 micrograms lead. This means that only fair precision (0.4%) can be obtained with samples of 10 ppm. lead. This research does, however, indicate that gas source mass spectrometry may be able to compete with solid source techniques, provided the sensitivity of the gas source instruments can be increased sufficiently. This is important, since it appears that gas source analyses are more reproducible (Ulrych, 1962) if intercomparison techniques can be used. This development would offer some interesting possibilities indeed.

The present writer has also explored the mass spectrometric aspects of analysing small tetramethyllead samples, a topic about which little was known. A most exciting development appeared in this phase of the research - the first reported occurrence of lead isotope fractionation. Such fractionation appeared if the sample passed from the sample line into the mass spectrometer under conditions of molecular flow. This unexpectedly limits small sample analyses to a sample line pressure of not less than about 1.0 cm. Hg, which is just below the usual operating pressure of the present instrument. Thus, with the present mass spectrometer sensitivity, smaller samples (< 500 micrograms lead) cannot be analysed as pure tetramethyllead; if they are initially purified a carrier must be added to bring the pressure up above the molecular range.

More significant, probably, are the geophysical aspects of lead isotope fractionation in nature, and the effects of fractionation on the interpretation of leads in terms of lead isotope models. The present writer's preliminary exploration of this aspect suggests that such fractionation is likely to be rare except, possibly, in leads derived from sea water.

One other aspect of mass spectrometry has also been clarified. The present research has shown that pressure scattering - the scattering of trimethyllead ions during their passage through the mass spectrometer - is distinctly asymmetrical in character. The spectral peaks exhibit a previously unsuspected extreme down mass tailing. A correction for this scattering has been devised and is shown to result in more reproducible analyses.

The contribution of this thesis to interpretation of lead isotope abundances has been four-fold. Firstly, the results of the lead isotope analyses of samples from southwestern Finland show that the previously reported primary isochrons for this area are most probably due to errors in measuring the lead 204 abundance. This is added support for the primary lead model proposed by Russell (1956). Secondly, it has been shown that the leads in the conformable chalcopyrite deposits of Mt. Isa are not of direct primary origin, although those of the massive lead-zinc deposits apparently are. Thirdly, it

has been shown that the lead in ultrabasic sulfides are not necessarily primary. Fourthly, it is here suggested that primary leads, excepting those that have had contact with the sea, should have sulfur isotope ratios which correspond closely, in most cases, to the meteoritic value.

The new analyses for southern Finland can be used to reinterpret the older lead isotope data; the resulting interpretation is more in accord with age determinations based on other methods. The first event occurred 2800 million years ago when primary lead was emplaced in the ancient Saamian basement rocks. At 1800 million years a second orogeny, the Karelian - Svecofennian event, introduced more primary lead, some of which mixed with the older primary lead. The previously reported 2100 million year age of the Karelian event is incorrect since it fails to account for this primary lead mixture. A third event occurred at 1500-1650 million years, the time of intrusion of the Rapakivi granites. One of the earlier reported analyses for Sottunga (midway between southern Finland and Sweden) appears to reflect the effects of a fourth period, the 1000 million year Gothic Belt event of southern Norway and Sweden.

The composition of the lead in the conformable chalcopyrite bodies of Mt. Isa is quite different from that in the primary massive lead-zinc bodies. These

deposits could have been the result of metal-bearing solutions entering an enclosed bay. Remobilized sea water leads and/or epigenetic replacement seem to be less likely possibilities when both the lead and sulfur isotope data are considered.

Samples of sulfide obtained from the ultrabasic Stillwater Complex, Montana, appear to contain multi-stage lead. The events of this growth are in accord with those suggested earlier by Catanzaro (1961) on the basis of his study of discordant zircons: >3000 million years, 2700 million years, and approximately 120 million years. On the other hand, a sample from the ultrabasic deposit near Hope, B.C. could be of primary origin. More careful sampling, and an increase in gas source mass spectrometer sensitivity is required before the Stanton and Russell (1959) primary lead hypothesis can be adequately tested in terms of ultrabasic sulfides.

APPENDICES

"-the book of nature is written in the mathematical language,...without its help it is impossible to comprehend a single word of it."

-Galileo Galilei as quoted by A. Koestler in The Sleepwalkers.

Appendix A.1. Isotopic Fractionation and Molecular and Viscous Flow.

A.1.1 General Definitions

Most of the basic definitions were found in the review by Loevinger (1949).

(1) The Conductance and Flow

The conductance C of a pipe through which gas is flowing may be defined by:

$$C = \frac{Q}{P - P_2} \qquad \text{(A.1-1)}$$

where P = pressure at entrance of pipe

P_2 = pressure at exit of pipe.

Q is proportional the number of molecules passing a plane in the pipe in a given time, and is defined by:

$$Q = P_z \left.\frac{dV}{dt}\right|_z$$

where $\left.\frac{dV}{dt}\right|_z$ = volume of gas flowing per unit time across any plane z in the pipe.

P_z = pressure in that plane.

(2) Flow through Circular Pipes: General

If the density in a flow system increases beyond a point given approximately by the Reynolds' number:

$$R_e = \frac{Dv\delta}{\eta} \qquad \text{(A.1-2)}$$

where D = diameter of pipe

V = velocity of gas

δ = density of gas

η = viscosity of gas.

the flow may change from laminar (viscous) to turbulent. This transition is defined roughly by:

$R_e > 2{,}200$ - turbulent flow

$R_e < 1{,}200$ - viscous flow.

The type of flow in the intermediate region depends upon conditions at inlet and outlet of the pipe.

With viscous flow only the molecules near the pipe walls actually collide with the walls; most of the collisions are intermolecular. Hence the shape and size of the pipe have a greater effect than surface conditions. If the pressure is lowered sufficiently the flow will change from viscous to molecular. The flow is described as molecular when few inter-gas molecule collisions occur and wall effects predominate.

The transition between molecular and viscous flow depends upon the pressure. For air at 20°C., the flow is viscous if (Loevinger, 1949):

$$\gamma < D/100$$

and molecular if:

$$\gamma > D/3$$

where D = diameter of pipe in cm.

γ = mean free path length in cm.

In the intermediate range the flow will change from viscous to molecular as the gas passes down the pipe. In such a case the flow is called "mixed viscous and molecular flow".

(3) Viscous Flow through Circular Pipes

Loevinger (1949) quotes Kundsen's semi-empirical conductance formula for mixed viscous and molecular flow (c.g.s. units):

$$C = \frac{\pi D^4 \bar{P}}{128 \eta L} + \frac{1}{6}\sqrt{\frac{2\pi kT}{m_0}}\,\frac{D^3}{L}\left[\frac{1+\sqrt{\frac{m_0}{kT}}\,\frac{D\bar{P}}{\eta}}{1+1.24\sqrt{\frac{m_0}{kT}}\,\frac{D\bar{P}}{\eta}}\right] \qquad (A.1\text{-}3)$$

where L = length of pipe

k = Boltzman's constant

T = °K

m_0 = mass of molecule of gas

$\bar{P}$ = average pressure in the pipe.

This formula appears to be correct within a few percent (Adzumi, 1937; Halsted and Nier, 1950).

For high pressures this becomes the viscous conductance:

$$C = \frac{\pi D^4}{128 \eta L}\bar{P} \qquad (A.1\text{-}4)$$

or

$$C = C_v \bar{P} \qquad (A.1\text{-}5)$$

Hence

$$C_v \bar{P} = \frac{Q}{P - P_2} = \frac{P_2}{P - P_2}\left.\frac{dV}{dt}\right|_2 \qquad (A.1\text{-}6)$$

If $P_2 \ll P$, and the volume rate of flow is measured from the sample line ($P_2 = P$):

$$C_v \bar{P} \simeq \frac{dV}{dt} \qquad (A.1\text{-}7)$$

(4) Molecular Flow through Circular Pipes

For low pressures equation (A.1-3) becomes the expression for molecular conductance:

$$C = \frac{1}{6}\sqrt{\frac{2\pi kT}{m_o}}\,\frac{D^3}{L} = C_m \qquad \text{(A.1-8)}$$

C_m is a constant for a given pipe and gas at a constant temperature. From equation (A.1-1) and (A.1-2) we find:

$$C_m = \frac{dV}{dt} \qquad \text{(A.1-9)}$$

where the volume rate of flow is measured from the sample line.

A.1.2 Derivation of Pressure vs. Time Models.

(1) Viscous Model

The rate of change of mass m of the gas in the sample line, for a constant volume V, is

$$\frac{dm}{dt} = -\left[\frac{m}{V}\right]\frac{dV}{dt}$$

at the sample line pressure P, that defines dV/dt. By equation (A.1-7):

$$\frac{dm}{dt} \cong -\frac{m}{V}\frac{dV}{dt} \cong -\frac{m}{V}C_v\bar{P}$$

Since the pressure in the mass spectrometer is much lower (approximately 10^{-4} to 10^{-6} mm. Hg) than that in the sample line (approximately 1 cm. Hg) the average pressure

$$\bar{P} = \frac{P + P_2}{2} \cong \frac{P}{2}$$

thus

$$\frac{dm}{dt} \cong \frac{-m\,C_v\,P}{2V}$$

Assuming P is proportional to m, over the pressure range considered, then;

$$\frac{dm}{m} \cong \frac{dP}{P} \qquad \text{(A.1-10)}$$

or

$$\frac{dP}{dt} \cong \frac{-P_m C_v P}{m\, 2V} \cong \frac{-C_v P^2}{2V}$$

thus:

$$\frac{dP}{P^2} \cong \frac{-C_v\, dt}{2V}$$

Integrating:

$$\frac{1}{P} \cong \frac{C_v t}{2V} + \frac{1}{P_o} \qquad \text{(A.1-11)}$$

since at $t = 0$, $P = P_o$. This equation shows that for a viscous leak the relation $1/P$ vs. t will be a straight line.

(2) Molecular model

In this case, again:

$$\frac{dm}{dt} \cong \frac{-m}{V} \frac{dV}{dt}$$

so by applying equations (A.1-9) and (A.1-10) one obtains:

$$\frac{dP}{P} \cong -\frac{C_m\, dt}{V}$$

Integrating with $\ln P = \ln P_o$ at $t = 0$, then

$$\ln\left[\frac{P_o}{P}\right] \cong \frac{C_m t}{V} \qquad \text{(A.1-12)}$$

A.1.3 Isotopic Fractionation due to Viscous and Molecular Flow

(1) Fractionation and Viscous Flow

Under viscous flow conditions gas molecule interactions are important and the P vs. t equations cannot be applied independently for the individual isotopic species (Dr. T.T. Ulrych, personal communication). This is in contrast to

molecular flow conditions under which the gas molecules move independently of each other.

Experimental tests have shown that no fractionation occurs in the present system with viscous flow. (Section 2.1).

(2) Fractionation and Molecular Flow

The molecular flow equation (A.1-12) may be rewritten as

$$P \cong P_o e^{-\frac{C_m t}{V}}$$

According to Halsted and Nier (1950), for molecular flow through the leak and out of the source region, the ratios are:

$$\frac{I_1}{I_2} \cong \frac{P_1}{P_2}$$

Hence

$$\frac{I_1}{I_2} \cong \frac{\left[P_o e^{-\frac{C_m t}{V}}\right]_1}{\left[P_o e^{-\frac{C_m t}{V}}\right]_2}$$

Since for isotope i (equation A.1-8)

$$(C_m)_i = (\text{CONSTANT}) \frac{1}{\sqrt{(m_o)_i}}$$

and since the ratio of the mass of a molecule is proportional to the molecular weight

$$\sqrt{\frac{(m_o)_1}{(m_o)_2}} = \sqrt{\frac{M_1}{M_2}}$$

where M_i = molecular weight of isotopic species i, then

$$\frac{I_1}{I_2} \cong \frac{(P_o)_1}{(P_o)_2} \exp\left[\left(\sqrt{\frac{M_1}{M_2}} - 1\right) \frac{(C_m)_1 t}{V}\right]$$

or
$$R \cong R_o \exp\left[\left(\sqrt{\frac{M_1}{M_2}} - 1\right)\frac{(C_m)_1 t}{V}\right] \qquad \text{(A.1-14)}$$

If one considers this in terms of the fraction F_1 (of the total mass m_1 of the first isotopic species in the sample line) that has been depleted:

$$F_1 \cong \frac{(P_o)_1 - (P)_1}{(P_o)_1} \cong 1 - \exp\left[-(C_m)_1 t / V\right]$$

Then
$$\exp\left[(C_m)_1 t / V\right] \cong 1 - F_1$$

or
$$t \cong \frac{V}{(C_m)_1} \ln\left[\frac{1}{1 - F_1}\right] \qquad \text{(A.1-15)}$$

This equation gives the time t at which the depletion will be F_1. By substituting (A.1-15) into (A.1-14) one finds

$$R \cong R_o \exp\left[\left(\sqrt{\frac{M_1}{M_2}} - 1\right) \ln\left(\frac{1}{1 - F_1}\right)\right]$$

therefore
$$R \cong R_o \left[\frac{1}{1 - F_1}\right]^{\sqrt{\frac{M_1}{M_2}} - 1} \qquad \text{(A.1-16)}$$

For small changes in R we can replace $F_1 \cong F$, where F is the fractional depletion of the whole sample (e.g. based on the total, rather than the partial, pressure decrease). Thus

$$R \cong R_o \left[\frac{1}{1 - F}\right]^{\sqrt{\frac{M_1}{M_2}} - 1} \qquad \text{(A.1-17)}$$

for small changes in R. This equation, as it is applied in section 2.1, agrees closely with the observed results.

Equation (A.1-17) appears to be at least analogous to that derived for distillation processes (Rayleigh, 1896).

Appendix A.2 Asymmetrical Pressure Scattering

A.2.1 General Aspects

Studies of scattering in a mass spectrometer have suggested several possible characteristics that correspond fairly well to those observed.

(1) The density at the collector of the scattered ions should be proportional to the pressure. This should be true to the extent that the pressure is the same throughout the scattering region.

(2) If an asymmetrical exists between the density of ions scattered up and down mass it should be independent of the pressure. This was correct within a few percent.

(3) The Born approximation for the scattering amplitude of a screened coulomb potential (Mandl, 1957) probably describes basically the type of scattering encountered.

(4) The presence of a magnetic field can cause asymmetric scattering. Calculations for scattered ion

densities in a 180° instrument showed that asymmetries occur in the first 90° of the field; which cancel those in the second.

(5) A graphical study of scattering in a 90° magnetic field showed that the net scatter would be asymmetric with a higher down mass density. This type of asymmetry is actually observed with the present mass spectrometer.

A.2.2 Experiment Aspects

1. Tailing coefficients from the trimethyl bismuth Spectra

A sample of trimethyl bismuth was prepared and analysed on the mass spectrometer. Twenty-one spectra were obtained from which the tailing coefficients were calculated and averaged (Table A.2-1); for example:

$$(0.5u) = \left[\frac{\text{Averaged measurement from base line to spectrum 0.5 mass units up mass from the main peak}}{\text{Average main peak height from base line.}}\right] \quad \text{(A.2.1)}$$

$$= 5.39 \times 10^{-3} \quad (\text{at } P = 4.0 \times 10^{-6} \text{ mm. Hg})$$

The results were plotted earlier (Diagram 2.11).

2. Coefficient Averaging Procedure

An averaging process was used to minimize the errors of calculating the coefficients for individual analyses. The averaged (no subscript) coefficient was based on the measured (subscript m) coefficient plus asymmetric factors

Table (A.2-1) Tailing Coefficients (x 10^{-3}) for a Pressure of 4.0×10^{-6} mm. Hg (250 Mass Range).

0.5u	1u	2u	3u	0.5d	1d	2d	3d
5.39	1.61	0.29	0.00	7.69	2.86	1.26	0.75

Table (A.2-2) Asymmetry Factors, Relating the Various Tailing Coefficients. (250 Mass Range).

Numerator / Denominator	0.5u	1u	2u	0.5d	1d	2d	3d	4d	5d
0.5u	1.00	0.30	0.06		0.53	0.23	0.14		
1u		1.00	0.20			0.78	0.47		
2u			1.00						
0.5d	0.70	0.21	0.04	1.00	0.37	0.16	0.10		
1d	1.89	0.56	0.10		1.00	0.44	0.26	0.19	0.15
2d			0.23			1.00	0.60	0.42	
3d							1.00		
4d								1.00	
5d									1.00

Example: $\frac{1u}{1d} = 0.56$

obtained from Table (A.2-2) times the larger measured coefficients

$$\left.\begin{aligned} (1d) &= (1d)m \\ (2d) &= \frac{(2d)m + (0.44)(1d)m + (0.78)(1u)m}{3} \\ (1u) &= \frac{(1u)m + (0.56)(1d)m}{2} \end{aligned}\right\} \quad (A.2\text{-}2)$$

etc. Table (A.2-3) illustrates the result of this process. The first row of values are the tailing coefficients obtained only from trial 11 of the 21 bismuth spectra. These should correspond to the values in the second row, the coefficients obtained by averaging the results of the 21 spectra. A considerable difference is evident. If the measured coefficients of the first row are recalculated according to averaging processes (A.2-2) a much better agreement is possible (third row, Table A.2-3).

3. Asymmetric Tailing Coefficients for Trimethyllead

For trimethyllead the tailing coefficients were based on the measurements illustrated in Diagram (A.2-1). The lower case letters (a_8, etc,) were measured at the center of the corresponding peaks from the curved base lines sketched under the peaks, to the base line determined by that at mass 256, plus drift. The upper case letters A_1, A_2, and A_3 were the peak heights measured with respect to the 256 base level. A_9, A_0, and A_4 are measured with respect to the curved base lines as shown. As noted in section 2.2.3 the base line below mass 248 is higher than

Table A.2-3: Example of Averaged Pressure Scattering Coefficients (x 10^{-3}) for a Pressure of 4.0×10^{-6} mm. Hg. ($Bi(CH_3)_3^+$ 250 Mass Range.)

	0.5u	1u	2u	0.5d	1d	2d	3d
Measured (Trial 11)	5.16	1.45	0.31	8.03	3.00	1.45	0.95
Ave. 21 Spectra	5.39	1.61	0.29	7.69	2.86	1.26	0.75
Averaged (Trial 11)	5.38	1.59	0.31	—	2.90	1.28	0.79

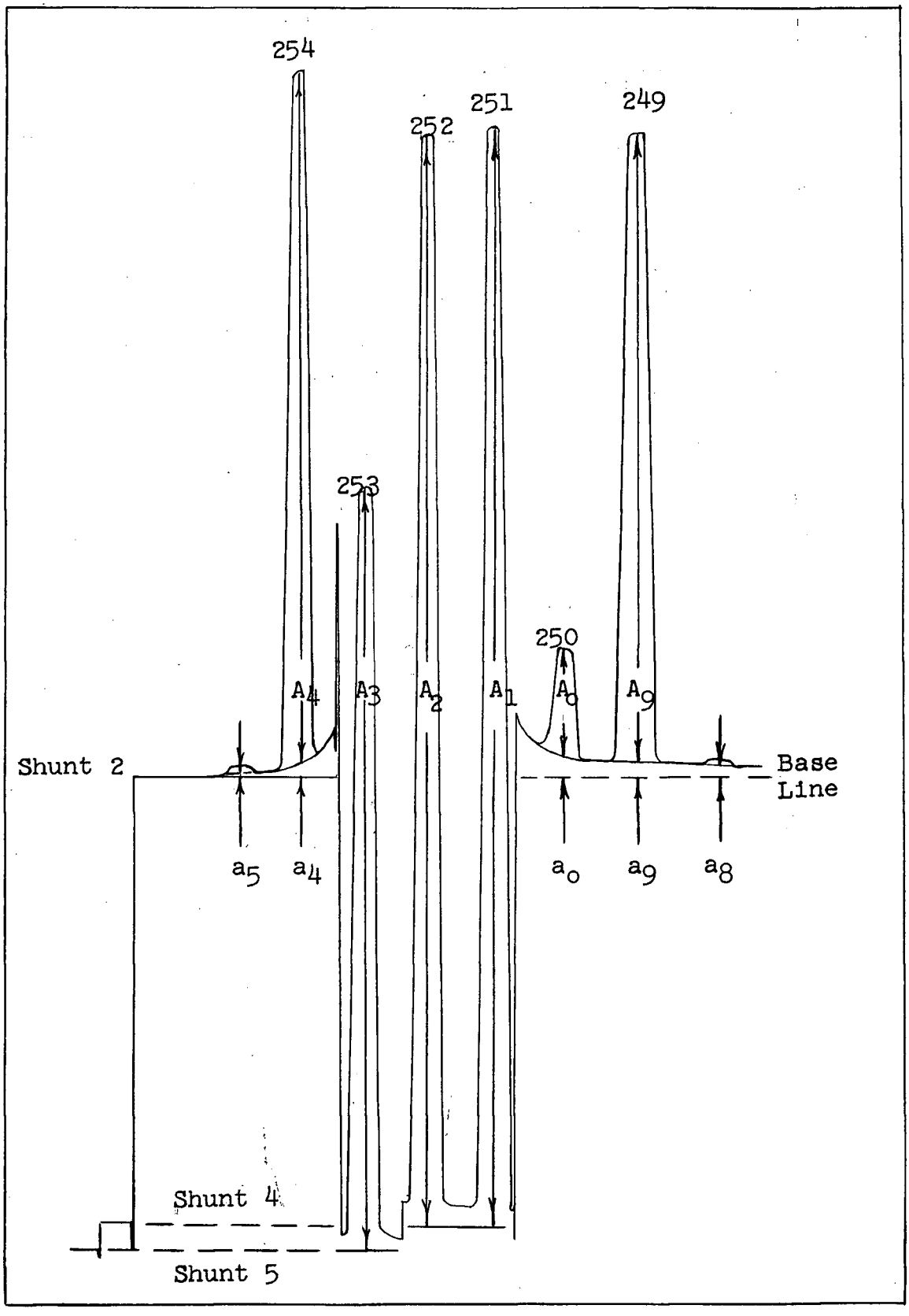

Diagram A.2-1. Pressure Scattering Measurements from the Trimethyllead Spectrum

that at 256, and dependent upon the pressure of the sample (Diagram A.2-2). Below mass 248 it levels off, and extends at least 8 mass units down to the dimethyllead spectrum. This is mainly the result of the extreme down mass tailing of masses 251, 252, and 253. The base line at mass 256 is not affected by the presence of a sample and so represents the true base level.

The lower case letters represent the tailing values of the various peaks; e.g. (neglecting A_o and A_4):

$$a_8 = (1d)A_9 + (3d)A_1 + (4d)A_2 + (5d)A_3$$

The known asymmetries between these coefficients can be obtained from Table (A.2-2). (These are assumed to be the same for both $Pb(CH_3)_3^+$ and $Bi(CH_3)_3^+$.)

$$a_8 = (1d)A_9 + (0.26)A_1 + (0.19)A_2 + (0.15)A_3$$

the tailing coefficient is thus

$$(1d)_{m1} = a_8/\left[A_9 + (0.29)A_1 + (0.19)A_2 + (0.15)A_3\right]$$

Similarily (again neglecting some of the small peaks)

$$(1d)_{m2} = a_0/\left[(0.56)A_9 + A_1 + (0.44)A_2 + (0.26)A_3\right]$$

$$(2d)_m = a_9/\left[A_1 + (0.60)A_2 + (0.42)A_3\right]$$

$$(2u)_m = a_5/\left[(5.00)A_4 + A_3\right]$$

The value of (1u) was not calculated from measured values since it is very difficult to draw a consistant base line beneath the mass 254 peak. The final coefficients were calculated by applying the averaging process described above:

$$(1d) = \frac{(1d)_{m1} + (1d)_{m2}}{2}$$

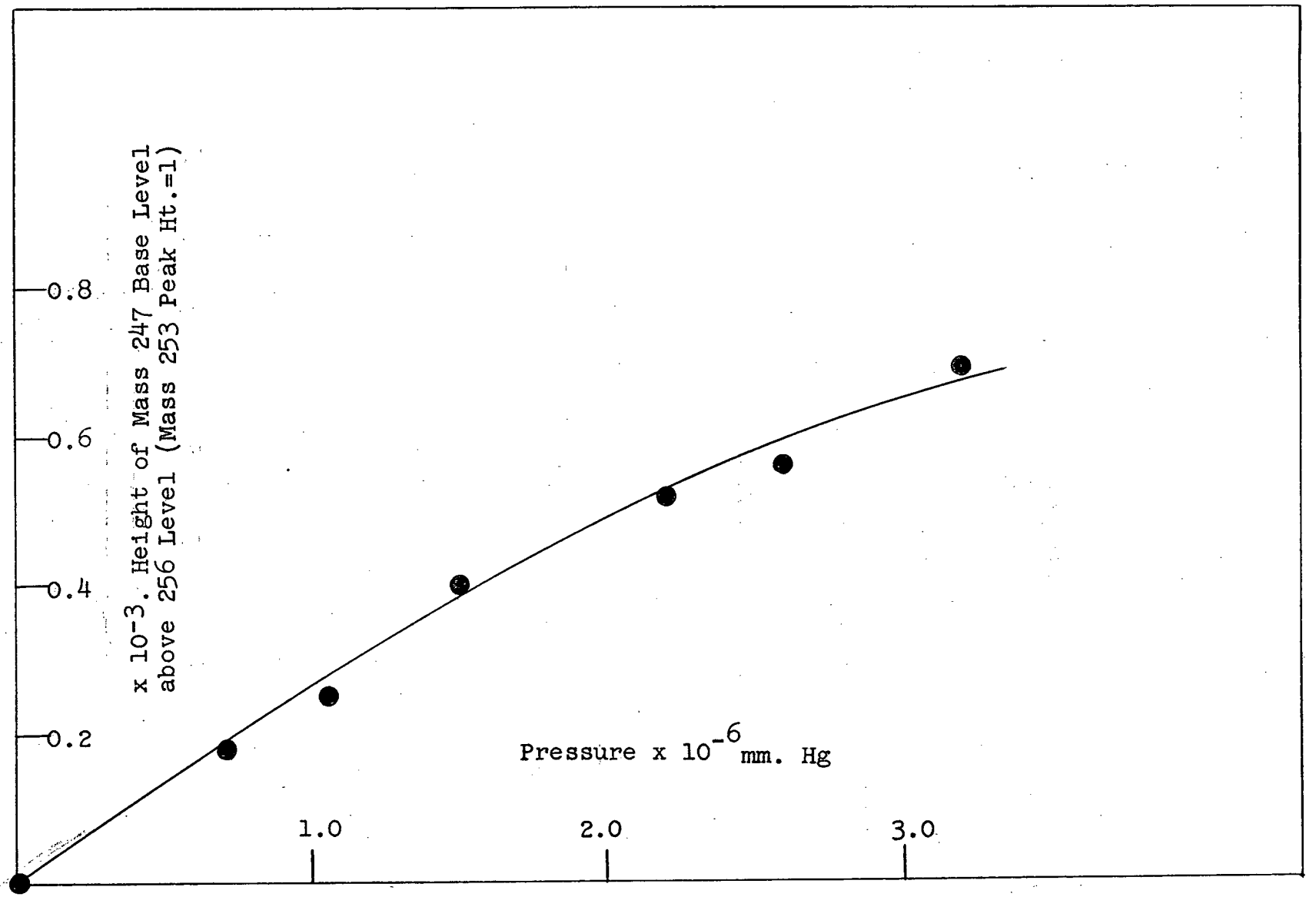

Diagram A.2-2. The Effect of Asymmetrical Pressure Scattering on the Mass 247 Base Level in the Trimethyllead Spectrum

$$(2d) = \frac{(2d)_m + (0.44)(1d)_m + (0.78)(1u)_m}{3}$$

$$(1u) = (0.56)(1d)_m$$

$$(2u) = \frac{(2u)_m + (0.20)(1u)_m + (0.10)(1d)_m + (0.23)(2d)_m}{4}$$

$$(0.5u) = (1.89)(1d)_m$$

The formulae used to obtain the corrected peak height may be found in section 2.2.3.

4. The Presence of Bismuth

If bismuth is present in the sample it will appear as trimethyl bismuth mixed with the separated tetramethyllead. In this case, when the isotope ratios of lead are calculated, a value of K_{up} (C^{13}/C^{12}) must be substituted (0.03174 in the present case) and the 254 peak height ignored. The 253 peak must also be corrected for the K_{dn} (H^+ loss) factor of the bismuth peak:

$$(A_3^o)_{corr.} = A_3^o - K_{dn}\left[A_4^o - K_{up}\, A_3^o\right]$$

The A_3^o values refer to those which have been corrected for pressure scattering. The K_{dn} factor of trimethyl bismuth appears to be the same as that for the trimethyllead ion.

5. Example of Asymmetrical Pressure Scattering Correction: Mt. Isa #460

This sample of chalcopyrite was prepared with the

micro-lead technique and analysed at high pressure and low sensitivity. The data was processed in the usual way but without applying any corrections. The average peak heights of 12 pairs were so obtained:

A_9	A_o	A_1	A_2	A_3	A_4
1.2874	0.1678	21.5247	21.4373	47.6339	7.9500

with $K_{dn} = 0.00593$, $K_{up} = 0.03174$ Given.
The tailing or pressure scattering coefficients were obtained from Diagram 2.14, for a pressure of 3.8×10^{-6} mm. Hg (the response of the pressure gauge to acetone, the main impurity in these small samples, appears to correspond to that of tetramethyllead):

$(0.5u) = 5.40 \times 10^{-3}$ $\quad$ $(1u) = 1.65 \times 10^{-3}$

$(1d) = 2.80 \times 10^{-3}$ $\quad$ $(2u) = 0.30 \times 10^{-3}$

$(2d) = 1.25 \times 10^{-3}$

The correction formula of section 2.2.3 were used to obtain the true peak heights.

$$A_9^o = 1.2874 + 1.2874 \quad (5.40 \times 10^{-3})$$
$$= 1.2944$$
$$A_0^o = 0.1678$$
$$A_1^o = 21.5247 - (0.00280)(21.4373) - (0.00125)(47.6339)$$
$$= 21.4052$$
$$A_2^o = 21.4373 - (0.00165)(21.5247) - (0.00280)(47.6339) - (0.00125)(7.9500)$$
$$= 21.2585$$

$$A_3^o = 47.6339 - (0.00165)(21.4373) - (0.00030)(21.5247) - (0.0028)(7.9500)$$

$$= 47.5689$$

$$A_4^o = 7.9500$$

The bismuth correction was also computed

$$(A_3^o)_{corr.} = 47.5687 - (0.00593)\left[7.9500 - (0.03174)(47.5689)\right]$$

$$= 47.5305$$

The corrected peak heights were then used to recalculate the isotope ratios.

For the larger, normal sensitivity samples, the tailing coefficients may be calculated directly from the spectra.

A.3 Lead Isotope Models

A.3.1 Basic equations

The mathematical models discussed in this section consist of sets of equations which are developed, according to certain assumptions, to relate the changes in the lead isotope ratios to the time and the relative proportions of lead, uranium and thorium. The three heavier lead isotopes are the end products of the three radioactive series:

$$\begin{aligned} {}_{92}U^{235} &= {}_{82}Pb^{207} + 7He^4 + \text{energy} \\ {}_{92}U^{238} &= {}_{82}Pb^{206} + 8He^4 + \text{energy} \\ {}_{90}Th^{232} &= {}_{82}Pb^{208} + 6He^4 + \text{energy} \end{aligned} \qquad \text{(A.3-1)}$$

The abundance of lead 204 has remained unchanged since the beginning of geologic time. If it is assumed that

(1) at the beginning of geologic time (t_o years ago) all lead was of a unique composition (primordial lead);

(2) equations (A.2-1) are the only causes of change in the isotopic abundances; and,

(3) the radioactive decay law applies; then the relative isotopic abundances at any time t, are given by the integral equations:

$$\left.\begin{aligned} Pb^{206}/Pb^{204} &= x = a_o + \alpha\int_t^{t_o} V\lambda e^{\lambda t}dt \\ Pb^{207}/Pb^{204} &= y = b_o + \int_t^{t_o} V\lambda' e^{\lambda' t}dt \\ Pb^{208}/Pb^{204} &= z = c_o + \int_t^{t_o} W\lambda'' e^{\lambda'' t}dt \end{aligned}\right\} \quad (A.3\text{-}2)$$

where t is measured positively into the past. The constants involved are given in Table (A.3-1). a_o, b_o, c_o are the primordial abundances determined from meteoritic triolites. t_o was also obtained from meteoritic data.

Equations (A.3-2) are quite general since V and W are unspecified functions of time and place. The different lead isotope models have been developed by applying different assumptions to these basic equations.

A.3.2 Single-Stage Models

1. Isochron Model

Gerling (1942), Holmes (1946), and Houtermans (1946)

Table (A.3-1) Symbols and Constants Used in Age Determination

1. Symbols

Isotope Ratio	At Present t = 0	At Time t	At Time t_o
Pb^{206}/Pb^{204}	a	x	a_o
Pb^{207}/Pb^{204}	b	y	b_o
Pb^{208}/Pb^{204}	c	z	c_o
U^{238}/Pb^{204}	$\propto V$	$\propto V \exp(\lambda t)$	$\propto V \exp(\lambda t_o)$
U^{235}/Pb^{204}	V	$V \exp(\lambda' t)$	$V \exp(\lambda' t_o)$
Th^{232}/Pb^{204}	W	$W \exp(\lambda'' t)$	$W \exp(\lambda'' t_o)$

2. Constant Values

Constant	Parent atom	Value	Reference
λ	U^{238}	0.1537	1,2,3.
λ'	U^{235}	0.9722 $10^{-9}yr^{-1}$	4,2,3.
λ''	Th^{232}	0.0499	5,2,3.
$\propto$		137.8	6,4,7.
a_o		9.56	8
b_o		10.42	8
c_o		29.71	8
t_o		$4.55 \pm 0.03$by	8

References:

1. Kovarik et al (1955)
2. Aldrich and Wetherill (1958)
3. Russell and Farquhar (1960)
4. Fleming et al (1952)
5. Picciotto and Wilgain (1956)
6. Inghram (1947)
7. Senftle et al (1957)
8. Murthy and Patterson (1962)

constructed the first single stage model by assuming that leads developed in a series of locally closed systems. These leads developed in these local systems from time t_o, until time t when mineralization isolated the lead from uranium and thorium. Under this assumption equations (A.3-2) become

$$\left.\begin{aligned} x &= a_o + \alpha V(e^{\lambda t_o} - e^{\lambda t}) \\ y &= b_o + V(e^{\lambda' t_o} - e^{\lambda' t}) \\ z &= c_o + W(e^{\lambda'' t_o} - e^{\lambda'' t}) \end{aligned}\right\} \qquad \text{(A.3-3)}$$

where V and W will depend upon the local system abundances. If V is eliminated from the first two equations the result is the Houtermans' "isochron equation":

$$\phi = \frac{y - b_o}{x - a_o} = \frac{(e^{\lambda' t_o} - e^{\lambda' t})}{\alpha(e^{\lambda t_o} - e^{\lambda t})} \qquad \text{(A.3-4)}$$

This shows that leads, which are extracted from the various closed systems at the same time t, are linearly related in the x, y plot, e.g. they will lie along a "primary isochron" (See Diagram 4.1).

2. Primary Lead Model

The equations for this model are the same as those of the preceding section (A.3-3), the difference being that V and W are assumed constant in the primary lead system. Hence, at any given time, the lead isotope ratios are the same throughout the system.

A.3.3 Multi-stage Leads

The mathematical models for multi-stage leads are constructed by assuming that V and W are functions of time and place. Kanasewich (1962a, 1962b) assumed that V and W change discretely at the time of tectonic activity, and remain constant until the next event. Thus we have V_1 and W_1 from t_o to t_1, V_2 and W_2 from t_1 to t_2, etc., and equations (A.3-2) become:

$$(A.3\text{-}5)\begin{cases} x = a_o + \alpha V_1(e^{\lambda t_o} - e^{\lambda t_1}) + \alpha V_2(e^{\lambda t_1} - e^{\lambda t_2}) + \cdots \\ y = b_o + V_1(e^{\lambda' t_o} - e^{\lambda' t_1}) + V_2(e^{\lambda' t_1} - e^{\lambda' t_2}) + \cdots \\ z = c_o + W_1(e^{\lambda'' t_o} - e^{\lambda'' t_1}) + W_2(e^{\lambda'' t_1} - e^{\lambda'' t_2}) + \cdots \end{cases}$$

Stage 1 represents the growth in the primary system, (V_1, W_1), t_1 the initial mineralization time. At this time all the leads have the same isotopic composition (x_1. y_1, z_1) but they are placed into systems of different V_2 and W_2. Under these conditions, at any time t_2, $t_1 < t_2$, the lead isotope ratios (x,y) will be linearly related:

$$\frac{y - y_2}{x - x_2} = \frac{(e^{\lambda' t_1} - e^{\lambda' t_2})}{\alpha(e^{\lambda t_1} - e^{\lambda t_2})} \qquad (A.3\text{-}6)$$

The line through the various points (x,y) has a slope given by (A.3-6) and intercepts the primary growth curve at times t_1 and t_2 (Diagram 4.9). If these leads are extracted from their various systems at time t_2, and placed in a third set of systems (e.g. a second crustal environment), the results will no longer be simple unless extensive homogenization occurs. This point has been discussed

in section 4.4.4

A.3.4 Sea Water Leads

Chow and Patterson (1959, 1962), and Chow and Johnstone (1963), have published numerous sea water lead isotope analyses. Wampler (1963) has completed a study of leads in sedimentary pyrites. Generally speaking a two stage model:

$$\left.\begin{aligned} X &= a_o + \alpha V_1 (e^{\lambda t_o} - e^{\lambda t_1}) + \alpha V_2 (e^{\lambda t_1} - e^{\lambda t_2}) \\ y &= b_o + V_1 (e^{\lambda' t_o} - e^{\lambda' t_1}) + V_2 (e^{\lambda' t_1} - e^{\lambda' t_2}) \end{aligned}\right\} \quad (A.3\text{-}8)$$

has been fairly successful in predicting the observed results. This model assumes that lead is extracted from the primary system at some average time t_1, and emplaced in a crustal environment of V_2. The process of weathering will cause the lead to be extracted at some time t_2 and be carried into solution in the seas. The lead may then be precipitated as a trace element in pyrites, manganese nodules, and clays. The time interval represented by t_2 (the average time of leaching and deposition) is likely to be less than one million years. Equations (A.3-8) show that leads of the same t_1 and t_2 but different V_2 lie along a straight line.

R.D. Russell and W.F. Slawson have suggested (personal communication) a slightly different approach. One can assume that the time of leaching and deposition (t_2) is

the same, and that V_2 is fairly constant for rocks of one area. If we then leach lead from source rocks of different ages (t_1 varies) the resulting isotope ratios will lie along a curve:

$$\left.\begin{aligned} X &= a_0 + \alpha V_1 e^{\lambda t_0} - \alpha V_1 e^{\lambda t_1} + \alpha V_2 e^{\lambda t_1} - \alpha V_2 e^{\lambda t_2} \\ &\quad + \alpha V_1 e^{\lambda t_2} - \alpha V_1 e^{\lambda t_2} \\ X &= a_0 + \alpha V_1 (e^{\lambda t_0} - e^{\lambda t_2}) + \alpha (V_2 - V_1)(e^{\lambda t_1} - e^{\lambda t_2}) \\ X &= X_2 + \alpha \Delta V (e^{\lambda t_1} - e^{\lambda t_2}) \end{aligned}\right\} \quad \text{(A.3-9)}$$

where x_2 is the ratio, in the primary system, at the time of deposition t_2. Similarily:

$$y = y_2 + \Delta V (e^{\lambda' t_1} - e^{\lambda' t_2}) \qquad \text{(A.3-10)}$$

The difference between this model and the simple two stage model concerns the relative variation postulated in V_2 and t_1. Diagram (4.10) illustrates this for sea water leads deposited at time t_2. If the rocks being leached have a similar age (t_1), but have variations in V (V_1, etc.) then the model is two stage and the resulting leads lie along a straight line. If the variations in V are not significant, but the ages of the source rocks vary the leads could lie along the curve A-B-C-D. Theoretically, if ΔV is negative there is no reason why the leads cannot also lie along the reflection of this curve, below the primary growth curve. However, it is to be expected that ΔV will be mostly positive since the crustal rocks generally appear to have larger V ratios than the primary system.

Sea water leads would be expected to exhibit a considerable lead isotope ratio variation comparable to that found with present day samples (Chow and Patterson, 1962).

BIBLIOGRAPHY

Abel E.W., G. Nickless and F.H. Pollard, 1960. Vapor phase chromatography of organometallic compounds: alkyl derivatives of the Group IVa metals. Proceedings of the Chemical Society (London) 1960, 288.

Adzumi A., 1937. Studies on the flow of gaseous mixtures through capillaries. II: The molecular flow of gaseous mixtures. III: The flow of gaseous mixtures at medium pressures. Bulletin of the Chemical Society of Japan, 12, 285 and 292.

Aho A.E., 1956. Geology and genesis of ultrabasic nickel-copper-pyrrhotite deposits at the Pacific Nickel Property, southwestern British Columbia. Economic Geology, 51, 444.

Aldrich L.T. and G.W. Wetherill, 1958. Geochronology by radioactive decay. Annual review of Nuclear Science, 8, 257.

Allen A.D. and O.K. Rice, 1935. The explosion of azo-methane. American Journal of Chemistry, 57, 310.

Auger P.E., 1941. Zoning and district variations of the minor elements in pyrite of Canadian gold deposits. Economic Geology, 36, 401.

Ault W.U. and J.L. Kulp, 1959. Isotopic geochemistry of sulfur. Geochimica et Cosmochimica Acta, 16, 201.

Ault W.U. and J.L. Kulp, 1960. Sulfur isotopes and ore deposits. Economic Geology, 55, 73.

Austin C.F. and W.F. Slawson, 1961. Isotopic analyses of single galena crystals: a clue to history of deposition. American Mineralogist, 46, 1132.

Azzaria L.M., 1960. Distribution of copper, lead and zinc in the minerals of a granite. Ph.D. thesis, Department of Geology, University of Toronto.

Baikloh W. and G. Henke, 1937. Reduction of chromic oxide with hydrogen and solid carbon. Chemical Abstracts, 32, 2044c.

Bamford C.H., 1939. A study of organic nitrogen compounds. Part II: Aliphatic amines. Journal of the Chemical Society (London), 1939, 17.

Baskova Z.A. and G.I. Novikov, 1957. The evolution of small amounts of lead by a reducing calcination in vacuum. Geochemistry, 678.

Benson S.W., 1960. The Foundations of Chemical Kinetics. McGraw-Hill Publishers.

Blanchard R. and G. Hall, 1942. Rock deformation and mineralization at Mt. Isa. Australian Institute of Mining and Metallurgy Proceedings, #125, 1.

Bone W.A. and H.F. Coward, 1908. The thermal decomposition of hydrocarbons. Part I: methane, ethane, ethylene and acetylene. Transactions of the Chemical Society (London), Part II, 1197.

Brinton R.K. and D.H. Volman, 1952. Decomposition of di-t-butyl peroxide and kinetics of the gas phase reaction of t-butoxyl radicals in the presence of ethylenimine. Journal of Chemical Physics, 20, 25.

Bucher W.H., W.T. Thom Jr. and R.T. Chamberlin, 1934. Geological problems of the Beartooth Bighorn Region. Bulletin of the Geological Society of America, 45, 167.

Burlings R.L., 1952. The determination of geological time. Nucleonics, 10, 30.

Catanzaro F.J., 1961. A study of discordant zircons from the Little Belt (Montana), Beartooth (Montana), and Santa Catalina (Arizona) Mountains. Ph.D. thesis, Columbia University.

Chow T.J. and C.C. Patterson, 1959. Lead isotopes in manganese nodules. Geochimica et Cosmochimica Acta, 17, 21.

Chow T.J. and C.C. Patterson, 1962. The occurence and significance of lead isotopes in pelagic sediments. Geochemica et Cosmochimica Acta, 26, 263.

Chow T.J. and M.S. Johnstone, 1963. Lead isotopes in sediments of Hudson Bay and Baltic Sea. Transactions of the American Geophysical Union, 44, 890.

Clayton R.N. and S. Epstein, 1958. The relationship between O^{18}/O^{16} ratios in coexisting quartz, carbonate, and iron oxides from various geological deposits. Journal of Geology, 66, 352.

Collins C.B., J.R. Freeman and J.T. Wilson, 1951. A modification of the isotopic lead method for the determination of geologic ages. Physical Review, 82, 966.

Collins C.B., R.D. Russell and R.M. Farquhar, 1953. The maximum age of the elements and the age of the earth's crust. Canadian Journal of Physics, 31, 402.

Collins C.B., R.M. Farquhar and R.D. Russell, 1954. Isotopic constitution of radiogenic leads and the measurement of geological time. Bulletin of the Geological Society of America, 65, 1.

Crocco L., F. Glassman and I.E. Smith, 1959. Kinetics and mechanism of ethylene oxide decomposition at high temperatures. Journal of Chemical Physics, 31, 506.

Davidson C.F., 1962. The origin of some strata-bound sulfide ore deposits. Economic Geology, 57, 265.

Dawson Jr. H.J., 1963. Determination of methyl-ethyl lead alkyls in gasoline by gas chromatography with an electron capture detector. Analytical Chemistry, 35, 542.

Dechow E., 1960. Geology, sulfur isotopes and the origin of the Heath Steel ore deposits, Newcastle N.B., Canada. Economic Geology, 55, 539.

de Wet H., 1952. Reduction of chromium oxide and the production of chromium containing steels and alloys. Chemical Abstracts, 46, 9050h.

Diebler V.H. and F.L. Mohler, 1951. Mass spectra of some organo-lead and organo-mercury compounds. Journal of Research, National Bureau of Standards, Washington, 47, 337.

Dorfman L.M. and Z.W. Salsburg, 1951. The photochemical decomposition of gaseous di-t-butyl peroxide. Journal of the American Chemical Society, 73, 255.

Dunham K.C., 1964. Neptunist concepts in ore genesis. Economic Geology, 59, 1.

Dushman S., 1949. Scientific Foundations of Vacuum Technique. John Wiley and Sons, Publisher.

Eckelmann W.R. and A. Poldervaart, 1957. Geologic evolution of the Beartooth Mountains, Montana and Wyoming. Archean history of the Quad Creek area. Bulletin of the Geological Society of America, 68, 1225.

Edström J.O., 1953. The mechanism of reduction of iron oxides. Iron and Steel Institute Journal, 175, 289.

Eltenten G.C., 1947. Mass spectrometer studies of reactions, Part II. The thermal decomposition of some lower hydrocarbons. Journal of Chemical Physics, 15, 465.

Fleischer M., 1955. Minor elements in some sulfide minerals. Economic Geology Fiftieth Anniversary Volume, Part II, 970.

Fleming Jr. G.H., A. Ghiorso and B.B. Cunningham, 1952. Specific alpha activities and half lifes of U^{234}, U^{235}, and U^{236}. Physical Review, 88, 642.

Fletcher C.J.M. and G.K. Rollefson, 1936. The production of free radicals from ethylene oxide and the catalyis of other reactions by them. Journal of the American Chemical Society, 58, 2135.

Foose R.M., D.U. Wise and G.S. Garbarini, 1961. Structural geology of the Beartooth Mountains, Montana and Wyoming. Geological Society of America, Bulletin, 72, 1143.

Forst W. and O.K. Rice, 1963. The thermal decomposition of azomethane. I: Effect of added olefin and nitric oxide. Canadian Journal of Chemistry, 41, 562.

Friedman I., 1953. Deuterium content of natural water and other substances. Geochimica et Cosmochimica Acta, 4, 89.

Gallo., 1927. Reduction of iron ores with hydrogen. II: The behaviour of iron pyrites with hydrogen. Annals Chimica Applicata, 17, 39. (Chemical Abstracts, 21, 1243[1]).

Gallo G. and M. Del Guerra, 1951. The reaction of hydrogen with metallic oxides and sulfides. Annals Chimica (Rome), 41, 51. (Chemical Abstracts, 45, 8385e).

Gast P.W., J.L. Kulp and L.E. Long, 1958. Absolute age of early Precambrian rocks in the Bighorn Basin of Wyoming and Montana and southwestern Manitoba. Transactions of the American Geophysical Union, 39, 322.

Gay P.F. and M.W. Travers, 1937. On the thermal decomposition of dimethyl ether. Transactions of the Faraday Society, 33, 756.

Geller R.F., A.S. Creamer and E.N. Bunting, 1934. The System PbO-SiO_2. Journal of Research, National Bureau of Standards, 13, 243. Report 705.

George P. and A.D. Walsh, 1946. A note on the decomposition of tertiary alkyl peroxides. Transactions of the Faraday Society, 42, 94.

Gerling E.K., 1942. Age of the earth according to radioactive data. Comptes Rendus (Doklady) de l'Academie des Sciences de l'URSS, 34, 259.

Gesser H., J.T. Mullhaupt and J.E. Griffiths, 1957. The photolysis of trimethylamine. Journal of the American Chemical Society, 79, 4834.

Glazebrook H.H. and T.G. Pearson, 1936. Free Radicals and atoms in primary photochemical processes. The free propyl radical from di-isopropyl ketone. Journal of the Chemical Society (London), 1936, 1777.

Goldschmidt V.M., 1937. The principles of distribution of chemical elements in minerals and rocks. Journal of the Chemical Society, 1937, 655.

Gomberg M.G., 1900. An instance of trivalent carbon: triphenyl methyl. Journal of the American Chemical Society, 32, 757.

Grondĳs H.F. and C. Schouten, 1937. A study of Mt. Isa ores. Economic Geology, 32, 407.

Hall F.D. and H. Insley, 1947. Phase diagrams for ceramists. Journal of the American Ceramic Society, Part II, Nov.

Halsted R.E. and A.D. Nier, 1950. Gas flow through the mass spectrometer viscous leak. Review of Scientific Instruments, 21, 1019.

Harris G.M. and A.W. Tickner, 1948. The detection of free radicals in hydrogen atom reactions with organic molecules. Canadian Journal of Research, 26B, 343.

Harris Jr. R.L., 1959. Geological evolution of the Beartooth Mountains, Montana and Wyoming. Bulletin of the Geological Society of America, 70, 1185.

Harrison A.G. and H.G. Thode, 1958. Mechanism of the bacterial reduction of sulfate from isotopic fractionation studies. Transactions of the Faraday Society, 54, 84.

Hawley J.E. and I. Nickol, 1961. Trace elements in pyrite, pyrrhotite and chalcopyrite of different ores. Economic Geology, 56, 467.

Heckert W.W. and F. Mack, 1929. The thermal decomposition of gaseous ethylene oxide. Journal of the American Chemical Society, 51, 2706.

Heller Jr. C.A. and H.A. Taylor, 1953. The Pyrolysis of cadmium dimethyl. Journal of Physical Chemistry, 57, 226.

Helm D.F. and E.J. Mack, 1937. The thermal decomposition of gaseous silicon tetramethyl. Journal of the American Chemical Society, 59, 60.

Hess H.H., 1960. Stillwater Igneous Complex, Montana. Geological Society of America, Memoir 80.

Hinschelwood C.N. and W.K. Hutchison, 1926a. A comparison between unimolecular and bimolecular gaseous reactions. The thermal decomposition of gaseous acetaldehyde. Proceedings of the Royal Society (London), A111, 380.

Hinschelwood C.N. and W.K. Hutchinson, 1926b. A homogeneous unimolecular reaction. The thermal decomposition of acetone in the gaseous state. Proceedings of the Royal Society (London), A111, 245

Holmes A., 1946. An estimate of the age of the earth. Nature, 157, 680.

Houtermans F.G., 1946. Die isotopenhäufigkeiten im Naturalichen Blei und das Altes des Urans. Naturwissenschaften, 33, 185.

Howie R.A., 1955. The geochemistry of the Charnockite Series of Madras, India. Transactions of the Royal Society of Edinburgh, 62, Part 3, 725.

Huffman J.R., 1936. The thermal decomposition of acetone. Journal of the American Chemical Society, 58, 1815.

Inghnam H., 1947. Manhatten Project, Technical Series, Division II., 14, chapter 5, 35. McGraw-Hill Publishers.

Ingold K.U. and F.P. Lossing, 1953. Free radicals by mass spectrometry. III: Radicals in the thermal decomposition of some benzene derivatives. Canadian Journal of Chemistry, 31, 30.

Ishihara T. and K. Sudo, 1954. The dissociation pressure of pyrite. Chemical Abstracts, 48, 13321a.

Jensen M.L., 1959. Sulfur isotopes and hydrothermal mineral deposits. Economic Geology, 54, 374.

John F.P. and H.A. Taylor, 1939. The thermal decomposition of azomethane. Journal of Chemical Physics, 7, 470.

Kanasewich E.R., 1962a. Quantitative interpretation of of anomalous lead isotope abundances. Ph.D. thesis, Department of Physics, University of British Columbia.

Kanasewich E.R., 1962b. Approximate age of tectonic activity using anomalous lead isotopes. Geophysical Journal of the Royal Astronomical Society, 7, 158.

Kanasewich E.R. and W.F. Slawson, 1964. Precision intercomparisons of lead isotope ratios: Ivigtut, Greenland. Geochimica et Cosmochimica Acta, In Press.

Kistemaker J., 1953. The influence of fractionizing and viscosity effects in mass spectrometer gas handling systems. Mass Spectroscopy in Physics Research, U.S. National Bureau of Standards, Circular 522.

Kollar F., 1960. The precise intercomparison of lead isotope ratios. Ph.D. thesis, Department of Physics, University of British Columbia.

Kollar F., R.D. Russell and T.J. Ulrych, 1960. Precision intercomparison of lead isotope ratios: Broken Hill and Mt. Isa. Nature, 187, 754.

Kornilov I.I. and F.A. Krimlaeva, 1945. Relation between the velocity of reaction in solid solutions and the chemical composition of the equilibrium system. I: the velocity of the reduction of chromites and of oxides of iron and chromium. Chemical Abstracts, 42, 6214i.

Kouvo O. and J.L. Kulp, 1961. Isotopic composition of Finnish galenas. Annals of the New York Academy of Science, 91, 476.

Kovarik A.F. and N.I. Adams Jr., 1955. Redetermination of the disintigration constant of U^{238}. Physical Review, 98, 46.

Kulp J.L., R. Kologrivov, J. Engels, E.J. Catanzaro, H. Neumann and B. Nilssen, 1963a. Age of the Tordal, Norway Pegmatite - a correction. Geochimica et Cosmochimica Acta, 27, 847.

Kulp J.L. et al, 1963b. Investigations in isotopic geochemistry. Annual Report Number 8, Geochemistry Laboratory, Lamont Geological Observatory, Columbia University.

Laubengayer A.W. and W.F. Gilliam, 1941. The Alkyls of the third-group elements. I. Vapor-phase studies of the alkyls of aluminum, gallium and indium. Journal of the American Chemical Society, 63, 477.

Leermakers J.A., 1933a. The formation of methyl radicals in the decomposition of azomethane. Journal of the American Chemical Society, 55, 3499.

Leermakers J.A., 1933b. The effect of ethyl radicals on the thermal decomposition of azomethane. Journal of the American Chemical Society, 55, 4508.

Loevinger K., 1949. Fundamental considerations in vacuum practice. Vacuum Equipment and Techniques, Chapter 1. McGraw-Hill Publishers.

Lossing F.P. and A.W. Tickner, 1952. Free radicals by mass spectrometry. I: The measurement of methyl radical concentrations. Journal of Chemical Physics, 20, 907.

Lossing F.P., K.U. Ingold and I.H.S. Henderson, 1953a. The study of free radicals by mass spectrometry. Applied Mass Spectrometry, Institute of Petroleum Conference, 102.

Lossing F.P., K.U. Ingold and A.W.T. Tickner, 1953b. Free radicals by mass spectrometry. Part II: the thermal decomposition of ethylene oxide, propylene oxide, dimethyl ether, and dioxane. Discussions of the Faraday Society, 14, 34.

Love L.G. and D.O. Zimmerman, 1961. Bedded pyrite and microorganisms from the Mt. Isa shale. Economic Geology, 56, 873.

Love L.G., 1962. On the origin of some strata bound sulfide ore deposits. Economic Geology, 57, 460

Mandl F., 1957. Quantum Mechanics, 151. Butterworth Publishers.

Mason B., 1958. Principles of Geochemistry, John Wiley and Sons, Publishers.

Mataba S. and T. Unotoro, 1951. The equilibrium amoung iron, sulfur and hydrogen at high temperatures. II: The reduction equilibrium of ferrous sulfide by hydrogen. Chemical Abstracts, 45, 7005g,h.

McKewan W.M., 1960. Kinetics of iron oxide reduction. Transactions of the American Institute of Mining, Metallurgy and Petroleum Engineers, 218, 545.

McNesley J.R., T.W. Davis and A.S. Gordon, 1954. Pyrolysis of mixtures of acetone and acetone-d_6. Journal of the American Chemical Society, 76, 823.

Milas N.A. and D.M. Surgenor, 1946. Studies in organic peroxides. VIII: T-butyl hydroperoxide and di-t-butyl peroxide. Journal of the American Chemical Society, 68, 205.

Mohler F.L., 1960. Isotopic abundance ratios reported for reference samples stocked by the National Bureau of Standards. Technical Note 51. U.S. Department of Commerce, Washington 25, D.C.

Moorbath S. and H. Pauly, 1962. Rubidium-strontium and lead isotope studies on intrusive rocks from Ivigtut, South Greenland. Tenth Annual Progress Report for 1962, Department of Geology and Geophysics, Massachusetts Institute of Technology, 99-102.

Mueller K.H. and W.D. Waters, 1951. The thermal decomposition of ethylene oxide. Journal of the American Chemical Society, 73, 1458.

Mueller K.H. and W.D. Waters, 1954. The thermal decomposition of ethylene oxide. Journal of the American Chemical Society, 76, 330.

Murawski J., J.S. Roberts and M.Szwarc, 1951. Kinetics of the thermal decomposition of di-t-butyl peroxide. Journal of Chemical Physics, 19, 698.

Murphy V.R. and C.C. Patterson, 1962. Primary isochron of zero age for meteorites and the earth. Journal of Geophysical Research, 67. 1161.

Nerken A., 1956. Experiments on the Flow of Gases through leaks. Vacuum Symposium Transactions, 1956, 1.

Nier A.D., 1947. A mass spectrometer for isotope and gas analysis. Review of Scientific Instruments, 18, 398.

Niva K., Y. Katsufuji and T. Mackawa, 1956. The reduction process of iron pyrite. Chemical Abstracts, 50, 16600a.

Ostic R.G., 1963. Isotopic investigation of conformable lead deposits. Ph.D. thesis, Department of Physics, University of British Columbia.

Page M., H.O. Pritchard and A.F. Trotman-Dickenson, 1953. The thermal decomposition of azomethane. Journal of the Chemical Society (London), 1953, 3878.

Paneth F. and W. Hofeditz, 1929. Preparation of free methyl. Ber., 62B, 1335.

Parker W.W., G.Z. Smith and R.L. Hudson, 1961. Determination of mixed lead alkyls in gasoline by combined gas chromatographic and spectrophotometric techniques. Analytical Chemistry, 33, 1170.

Pascal P., 1945. Note sur la reductibilite de l'oxyde et d'hydroxyde chromiques. Bull. de la Soc. Chemique, 12, 627.

Peoples J.W., 1932. Geology of the Stillwater Igneous Complex (Beartooth Mountains, Montana). Ph.D. Thesis, Department of Geology, Princeton University.

Picciotto E. and S. Wilgain, 1956. Confirmation de la periode du thorium-232. Nilovo Cimento, Series 10, 4, 1525.

Quets J.M., M.E. Wadsworth and J.R. Lewis, 1960. Kinetics of hydrogen reduction of magnetite. Transactions of the American Institute of Mining, Metallurgy and Petroleum Engineers, 218, 545.

Raley J.H., F.F. Rust and W.E. Vaughan, 1948. Decompositions of di-t-alkyl peroxides. I: Kinetics. Journal of the American Chemical Society, 70, 88.

Ramsperger H.C., 1927. The decomposition of azomethane, a homogeneous unimolecular reaction. Journal of the American Chemical Society, 49, 912.

Rayleigh J.W.S., 1896. Theoretical considerations respecting the separation of gases by diffusion and similar processes. Philosophical Magazine, 42, 493.

Rebbert R.E. and K. Laidler, 1952. Kinetics of the decomposition of diethyl peroxide. Journal of Chemical Physics, 20, 574.

Riblett E.W. and L.C. Rubin, 1937. The thermal decomposition of azomethane. Journal of the American Chemical Society, 59, 1537.

Rice F.O., W.R. Johnston and B.L. Evering, 1932. The thermal decomposition of organic compounds into free radicals. Journal of the American Chemical Society, 54, 3529.

Rice F.O. and R.E. Vollrath, 1929. The thermal decomposition of acetone in the gaseous state. Proceedings of the National Academy of Science (Washington), 15, 702.

Rice F.O. and M.D. Dooley, 1933. The thermal decomposition of organic compounds from the standpoint of free radicals. IV: The dehydrogenation of paraffin hydrocarbon and the strength of the C-C bond. Journal of the American Chemical Society, 55, 4245.

Rice F.O. and K.F. Herzfeld, 1934. The thermal decomposition of organic compounds from the standpoint of free radicals. VI: The mechanism of some chain reactions. Journal of the American Chemical Society, 56, 284.

Rice F.O. and W.R. Johnston, 1934. The thermal decomposition of organic compounds from the standpoint of free radicals. V: The strength of bonds in organic molecules. Journal of the American Chemical Society, 56, 214.

Rice F.O. and K.K. Rice, 1935. The Aliphatic Free Radicals, John Hopkins Press.

Rice F.O. and C.J. Grelecki, 1957. An active species formed in the electrical decomposition of dimethylamine. Journal of Physical Chemistry, 61, 824.

Russell R.D., 1956. Interpretation of lead isotope abundances. Proceedings of the Second Conference on Nuclear Processes in Geological Settings, 68.

Russell R.D. and R.M. Farquhar, 1960. Lead Isotopes in Geology. Interscience Publishers.

Rust F.F., F.H. Seubold and W.F. Vaughan, 1948. Decomposition of di-t-alkyl peroxides. II: Reactions of the resultant free radicals. Journal of the American Chemical Society, 70, 95.

Sathyamurthy T.V., S. Swaminathan and L.M. Yeddanapalli, 1950. Kinetic study of thermal decomposition of tin and silicon tetramethyls. Journal of the Indian Chemical Society, 27, 10.

Schütze W., 1962. Über die datierung von Pb - mineralen. Geochimica et Cosmochimica Acta, 26, 617.

Schwab G.M. and J. Philinis, 1947. Reactions of iron pyrite: its thermal decomposition, reduction by hydrogen and air oxidation. Journal of the American Chemical Society, 69, 2588.

Seddon R.V. and M.W. Travers, 1936. On the thermal decomposition of acetaldehyde and ethylene oxide. Proceedings of the Royal Society of London, A156, 234.

Sehon A.H. and M. Szwarc, 1950. The $(CH_2 = CH - CH_2) - CH_3$ bond dissociation energy and the heat of formation of the alkyl radical. Proceedings of the Royal Society of London, A202, 263.

Senftle F.E. and J.T. Bracken, 1955. Theoretical effect of diffusion on isotopic abundance ratios in rocks and associated fluids. Geochimica et Cosmochimica Acta, 1, 61.

Senftle F.E., L.R. Stieff, F. Cuttilta and P.K. Kuroda, 1957. Comparison of the isotopic abundance of U^{235} and U^{238} and the radium activity ratios in Colorado Plateau Uranium ores. Geochimica et Cosmochimica Acta, 11, 189.

Silverman S.R., 1951. The isotope geology of oxygen. Geochimica et Cosmochimica Acta, 2, 26.

Simard G.L., J. Steger, T. Mariner, D.J. Salley and V.Z. Williams, 1948. In situ study of the thermal decomposition of ethylene oxide in infra-red spectrometry. Journal of Chemical Physics, 16, 836.

Simonen A., 1960. Pre-Quaternary rocks in Finland. Bull. Comm. Geol. Finlande, No. 191.

Slawson W.F. and R.D. Russell, 1962. Concerning the occasional presence of a contaminant in tetramethyllead. Mikrochimica Acta, 4, 201.

Smith F.G., 1963. Physical Geochemistry. Addison-Wiley Publishers.

Stacey J.S., 1962. A method of ratio recording for lead isotopes in mass spectrometry. Ph.D. Thesis, Department of Physics, University of British Columbia.

Stanton R.L. and R.D. Russell, 1959. Anomalous leads and the emplacement of lead sulfide ores. Economic Geology, 54, 588.

Stanton R.L., 1955. The genetic relationship between limestones, volcanic rocks and certain ore deposits. Australian Journal of Science, 17, 173.

Stanton R.L., 1960. General features of conformable "pyritic" orebodies. Canadian Mining and Metallurgical Bulletin, LXIII, 22.

Steacie E.W.R., 1954. Atomic and Free Radical Reactions. Volumes 1 and 2, Reinhold Publisher.

Steel C. and A.F. Trotman-Dickenson, 1959. Kinetics of the thermal decomposition of azomethane. Journal of the Chemical Society (London), 1959, 975.

Sudo K., 1948. Fundamental researches on smelting of sulfide ores. IV: The equilibrium in the reduction of solid lead sulfide by hydrogen gas. Chemical Abstracts, 45, 10011f,g,h.

Surkan A.J., 1956. Sources of lead ions for mass spectrometry. M.A. Thesis, Department of Physics, University of Toronto.

Szwarc M., 1949. The C-C bond energy in ethylbenzene. Journal of Chemical Physics, 17, 431.

Szwarc M., 1950. The determination of bond dissociation energies by pyrolitic methods. Chemical Reviews, 47, 75.

Szwarc M. and A.H. Sehon, 1950. The dissociation energies of the C-H bond in propylene and the C-C bond in 1-butene. Journal of Chemical Physics, 18, 237.

Tatsumoto M. and C.C. Patterson, 1963. The concentration of common lead in sea water. Nuclear Geophysics, National Academy of Science - National Research Council, Washington D.C., Publication 1075, 167.

Tauson L.V. and E.A. Kravckenkov, 1956. The nature of the distribution of lead and zinc in the minerals of the Caledonian Granitoids of Suramir Batholith. Geochemistry #1, 81.

Taylor H.A., 1932. The thermal decomposition of dimethylamine. Journal of Physical Chemistry, 36, 1960.

Terenin A. and H. Neujmin, 1935. Photo-disintegration of polyatomic molecules in the Schuman Ultraviolet. Journal of Chemical Physics, 3, 436.

Thiele J., 1909. Hydrazo- and azomethane. Chemical Abstracts, 3, 2568.

Thode H.G., A.G. Harrison and J. Monster, 1960. Sulfur isotope fractionation in early diagenesis of recent sediments of Northeast Venezuela. American Association of Petroleum Geologists, Bulletin, 44, 1809.

Thode H.G., J.GMonster and H.B. Dunford, 1961. Sulfur isotope geochemistry. Geochimica et Cosmochimica Acta, 25, 159.

Thode H.G., H.B. Dunford and M. Shima, 1962. Sulfur isotope abundances in rock of the Sudbury District and their geological significance. Economic Geology, 57, 565.

Thompson H.W. and M. Meissner, 1938. The kinetics of the thermal decomposition of alkylene oxides. II: Propylene oxide. Transactions of the Faraday Society, 34, 1222.

Tilton G.R., C.C. Patterson, H. Brown, M. Inghram, R. Hayden, D. Hess and E. Larson Jr., 1955. Isotopic composition and distribution of lead, uranium, and thorium in a Precambrium Granite. Bulletin of the Geological Society of America, 66, 1131.

Travers M.W., 1937a. On the thermal decomposition of ethane, ethylene, acetaldehyde, etc. Transactions of the Faraday Society, 33, 735.

Travers M.W., 1937b. A critical study of some recent investigations on thermal changes in simple organic compounds. Transactions of the Faraday Society, 33, 1937.

Tropsch H., C.I. Parrish and G. Egloff, 1936. High-temperature pyrolysis of gaseous olefins. Industrial and Engineering Chemistry, 28, 581.

Tudge A.P. and H.G. Thode, 1950. Thermodynamic properties of isotopic compounds of sulfur. Canadian Journal of Research, 28B, 567.

Ulrych T.J., 1960. The preparation of lead tetramethyl for mass spectrometer analysis. M.Sc Thesis, Department of Physics, University of British Columbia.

Ulrych T.J., 1962. Gas source mass spectrometry of trace leads from Sudbury, Ontario. Ph.D. Thesis, Department of Physics, University of British Columbia.

Vaasjoki O. and O. Kouvo, 1959. A comparison between common lead isotopic composition and minor base metal contents of some Finnish galenas. Economic Geology, 54, 301.

Wampler J.M., 1963. An isotopic study of lead in sedimentary pyrite. Ph.D. Thesis, Columbia University.

Wanless R.K., R.W. Boyle and J.A. Lowden, 1960. Sulfur isotope investigations of the gold-quartz deposits of the Yellowknife District. Economic Geology, 55, 1591.

Waring C.E. and W.S. Horton, 1945. The kinetics of the thermal decomposition of gaseous tetramethyl tin. Journal of the American Chemical Society, 67, 540.

Waters W.A., 1948. The Chemistry of Free Radical Reactions. Oxford Publishers.

Wedepohl K.H., 1956. Untersuchungen zur Geochemie des Bleis. Geochimica et Cosmochimica Acta, 10, 69.

Wetherill G.W., O. Kouvo, G.R. Tilton and P.W. Gast, 1962. Age measurements on rocks from the Finnish Precambrian. Journal of Geology, 70, 74.

Whittles A.B.L., 1960a. The precise measurement of mass spectrometer ion currents. M.Sc. Thesis, Department of Physics, University of British Columbia.

Whittles A.B.L., 1960b. Voltage coefficient of Victoreen High-Meg resistors. Review of Scientific Instruments, 31, 208.

Whittles A.B.L., 1962. The elusive isochron. Transactions of the American Geological Association, 71, 245.

Williams D., 1960. Genesis of sulfide ores. Proceedings of the Geological Association, 71, 245.

Winkler C.A. and C.N. Hinschelwood, 1935a. The thermal decomposition of acetaldehyde. Proceedings of the Royal Society of London, A149, 355.

Winkler C.A. and C.N. Hinschelwood, 1935b. The thermal decomposition of acetone vapor. Proceedings of the Royal Society of London, A149, 340.

Yeddanapalli L.M. and C.C. Schubert, 1946. Thermal and photochemical decomposition of gaseous aluminum trimethyl. Journal of Chemical Physics, 7, 1.

Zhirov K.K. and S.I. Zykov, 1956. Metamorphism and the time of formation of granites as based on isotopic analyses of lead. Geochemistry, 684.